Driven particle in a random landscape: Disorder correlator, avalanche distribution, and extreme value statistics of records

Pierre Le Doussal and Kay Jörg Wiese

CNRS-Laboratoire de Physique Théorique de l'Ecole Normale Supérieure, 24 rue Lhomond, 75231 Paris Cedex, France
(Received 30 October 2008; published 7 May 2009)

We review how the renormalized force correlator $\Delta(u)$, the function computed in the functional renormalization-group (RG) field theory, can be measured directly in numerics and experiments on the *dynamics* of elastic manifolds in the presence of pinning disorder. We show how this function can be computed analytically for a particle dragged through a one-dimensional random-force landscape. The limit of small velocity allows one to access the critical behavior at the depinning transition. For uncorrelated forces one finds three universality classes, corresponding to the three extreme value statistics, Gumbel, Weibull, and Fréchet. For each class we obtain analytically the universal function $\Delta(u)$, the corrections to the critical force, and the joint probability distribution of avalanche sizes s and waiting times w. We find $P(s) = P(w)$ for all three cases. All results are checked numerically. For a Brownian force landscape, known as the Alessandro, Beatrice, Bertotti, and Montorsi (ABBM) model, avalanche distributions and $\Delta(u)$ can be computed for any velocity. For two-dimensional disorder, we perform large-scale numerical simulations to calculate the renormalized force correlator tensor $\Delta_{ij}(\vec{u})$, and to extract the anisotropic scaling exponents $\zeta_x > \zeta_y$. We also show how the Middleton theorem is violated. Our results are relevant for the record statistics of random sequences with linear trends, as encountered, e.g., in some models of global warming. We give the joint distribution of the time s between two successive records and their difference in value w.

I. INTRODUCTION

Elastic objects driven through a disordered environment are ubiquitous in nature, including magnets [1,2], superconductors [3,4], density waves [5,6], wetting [7,8], dry friction [9], dislocation [10], crack propagation [11], and earthquake dynamics [12]. These phenomena can be studied by different theoretical approaches, including phenomenological arguments [3], mean field models [13], functional renormalization group for statics [14–40] and driven dynamics [41–48]. They were also studied with numerical techniques [49–52]. In several cases the experimental results seem to be in reasonable agreement with the theory (see [53] for vortex lattices, [54] for ferroelectrics, and [1] for magnetic interfaces), but some discrepancies are still manifest, at least with the simplest theories, in some cases, e.g., the depinning of the contact line of a fluid [7,8,48].

Recent theoretical progress allows not only for qualitative, but also for quantitative tests. On one hand, for interfaces, powerful algorithms now allow one to find the exact depinning threshold and critical configuration on a cylinder [52,55] and to study creep dynamics [56]. On the other hand the functional renormalization group (FRG) has been extended beyond the lowest order (one loop), and it was shown that differences between statics and depinning become manifest only at two loops [14,41], i.e., to second order in an expansion in $d=4-\epsilon$ where d is the internal dimension of the manifold. Such differences appear for instance in the roughness exponent ζ. The FRG is a field theoretic tool for disordered systems, which captures the complex glassy physics of numerous metastable states at the expense of introducing, rather than a single coupling as in standard critical phenomena, a function, $\Delta(u)$, of the displacement field u, which flows to a fixed point (FP) $\Delta^*(u)$. This FP is nonanalytic, as

is the effective action of the theory. The nonanalyticity is a rather unconventional feature, and the validity of the approach has been questioned: one could argue that, although $\Delta^*(u)$ is perturbative near $d=4$, the second derivative $\Delta''(0)$ has gone to infinity, hence we have left the domain controlled by perturbation theory. To put this criticism to rest, one first shows how an observable of the experimental system can be defined, which is identical to the field theoretic disorder correlator $\Delta(u)$: the idea [57] is to add a quadratic confining potential to the system, which formally acts as a mass for the elastic modes of the interface. The disorder correlator $\Delta(u)$ can then be measured directly as the second moment of the interface displacement.

This method has been used in a numerical simulation of interfaces in a disordered magnet, to compute numerically the zero-temperature FRG fixed-point function $\Delta(u)$ in the statics, for interfaces ($N=1$) using powerful exact minimization algorithms [58]. A variety of disorder types, random bond, random field, and periodic disorder were studied in various dimensions $d=0,1,2,3$. The results are close to one-loop predictions and deviations are consistent with two-loop FRG. The most important feature, namely a linear cusp in $\Delta(u)$, was clearly seen. These results come in strong support for the underlying hypothesis of a nonanalytic field theory, perturbatively accessible in a $d=4-\epsilon$ expansion.

In our Letter [59], we have extended the method of [57,58] to driven systems. In particular it allows one to measure the FRG fixed-point function $\Delta^*(u)$ near the depinning transition at velocity $v=0^+$. The form of this fixed point was obtained to one loop [43,44], but the remarkable fact is that it is only to two-loop order that it differs from the static fixed point [14,41]. Shortly after, this tiny difference was measured, beyond statistical uncertainties, together with the predicted linear cusp, in a numerical study [60] of a line driven in a one-dimensional medium.

In this situation, it is useful to find a simple model, which can be solved analytically, and exhibits many features of the more complicated situation. Such a model is a particle in a random-force landscape, pulled by a moving spring. Since there is no internal degree of freedom, it is the $d=0$ limit of the depinning fixed point for interfaces. Similar $d=0$ toy models were very useful in the study of the statics. The universality classes there were found to be parametrized by the exponent $\zeta \geqslant 1$, with a (presumably unique) universal fixed-point function $\Delta(u) = -R''(u)$ in each case, with $R(u) \sim |u|^\gamma$ at large $|u|$, with $\gamma = 4 - 4/\zeta$. Only in some cases this function was obtained analytically, e.g., for the case $\zeta = 4/3$ of the Sinai model [57], which corresponds to the random-field disorder class. It is thus quite interesting to obtain the corresponding results for the depinning fixed point. Of course another application of the $d=0$ model is driving a fixed-size manifold over very large distance, it eventually behaves again as a particle with some effective random-force landscape.

The aim of this paper is to give a detailed account of the results summarized in [59], and to present some different ones. We summarize the basic ideas in Sec. II, relegating details of the field-theoretic derivation in Appendix A.

In Sec. III, we give a detailed derivation of the analytical results for the $d=0$ particle model, focusing there on uncorrelated random forces. This yields an exponent ζ in a continuous range $0 < \zeta \leqslant 2$ with corresponding fixed-point functions $\Delta(u)$ easier to compute than in the statics. The result depends on the tail of the distribution of the local random force, i.e., we find the three main universality classes of extreme value statistics: The Gumbel, Weibull, and Frechet distribution.

In Sec. IV, we calculate analytically the joint avalanche size s and waiting time w distribution. The avalanche distribution was computed recently [61] in a $d = 4 - \epsilon$ expansion using FRG, and the present results hence correspond to the $d=0$ limit. There it was shown how the avalanche distribution is related to the nonanalyticity of the set of all cumulants of the displacement field.

Interestingly, the problem of a particle driven in one dimension is related to the so-called record statistics [62,63]. If the particle is pulled by a spring the problem is related to record statistics for random sequences with linear trends [64], whose interest has been revived in the context of global warming models [65]. Translated into the language of records, we obtain in Sec. IV, the joint distribution of the time s between two successive records and their difference in value, w, for a sequence of independent and identically distributed (IID) random variables with trends, i.e., variables $Y_n = X_n + cn$ where X_n are IID random variables, and c a drift. These results are obtained for the three classes of extremal statistics.

In Sec. V, we check some of our above results numerically; we also study numerically a particle driven at nonzero velocity $v > 0$, and find that the velocity smoothens the cusp in the force correlator.

In Sec. VI we consider long-range correlated random-force landscapes, specifically the case of a Brownian force. For this model, known as the Alessandro, Beatrice, Bertotti, and Montorsi (ABBM) model for domain wall motion, re-markably, the stationary distribution of instantaneous velocities can be computed [66] for any nonzero average driving velocity $v > 0$. From that we obtain $\Delta(u)$ for any $v > 0$. We also compute the quasistatic $\Delta(u)$ and avalanche distribution. It matches with the limit $v \to 0^+$, and shows how the cusp is smoothened at $v > 0$.

In Sec. VII we summarize some known results and some alternate ones, common to record statistics and to the present model of a driven particle, either with no mass (fixed-force driving, symmetric records), or with a mass (fixed-velocity driving, records with drifts). In particular we study in detail the record statistics for a Levy-walk landscape with drift.

Finally we address the outstanding question of the depinning for systems which can move in more than one direction, also termed "$N > 1$," with N the number of components of the displacement field u (e.g., $N = 2$ for a line moving in three dimension). In particular there is still no satisfactory field theoretic description for this case based on FRG. This question was studied by Ertaş and Kardar [67], but they made the approximation that the disorder correlator only depends on the direction in which the system is driven. Considering two manifolds which are driven on trajectories far apart in the transversal direction, their renormalized disorder correlators should be independent, questioning the assumptions in the Ertaş-Kardar approach. We have studied this situation in the field theory [68] (see also some study at $v > 0$ in [69]), but consistent and *stable* solution of the fixed-point equations seem quite complicated and are still lacking. In this situation it is important to have some numerical results as guide for the analytical treatment. In Sec. VIII we therefore discuss the changes necessary to study an elastic manifold driven through a higher-dimensional random environment, and complement this in Sec. IX by a numerical study of a particle dragged through a random-energy landscape. Especially, we show numerically, that the scaling exponents ("roughness") in the direction of the driving ζ_x and perpendicular to it ζ_y are different, and satisfy $\zeta_x > \zeta_y$. We also find that the cross correlator in the transversal direction (i.e., the force correlator between forces in the direction x of the driving, and its transversal one y, measured as a function of the transversal distance u_y, $\Delta_{xy}(u_x = 0, u_y)$, is nonvanishing.

II. SUMMARY OF THE METHOD

We consider the equation of motion for the overdamped dynamics of an elastic manifold parametrized by its time-dependent displacement field $u(x,t)$,

$$\eta \partial_t u(x,t) = F_x[u(t); w(t)],$$

$$F_x[u;w] = m^2[w - u(x)] + c\nabla_x^2 u(x) + F(x,u(x)), \quad (1)$$

where $F_x[u(t); w(t)]$ is the total force exerted on the manifold [we note $u(t) = \{u(x,t)\}_{x \in \mathbb{R}^d}$ is the manifold configuration, x being its d-dimensional internal coordinate]; η is the friction coefficient and c the elastic constant. Here at the bare level, the random pinning force is $F(x,u) = -\partial_u V(x,u)$ and the random potential V has correlations $\overline{V(0,x)V(u,x')} = R_0(u)\delta^d(x - x')$. We consider first random-bond bare disorder with a short-ranged $R_0(u)$. We have added a har-

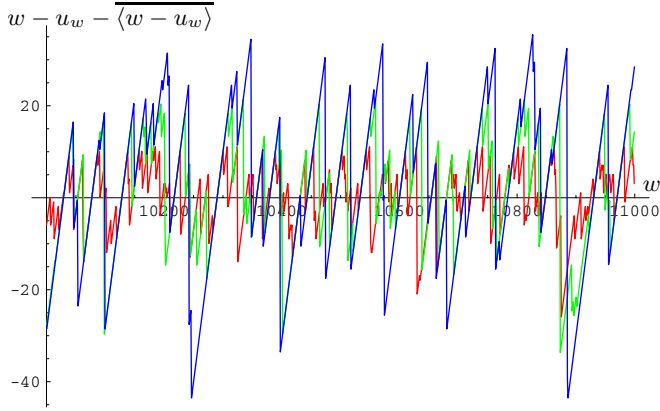FIG. 1. (Color online) Dynamical shocks (avalanches): position of a particle u_w pulled by a spring, of varying equilibrium position w, in a one-dimensional random force landscape (with forces uniformly distributed between 0 and 1). The quasistatic motion shows a succession of jumps, also called shocks. Decreasing the spring constant (the mass) from $m^2 = 0.01$ (red) over $m^2 = 0.03$ (green) to $m^2 = 0.001$ (blue), the shocks become larger and larger.

monic coupling to an external variable $w(t)$, a given function of time (in most cases we choose it uniform in x). This is the simplest generalization of the statics, where $w(t) = w$ is time independent. It is useful to define the fixed-w energy

$$\mathcal{H}_w[u] = \int d^d x \frac{m^2}{2} [u(x) - w]^2 + V(x, u(x)) \qquad (2)$$

associated to the force $F_x[u; w] = -\frac{\delta H_w[u]}{\delta u(x)}$. If $w(t)$ is an increasing function of t the model represents an elastic manifold "pulled" by a spring, see Fig. 1.

We first describe qualitatively how to measure the FRG functions and later justify why the relation is expected to be exact. We are interested in the observable $w(t) - \langle \bar{u}(t) \rangle$ where $\bar{u}(t) = L^{-d} \int d^d x u(x, t)$ is the center of mass position, and $\langle \cdot \rangle$ denotes thermal averages, i.e., the ground state at zero temperature. It represents the shift between the translationally averaged displacement and the center of the well, i.e., the extension of the spring. It is thus proportional to the pulling force on the manifold, hence to the translationally averaged pinning force minus the friction force, i.e., $w(t) - \bar{u}(t) = m^{-2} [\eta v(t) - \int_x F(x, u(x, t))]$ (if we use periodic boundary conditions inside the manifold). Of particular interest are

$$\overline{w(t) - \langle \bar{u}(t) \rangle} = m^{-2} f_{av}(t),$$

$$\overline{[w(t) - \langle \bar{u}(t) \rangle][w(t') - \langle \bar{u}(t') \rangle]}^c = m^{-4} L^{-d} D_w(t, t'), \qquad (3)$$

where connected means with respect to the double average $\overline{\langle \cdots \rangle}$. If we consider a function $w(t)$ such that $dw(t)/dt > 0$, one can also write

$$D_w(t, t') = \Delta_w(w(t), w(t')). \qquad (4)$$

As written, the function Δ_w may in general depend on the history $w(t)$. However, we expect that for fixed L, m and slow enough $w(t)$, e.g., $w(t) = vt$ with $v \to 0^+$, one has $\Delta_w(w(t), w(t')) \to \Delta[w(t) - w(t')]$. This function $\Delta(w - w')$, which is independent of the process $w(t)$, is the one defined

in the F.T. The derivation of this property is given in Appendix A to which we refer the reader for technical details. Note that we are discussing now $N = 1$ systems (interfaces), subtleties related to $N > 1$ are discussed in Sec. VIII.

Let us now describe $T = 0$ depinning. Quasistatic depinning is studied as the limiting case where $dw/dt \to 0^+$. The quasistatic motion can be described as follows (in the continuum model). One starts in a metastable state $u_0(x)$ for a given $w = w_0$, i.e., a zero-force state $F_x(u_0(x); w) = 0$ which is a local minimum of $H_{w_0}[u]$ with a positive barrier. One then increases w. For smooth short-scale disorder, the resulting deformation of $u(x)$ is smooth. At some $w = w_1$, the barrier vanishes. For $w = w_1^+$ the manifold moves downward in energy until it is blocked again in a metastable state $u_1(x)$ which again is a local minimum of $H_{w_1}[u]$. We are interested in the center of mass (i.e., translationally averaged) displacement $\bar{u} = L^{-d} \int d^d x u(x)$. The above process defines a function $\bar{u}(w)$ which exhibits jumps at the set w_i. Note that time has disappeared: evolution is only used to find the next location. The first two cumulants

$$\overline{w - u(w)} = m^{-2} f_c, \qquad (5)$$

$$\overline{[w - u(w)][w' - u(w')]}^c = m^{-4} L^{-d} \Delta(w - w') \qquad (6)$$

allow a direct determination of the averaged (m dependent) critical force f_c and of $\Delta(w)$. Note that $u(w)$ a priori depends on the initial condition and on its orbit but at fixed m one expects an averaging effect when w is moved over a large region. This is further discussed below. Note that the definition of the (finite size) critical force is very delicate in the thermodynamic limit [38].

Elastic systems driven by a spring and stick-slip type motion were studied before, e.g., in the context of dry friction. The force fluctuations and jump distribution were studied numerically for a string driven in a random potential [70]. However, the precise connection to quantities defined and computed in the field theory has to our knowledge not been made. The dependence in m for small m predicted by FRG, $\Delta(w) = m^{\epsilon - 2\zeta} \widetilde{\Delta}(w m^{-\zeta})$, is consistent with observations of [70] but the resulting $\widetilde{\Delta}(w)$ has never been measured. Fully connected mean-field models of depinning also reduce to a particle pulled by a spring, together with some self-consistency condition. Reference [44] discusses related issues in an expansion around mean field. As discussed below, our main remarks here are much more general, independent of any approximation scheme, and provide a rather simple and transparent way to attack the problem.

Note that the manifold in the harmonic well can be approximated by $(L/L_m)^d$ roughly independent pieces with $L_m \sim 1/m$. The motion of each piece over large distances resembles the one of a particle, i.e., a $d = 0$ model, but with a rescaled unit of distance in the u direction, $u_m \sim L_m^\zeta \sim m^{-\zeta}$. The "effective force" landscape seen by each piece becomes uncorrelated on such distances, and its amplitude scales as $F_m \sim m^2 u_m$. Hence one is in a bulk regime not dominated by extremes, i.e., $\Delta(w)$ probes only motion over order one unit. It is easy to check that an arbitrary initial condition joins the common unique orbit after about one correlation length.
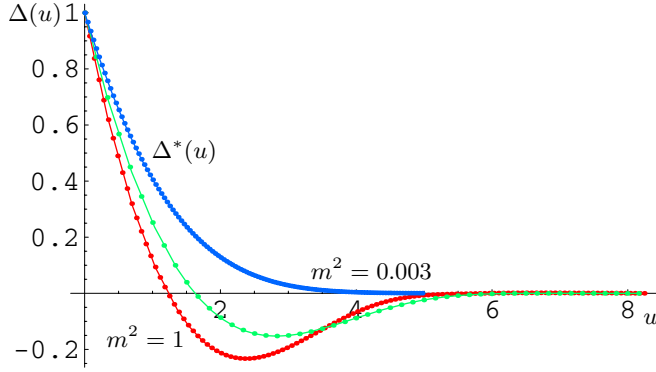
FIG. 2. (Color online) (a) The measured correlator $\Delta(u)$ for a particle pulled in a random potential [i.e., random-bond (RB) disorder] distributed uniformly in $[0,1]$, and rescaled such that $\Delta(0)=1$ and $\int_0^\infty du|\Delta(u)|=1$. From bottom [which has $\int_0^\infty du\Delta(u)\approx 0$] to top the mass decreases from $m^2=1$ (red) to $m^2=0.5$ (green) to $m^2=0.003$ (blue), where it has (up to small corrections) converged to the fixed point $\Delta^*(u)$. This demonstrates in $d=0$ the expected crossover from random-bond to random-field disorder (see text). Note that the fixed point has a cusp singularity at $u=0$.

Hence the $d=0$ model (see Fig. 2) suggests that starting the quasistatic motion in u_0 and driving the manifold over $w\sim L_m^\zeta$ should then result in all orbits either converging or having statistically identical properties. Note that if the manifold is driven over more than L^ζ, a crossover to $d=0$ behavior and extremal statistics occurs, as studied in the next section.

The averaged critical force, defined in Eq. (5), should, for $d>0$, go to a finite limit, with $f_c(m)=f_c^\infty+Bm^{2-\zeta}$ from finite-size scaling. This has been recently tested in the numerics [60]. Although f_c is not universal and depends on short-scale details, one easily sees that $-m\partial_m f_c(m)$ depends only on one unknown scale. We note that the definition (5) coincides with the one proposed recently as the maximum depinning force for all configurations having the same center of mass u_0 [39]. Since $\bar{u}-w$ is a fluctuating variable of order $(L/L_m)^{-d/2}$, the two definitions should coincide in the limit where $L\to\infty$, before $m\to 0$. The one point distribution of the critical force is obtained from the distribution of $w-u(w)$, and to one loop is identical to the one obtained in [39] provided one uses there the massive scheme.

Let us now recall the field-theory predictions: The FRG equation at two-loop order for the (rescaled) force correlator are [14]

$$-m\partial_m\Delta(u) = (\epsilon-2\zeta)\Delta(u)+\zeta u\Delta'(u)$$
$$-\frac{d^2}{du^2}\left\{\frac{1}{2}[\Delta(u)-\Delta(0)]^2\right\}$$
$$+\frac{d^2}{du^2}\{\Delta'(u)^2[\Delta(u)-\Delta(0)]+\lambda\Delta'(0^+)^2\Delta(u)\}.$$
$$(7)$$

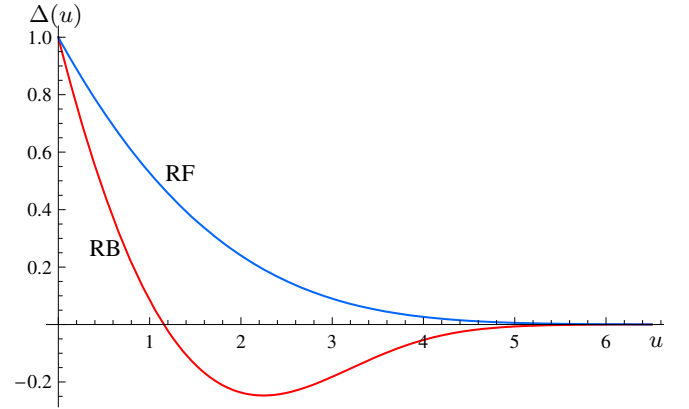$\lambda=-1$ describes the statics, and $\lambda=1$ the depinning. For the statics, $\Delta(u)$ admits a potential solution (random-bond universality class) $\Delta(u)=-R''(u)$, with $R(u)$ decaying to 0 as $u\to\infty$, as illustrated on Fig. 3. This implies that the integral $\int_0^\infty du\Delta(u)$ remains unrenormalized. However at depinning, it flows, and no potential solution exists. For a large class of bare disorder, the model should renormalize, as m decreases, to the random-field fixed-point solution, $\Delta_{\rm RF}^*(u)$, which is monotonically decaying and strictly positive. For the $d=0$ toy model discussed in the next section, this crossover is nicely seen in our numerical simulation with decreasing m, as is illustrated on Fig. 2. Therefore, in the following, we can focus on the random-field universality class, i.e., short-range correlated random forces.

FIG. 3. (Color online) Fixed-point functions $\Delta^*(u)$ for random-bond (RB) and random-field (RF) disorder (arbitrary scale).

III. PARTICLE IN SHORT-RANGE RANDOM-FORCE LANDSCAPE ($D=0$): EXACT RESULTS

We now study the model in $d=0$, i.e., a particle with equation of motion

$$\eta\partial_t u = m^2(w-u)+F(u). \quad (8)$$

In the quasistatic limit where w is increased slower than any other time scale in the problem, the zero force condition $F(u)=m^2(u-w)$ determines $u(w)$ for each w, starting from some initial condition. The graphical construction of $u(w)$ is well known from studies of dry friction. When there are several roots one must follow the root as indicated in Fig. 4, where $F(u)$ is plotted versus $m^2(u-w)$. This results in jumps and different paths, $u^\uparrow(w)$ and $u^\downarrow(w)$, respectively, for motion to the right (forward) and to the left (backward). Let us call A the area of this hysteresis loop (the area of all colored and/or shaded regions in Fig. 4). It is the total work of the friction force when moving the center of the harmonic well quasistatically once forth and back, i.e., the total dissipated energy. The above definition of the averaged critical force (5), assuming the landscape statistics to be translationally invariant and that one can replace disorder averages by translational ones over a large width M (which certainly holds if force correlations are short-range correlated), gives

$$f_c = m^2\overline{(w-u_w)}^{\rm tr} = \frac{m^2}{M}\int_0^M dw(w-u_w). \quad (9)$$
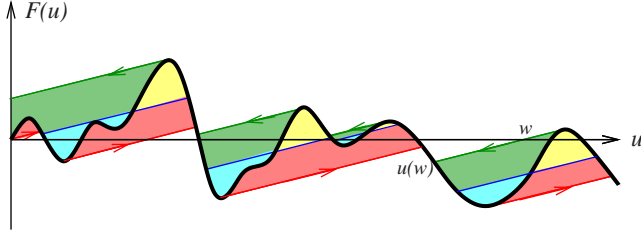
Hence, subtracting the two paths gives

FIG. 4. (Color online) Construction of $u(w)$ in $d=0$, for the pinning force $F(u)$ (bold black line). The two quasistatic motions driven to the right and to the left are indicated by red and green arrows, and exhibit jumps ("dynamical shocks"). The position of the shocks in the statics is shown for comparison, based on the Maxwell construction (equivalence of light blue and yellow areas, both bright in black and white). The critical force is $1/(2M)$ times the area bounded by the hull of the construction.

$$f_c := \frac{1}{2}(f_c^\uparrow - f_c^\downarrow)$$

$$= \lim_{M \to \infty} \frac{m^2}{2M} \int_0^M dw[u^\downarrow(w) - u^\uparrow(w)]$$

$$= \lim_{M \to \infty} \frac{A}{2M}, \qquad (10)$$

where we have used $\int u\,dw = \int w\,du$ and $f_c^\downarrow < 0$. One can check that for $m \to 0$ this definition of f_c becomes identical to the one on a cylinder, f_d, which for a particle $(d=0)$ is $2f_d = f_d^\uparrow - f_d^\downarrow = \max_u F(u) - \min_u F(u)$ with $2f_d M = \lim_{m \to 0} A(m)$. Since A depends on the starting point, this definition holds after a complete tour, where the maximum (minimal) pinning force was selected. One can also compare with the definition of shocks in the statics. There, the effective potential is a continuous function of w. Therefore, when making a jump, the integral over the force must be zero, which amounts to the Maxwell construction of Fig. 4.

A. Short-range correlated force: A discrete model

Let us now consider the asymptotic forward process $u(w) := u^\uparrow(w)$, defined in general as the *smallest root* of the equation $F(u) = m^2(u-w)$. The set of points $[u, F(u)]$ is the lightened portion of the $F(u)$ curve, the rest being the shadow. If one starts in the shadow at w_0 one joins at w_1 the asymptotic process for all $w > w_1$. The difference $w_1 - w_0$ is finite for finite m, hence we will only study the asymptotic process. Note that the area of the shadow per unit length is the critical force.

We now study short-range correlated random force landscapes. In the limit of interest, $m \to 0$, the scale of jumps becomes large, and the finite range should be unimportant. Hence it is equivalent, and more convenient, to consider a discrete model, u being integers. The variable w can be kept real. One considers a discrete landscape $F(u) = F_i$ independently distributed with $P(F)$, and i integer variable. The process $u(w)$ is then defined on integers. Its definition is shown in Fig. 5.
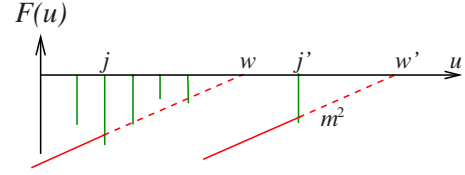

FIG. 5. (Color online) Construction of $u(w)$ in $d=0$ for the forward motion in the discretized model. The vertical lines are the force barriers, the (red) increasing lines the spring force $m^2(u-w)$. A particle moves from left to right, until it is stopped by a barrier (when the lines for spring force and barrier forces intersect).

Let us compute for $w' > w$ the following joint probabilities:

$$P_w(j,F) := \text{Prob}(u(w) = j \text{ and } F_j = F), \qquad (11)$$

$$P_{w;w'}(j,F;j',F') := \text{Prob}(u(w) = j \text{ and } F_j = F \text{ and } u(w') = j'$$
$$\text{and } F_{j'} = F'). \qquad (12)$$

We define

$$H(F) = \int_F^{+\infty} P(f)df = 1 - \int_{-\infty}^F P(f)df. \qquad (13)$$

Since for $u(w) = j$ to hold one must have all $F_k > m^2(k-w)$ for all $k < j$ and $F_j < m^2(j-w)$, see Fig. 5, one has

$$P_w(j,F) = P(F)\theta(m^2(j-w)-F) \prod_{k=-\infty}^{j-1} H(m^2(k-w)),$$

$$P_w(j) = \{1 - H(m^2(j-w))\} \prod_{k=-\infty}^{j-1} H(m^2(k-w)), \qquad (14)$$

where the first line integrated over F yields the second [and $\theta(x)$ denotes the unit step function]. One easily checks that $\sum_{j=-\infty}^{j=+\infty} P_w(j) = 1$.

Next for $j' > j$ one has

$$P_{w;w'}(j,F,j',F') = P(F)\theta(m^2(j-w)-F)\theta(F-m^2(j-w'))$$

$$\times \prod_{k=-\infty}^{j-1} H(m^2(k-w))P(F')$$

$$\times \theta(m^2(j'-w')-F') \prod_{k=j+1}^{j'-1} H(m^2(k-w'))$$

$$\qquad (15)$$

with the convention that for $j' = j+1$, the factor $\prod_{k=j+1}^{j'-1} H[m^2(k-w')] = 1$, and for $j = j'$,

$$P_{w;w'}(j,F,j,F') = \delta(F-F')P(F)\theta(m^2(j-w')-F)$$

$$\times \prod_{k=-\infty}^{j-1} H(m^2(k-w)). \qquad (16)$$

Integrating over the forces we obtain the one-point and two-point probability for the process $u(w)$. They read, in compact

notations with $H_k^w := H[m^2(k-w)]$, and nonzero only for $j' \geq j$,

$$P_w(j) = (1 - H_j^w) \prod_{k=-\infty}^{j-1} H_k^w, \tag{17}$$

$$P_{w;w'}(j,j') = (H_j^{w'} - H_j^w)(1 - H_{j'}^{w'}) \prod_{k=-\infty}^{j-1} H_k^w \prod_{k=j+1}^{j'-1} H_k^{w'}$$

$$+ \delta_{jj'}(1 - H_j^{w'}) \prod_{k=-\infty}^{j-1} H_k^w \tag{18}$$

$$= \frac{P_w(j)}{1 - H_j^w} \left[(H_j^{w'} - H_j^w)(1 - H_{j'}^{w'}) \prod_{k=j+1}^{j'-1} H_k^{w'} + \delta_{jj'}(1 - H_j^{w'}) \right], \tag{19}$$

with the convention that for $j'=j$, the factor $\prod_{k=j+1}^{j'-1} H_k^{w'} = 0$. Using that $\sum_{j'>j}(1 - H_{j'}^{w'})\prod_{k=j+1}^{j'-1} H_k^{w'} = 1$ one checks the normalization $\sum_{j' \geq j} P_{w;w'}(j,j') = P_w(j)$.

B. Continuum limit for one-point distribution

For small m the continuum limit can be taken as

$$P_w(j) \approx \{1 - H(m^2(j-w))\} \exp\left(\int_{-\infty}^{j} dy \ln H(m^2(y-w)) \right)$$

$$= \int_{-\infty}^{m^2(j-w)} df P(f)$$

$$\times \exp\left(\int_{-\infty}^{j} dy \ln\left(1 - \int_{-\infty}^{m^2(y-w)} P(l) dl \right) \right)$$

$$\approx \int_{-\infty}^{m^2(j-w)} df P(f) \exp\left(-\int_{-\infty}^{j} dy \int_{-\infty}^{m^2(y-w)} P(l) dl \right). \tag{20}$$

The last step is justified if the result is indeed dominated by the tail of $P(f)$ for f negative, which is at the heart of extremal statistics. That this is indeed true is justified *a posteriori*.

The quantity $m^2[w - u(w)] \equiv m^2(w-j)$ is the "local," i.e., fluctuating critical force, and its disorder average is $f_c(m) = m^2\overline{[w - u(w)]}$. Its distribution can be obtained from the one-point distribution $P_w(j)$. To rewrite Eq. (21) in a simpler form we define

$$a_w'(j) \equiv a'(j) := \int_{-\infty}^{m^2(j-w)} P(f) df, \tag{21}$$

$$a_w(-\infty) := 0. \tag{22}$$

Note that $a_w(+\infty) = +\infty$. The one-point distribution can thus be rewritten as

$$P_w(j) dj = e^{-a_w(j)} da_w(j). \tag{23}$$

Hence one can rewrite the first moment in the form

$$\overline{w - u(w)} = \int_{-\infty}^{\infty} dj P_w(j)(w - j) = \int_{-\infty}^{\infty} dj a_w'(j) e^{-a_w(j)}(w - j). \tag{24}$$

This means that the quantity a has a simple exponential distribution, hence one needs to invert the relation, i.e., find j as a function of a,

$$j = j(a;w) \leftrightarrow a_w(j) = a, \tag{25}$$

and use that a has an exponential distribution, to obtain any average, e.g.,

$$\overline{[w - u(w)]^p} = \int_0^{\infty} da e^{-a}[w - j(a;w)]^p, \tag{26}$$

for any p.

C. Distribution of critical force: The different disorder classes

We now obtain the universality classes for the one-point distribution of the process $u(w)$, i.e., for the distribution of critical forces. We define b, a rescaled version of a,

$$b(m^2(j-w)) := m^2 a. \tag{27}$$

Using Eq. (21), it can be written as

$$b(x) \equiv e^{-\beta(x)} = \int_{-\infty}^{x} dy \int_{-\infty}^{y} P(f) df. \tag{28}$$

The condition defines $a_w(j)$. We thus need to invert this relation to obtain j as a function of a. We do this for the three main disorder classes below.

1. Gumbel class (class Ia)

The first class contains distributions $P(F)$ with unbounded support and decaying exponentially fast at $F \to -\infty$ (in some broad sense defined below). One then finds the Gumbel distribution for the critical force, hence we call this class the Gumbel class.

Let us invert relation (27) and assume that the following expansion holds at small m:

$$m^2(j-w) = \beta^{-1}\left(\ln\frac{1}{m^2} - \ln a \right)$$

$$= -f_c^0(m) - \frac{\ln a}{\beta'(-f_c^0(m))} + (\beta^{-1})''\left(\ln\frac{1}{m^2} \right) \frac{(\ln a)^2}{2}$$

$$+ \cdots, \tag{29}$$

$$f_c^0(m) := -b^{-1}(m^2) \equiv -\beta^{-1}\left(\ln\frac{1}{m^2} \right), \tag{30}$$

where we know that a is a fluctuating number of order 1 with an exponential distribution, $P(a) = e^{-a}\theta(a)$. That gives the distribution of the variable $m^2(j-w)$. In particular since

$$-\int_0^{\infty} da e^{-a} \ln a = \gamma_E = 0.577\,216\ldots, \tag{31}$$

we obtain the asymptotics of the (averaged) critical force as

$$f_c(m) = f_c^0(m) - \frac{\gamma_E}{\beta'(-f_c^0(m))} + \cdots . \tag{32}$$

For this asymptotics to hold, the ratio of successive terms has to go to zero, equivalent to

$$\lim_{z \to \infty} \frac{d}{dz} \ln|(\beta^{-1})'(z)| \to 0. \tag{33}$$

This defines the Gumbel class Ia, together with the fact that the support is unbounded. An example is $\ln P(f) = -A(-f)^\gamma$ as $f \to -\infty$. Then

$$\beta(x) \approx_{x \to \infty} A(-x)^\gamma, \tag{34}$$

$$\beta^{-1}(y) \approx -(y/A)^{1/\gamma}, \tag{35}$$

$$-(\beta^{-1})'(y) \approx \frac{1}{\gamma A}\left(\frac{y}{A}\right)^{1/\gamma - 1}. \tag{36}$$

Hence class-Ia condition is satisfied for *any* γ, even for $\gamma < 1$. Note that preexponential algebraic factors do not change the result. The critical force becomes

$$m^2[u(w) - w] = m^2(j - w)$$

$$= -\left(\frac{\ln m^{-2}}{A}\right)^{1/\gamma} + \frac{\ln a}{A \gamma \left(\frac{\ln m^{-2}}{A}\right)^{1-1/\gamma}}$$

$$+ O\left(\frac{(\ln a)^2}{(\ln m^{-2})^{2-1/\gamma}}\right). \tag{37}$$

Defining the fluctuating critical force as $f_c(m) = m^2[w - u(w)]$ we find

$$f_c(m) = f_c^0(m) + cm^2\rho_m, \tag{38}$$

where $c = -\ln a$ has a Gumbel distribution $P(c) = e^{-c} \exp(-e^{-c})$ on the real axis $c \in]-\infty, \infty[$, with $\bar{c} = \gamma_E$ and

$$f_c^0(m) = A^{-1/\gamma}(\ln m^{-2})^{1/\gamma}. \tag{39}$$

One also finds

$$\rho_m = \frac{(\beta^{-1})'(\ln m^{-2})}{m^2} = \frac{1}{\gamma A^{1/\gamma} m^2 (\ln m^{-2})^{1-1/\gamma}}. \tag{40}$$

Since as confirmed below, $\rho_m \sim m^{-\zeta}$ is the unique scale appearing also in the second cumulant (the disorder correlator defined in FRG), we can identify for class Ia

$$m^{-\zeta} = m^{-2}(\ln m^{-2})^{1/\gamma - 1}. \tag{41}$$

Hence $\zeta = 2$, with additional logarithmic corrections, i.e., $\zeta = 2^+$ for $\gamma < 1$ and $\zeta = 2^-$ for $\gamma > 1$.

2. Class Ib: Bounded support with exponential singularity

An example of this class is

$$\beta(x) = A/(x + x_0)^\gamma, \tag{42}$$

$$\beta^{-1}(y) = -x_0 + (y/A)^{-1/\gamma}, \tag{43}$$

$$b(x) \sim e^{-A/(x+x_0)^\gamma}\theta(x + x_0), \tag{44}$$

$$P(f) \sim e^{-A/(f+x_0)^\gamma}\theta(f + x_0), \tag{45}$$

with $\gamma > 0$. One sees that the condition (33) is obeyed. Hence this is still the Gumbel class, although we introduce a distinction for convenience. A similar asymptotics can then be performed,

$$m^2(j - w) = -x_0 + \left(\frac{A}{\ln m^{-2}}\right)^{1/\gamma} + \frac{1}{\gamma}A^{1/\gamma}\frac{\ln a}{(\ln m^{-2})^{1+1/\gamma}}. \tag{46}$$

Apart from the bound x_0, the result is the same as in class I with $\gamma \to -\gamma$ (in the exponents only). Hence one finds again

$$f_c(m) = f_c^0(m) + cm^2\rho_m, \tag{47}$$

where $c = -\ln a$ has a Gumbel distribution $P(c) = e^{-c} \exp(-e^{-c})$ on the real axis $c \in]-\infty, \infty[$ with $\bar{c} = \gamma_E$ and

$$f_c^0(m) = x_0 - A^{1/\gamma}(\ln m^{-2})^{-1/\gamma}. \tag{48}$$

One also finds the characteristic scale $\rho_m \sim m^{-\zeta}$,

$$\rho_m = 1/[\gamma A^{-1/\gamma} m^2 (\ln m^{-2})^{1+1/\gamma}], \tag{49}$$

hence $\zeta = 2^+$.

3. Algebraic bounded support: Weibull class (class III)

The Weibull class, or class III, applies for a force distribution with bounded support (from below) and algebraic behavior near the edge. An example is

$$P(f) = \tilde{A}(f + x_0)^{\tilde\alpha}\theta(f + x_0), \tag{50}$$

$$b(x) = A(x + x_0)^\alpha\theta(x + x_0), \tag{51}$$

$$\alpha = 2 + \tilde\alpha, \tag{52}$$

$$A = \tilde{A}/[(2 + \tilde\alpha)(1 + \tilde\alpha)]. \tag{53}$$

One must have $\tilde\alpha > -1$, hence $\alpha > 1$. The box distribution corresponds to $\tilde\alpha = 0$, i.e., $\alpha = 2$. Here

$$b^{-1}(y) = -x_0 + (y/A)^{1/\alpha} \tag{54}$$

with $y \geq 0$. Hence analogously to Eqs. (29) and (30) we find from Eq. (27)

$$m^2[u(w) - w] = m^2(j - w) = b^{-1}(m^2a) = -x_0 + \left(\frac{m^2}{A}\right)^{1/\alpha}a^{1/\alpha}, \tag{55}$$

where we recall that a is a random variable with distribution $P(a) = e^{-a}\theta(a)$. For $\alpha \to \infty$ one recovers the Gumbel class. Hence one finds for the fluctuating critical force $f_c(m) = m^2[u(w) - w] = m^2(j - w)$,

$$f_c(m) = f_c^0(m) + cm^2\rho_m, \tag{56}$$

where now $c = -a^{1/\alpha}$ has a Weibull distribution $P(c) = \alpha(-c)^{\alpha-1}\exp[-(-c)^\alpha]$ with parameter α on the negative real axis $c \in]-\infty, 0[$ and

$$f_c^0(m) = x_0. \tag{57}$$

The averaged critical force is

$$f_c(m) = x_0 - \left(\frac{1}{A}\right)^{1/\alpha} m^{2/\alpha} \Gamma\left(1 + \frac{1}{\alpha}\right) + \cdots, \tag{58}$$

where we have used that $\int_0^\infty da e^{-a} a^{1/\alpha} = \Gamma(1 + \frac{1}{\alpha})$. One also finds that

$$\rho_m = A^{-1/\alpha} m^{-2(1-1/\alpha)}, \tag{59}$$

$$\zeta = 2 - \frac{2}{\alpha}, \tag{60}$$

with $1 < \alpha < \infty$, hence $0 < \zeta < 2$.

4. Fréchet class (class II)

The Fréchet class, or class II, is relevant for force distributions with large fluctuations, i.e., algebraic tails on an unbounded support. An example is $P(f) \approx \widetilde{A}(-f)^{-\widetilde{\alpha}} \Theta(-f)$, $\widetilde{\alpha} > 1$. One has $b(x) = A(-x)^{-\alpha}$ with $\alpha = \widetilde{\alpha} - 2$ and $\widetilde{A} = A(\widetilde{\alpha} - 2)(\widetilde{\alpha} - 1)$. Since $\beta(x) = -\ln A + \alpha \ln(-x)$ and $\beta^{-1}(y) \sim -e^{y/\alpha}$ one checks that the class-I condition (33) is not fulfilled. Let us first study $\widetilde{\alpha} > 2$, i.e., $\alpha > 0$,

$$m^2(j - w) = -A^{1/\alpha}\left(\frac{1}{m^2 a}\right)^{1/\alpha}. \tag{61}$$

Hence one finds for the fluctuating critical force $f_c(m) = m^2[u(w) - w] = m^2(j - w)$,

$$f_c(m) = c m^2 \rho_m, \tag{62}$$

where now $c = a^{-1/\alpha}$ has a Frechet distribution $P(c) = \alpha c^{-\alpha-1} \exp(-c^{-\alpha})$ with parameter $\alpha > 0$ on the positive real axis $c \in \,]0, \infty[$ and the average critical force is

$$\overline{f_c(m)} = \Gamma\left(1 - \frac{1}{\alpha}\right) m^2 \rho_m, \tag{63}$$

where we have used $\overline{c} = \int_0^\infty da e^{-a} a^{-1/\alpha} = \Gamma(1 - \frac{1}{\alpha})$ and

$$\rho_m = A^{1/\alpha} m^{-2(1+1/\alpha)}. \tag{64}$$

This corresponds to a roughness exponent

$$\zeta = 2 + \frac{2}{\alpha}. \tag{65}$$

Note that for $\alpha < 1$ ($\widetilde{\alpha} < 3$, $\zeta > 4$) the average critical force is infinite.

We will see that the Frechet class is a bit pathologic in the sense that $\Delta(0) = \infty$ for $\alpha < 2$. More generally cumulants of order larger than α are infinite, i.e., they are associated to a probability distribution with fat tails. This implies as usual that these quantities are dominated by the largest events, hence they are sensitive to how the continuous limit is constructed from the discrete model. For $\widetilde{\alpha} < 2$ the integral in Eq. (28) is divergent at its lower bound, hence undefined without a cutoff.

5. Comparison with extremal statistics

Until now it seems that we have recovered the standard extremal statistics classes for the distribution of the local critical force. On one hand this is not surprising, since one expects, qualitatively, that the critical force for two independent consecutive regions in one dimension be the maximum of the ones for each single region. This is certainly an exact statement for the zero-mass case recalled in Sec. VII. Here, it is quite consistent with the identification of $m^2[u(w) - w]$ as a fluctuating threshold force, a fact which maybe was not obvious from the start. However, note that the value of the parameter α of the extremal statistics classes is *shifted by one* from the value it takes if one models the total critical force as the extremal one $f_c = \min_i(\{f_c^i\})$ over $N \sim m^{-2}$ independent regions, each with its critical force f_c^i distributed with $P_c(f)$. In that case one has

$$\text{Prob}(f_c > x) = \left[\int_x^\infty P_c(f) df\right]^N \approx e^{-N \int_{-\infty}^x P_c(f) df} \tag{66}$$

which can be written equivalently as

$$b_c(x) := \int_{-\infty}^x P_c(f) df = \frac{a}{N}, \tag{67}$$

where a is a random variable of order 1 with an exponential distribution $P(a) = e^{-a} \theta(a)$. A comparison with Eq. (28) shows that the effective critical force in an independent region should be chosen with a distribution with a tail

$$P_c(f) = \int_{-\infty}^f P(f') df' \tag{68}$$

for large negative f. Hence there is a first coarse graining which transforms the tail of $P(f)$ into the tail of $P_c(f)$. Then one can think of the resulting critical force as the maximum over $N \sim m^{-2}$ independent random variables distributed with $P_c(f)$. Applied to Weibull and Frechet classes, Eq. (68) indeed accounts for the shift of the index α by one.

D. Two-point probabilities and the FRG correlator $\Delta(w)$

In addition to recovering the three extremal statistics classes, which, as explained above, is not surprising if one thinks in terms of coarse grained independent random variables, there is a second more remarkable property. We find here that the two-point correlation

$$\overline{[w - u(w)][w' - u(w')]}^c$$
$$= \int dj\, dj'\, P_{w,w'}(j, j')(w - j)(w' - j) - \overline{(w - j)(w' - j')}$$
$$= m^{-4} \Delta(w - w') \tag{69}$$

takes, for all three classes, the following form at small m:

$$\Delta(w) = m^4 \rho_m^2 \widetilde{\Delta}(w/\rho_m), \tag{70}$$

where the scale $\rho_m \sim m^{-\zeta}$ is the one identified in each case in the previous section, and the fixed-point function $\widetilde{\Delta}(w)$ only depends on the universality class: it is unique and identical

for all members of class I (Ia and Ib), continuously depending on α (hence ζ) for classes II and III.

Let us now give the joint probability in the continuum limit. From Eq. (18) and as was done to arrive to Eq. (23) one finds for $w' > w$

$$P_{w;w'}(j,j') = [a'_w(j) - a'_{w'}(j)]a'_{w'}(j')$$
$$\times e^{-a_w(j) - a_{w'}(j') + a_{w'}(j)}\theta(j' > j)$$
$$+ \delta(j - j')a'_{w'}(j)e^{-a_w(j)}. \quad (71)$$

Let us check the normalizations. Using that $\int_j^\infty dj' a'_{w'}(j')e^{-a_{w'}(j')} = e^{-a_{w'}(j)}$ one obtains (writing separately the two contributions)

$$\int_{-\infty}^\infty dj' P_{w;w'}(j,j') = [a'_w(j) - a'_{w'}(j)]e^{-a_w(j)} + a'_{w'}(j)e^{-a_w(j)}$$
$$= P_w(j). \quad (72)$$

A similar trick yields

$$\int_{-\infty}^\infty dj P_{w;w'}(j,j') = P_{w'}(j'). \quad (73)$$

Note also that

$$P_{w;w}(j,j') = P_w(j)\delta(j' - j). \quad (74)$$

For all three classes one finds, starting from Eqs. (37), (56), and (62), respectively,

$$j - w = -\frac{f_c^0(m)}{m^2} - \rho_m c(a), \quad (75)$$

with either $c(a) = -\ln a$ (class I), $c(a) = -a^{1/\alpha}$ (class III), or $c(a) = a^{-1/\alpha}$ (class II). Since the constant piece in Eq. (75) disappears when computing the connected moments, to compute Δ defined in Eq. (69) we can simply write

$$j - w = -\rho_m c(a), \quad j' - w' = -\rho_m c(a') \quad (76)$$

and to obtain the rescaled function, $\tilde{\Delta}$, we can further set $m = \rho_m = 1$ and write

$$\tilde{\Delta}(w - w') = \int dj dj' P_{w,w'}(j,j')c(a_w(j))c(a_{w'}(j')). \quad (77)$$

1. Calculation of $\Delta(w)$ for class I

We define $a_1 := a_w(j)$, $a_2 := a_{w'}(j)$, $a_3 := a_{w'}(j')$. Given the previous remark to compute the cumulants we can set

$$j - w = \ln a_1, \quad j - w' = \ln a_2, \quad (78)$$

$$j' - w' = \ln a_3, \quad a_2/a_1 = e^{-W}, \quad (79)$$

where we denote $W = w' - w > 0$. The joint probability (71) then reads

$$P_{w;w'}(j,j')dj dj' = da_1(1 - e^{-W})da_3 e^{-a_1(1-e^{-W})-a_3}\theta(j' > j)$$
$$+ \delta(j' - j)dj'e^{-W}da_1 e^{-a_1}. \quad (80)$$

This yields the second moment

$$\overline{(w - j)(w' - j')}^c = [1 - e^{-W}]\int_0^\infty da_1 \int_{a_1 e^{-W}}^\infty da_3$$
$$\times \exp(-a_1[1 - e^{-W}] - a_3)\ln a_1 \ln a_3$$
$$+ e^{-W}\left[W\overline{w - j} + \overline{(w - j)^2}\right] - \left(\overline{w - j}\right)^2. \quad (81)$$

Note the integration interval for a_3 which corresponds to $j' > j$ using Eq. (79). We recall that

$$\overline{w - j} = -\int_0^\infty da e^{-a}\ln a = \gamma_E, \quad (82)$$

$$\overline{(w - j)^2} = \int_0^\infty da e^{-a}(\ln a)^2 = \gamma_E^2 + \frac{\pi^2}{6}. \quad (83)$$

Thus we obtain

$$\tilde{\Delta}(W) = (1 - e^{-W})\int_0^\infty da_1 e^{-a_1(1-e^{-W})}\ln a_1$$
$$\times \int_{a_1 e^{-W}}^\infty da_3 e^{-a_3}\ln a_3 + e^{-W}\left(\gamma_E^2 + \frac{\pi^2}{6} + W\gamma_E\right) - \gamma_E^2. \quad (84)$$

The calculation is performed in Appendix B. The final result for the fixed-point function of class I is

$$\tilde{\Delta}(w) = \frac{w^2}{2} + \mathrm{Li}_2(1 - e^w) + \frac{\pi^2}{6} \quad (85)$$

where $\mathrm{Li}_n(z) = \sum_{k=1}^\infty z^k/k^n$. One can also use the alternative formula (B5). Another equivalent compact expression for the result is

$$\tilde{\Delta}(w) = \sum_{n=1}^\infty \frac{1 + nw}{n^2}e^{-nw}. \quad (86)$$

A numerical test is performed in Sec. V, see Fig. 11.

The behavior of the fixed-point function at small $w > 0$ is

$$\tilde{\Delta}(w) = \frac{\pi^2}{6} - w + \frac{w^2}{4} - \frac{w^3}{36} + \frac{w^5}{3600} - \frac{w^7}{211\,680} + O(w^9),$$

hence we confirm that *there is a cusp* and a power series expansion in $|w|$. The behavior at large w is easier obtained from Eq. (86) and reads

$$\tilde{\Delta}(w) = (w + 1)e^{-w} + \frac{1}{4}(2w + 1)e^{-2w} + \frac{1}{9}(3w + 1)e^{-3w}$$
$$+ O(e^{-4w}). \quad (87)$$

It is characteristic of short-ranged correlations in the force with an exponential decay.

2. Calculation of $\Delta(w)$ for class III

As for class I, we define $a_1 = a_w(j)$, $a_2 = a_{w'}(j)$, $a_3 = a_{w'}(j')$ with (attention: j is ahead of w)

$$j - w = a_1^{1/\alpha}, \tag{88}$$

$$j - w' = a_2^{1/\alpha}, \tag{89}$$

$$j' - w' = a_3^{1/\alpha}. \tag{90}$$

One must distinguish the cases $j > w'$ (then $j' > j$ is equivalent to $a_3 > a_2$ and $W = w' - w = a_1^{1/\alpha} - a_2^{1/\alpha}$) and $j < w'$, in which case $a_2 = 0$. There are thus two pieces for the part with $j' > j$,

$$d_1 := \overline{(j-w)(j'-w')}\big|_{j'=j}$$
$$= \int_w^{w'} dj \frac{da_1}{dj} e^{-a_1} \int_0^\infty da_3 e^{-a_3}(a_1 a_3)^{1/\alpha}$$
$$+ \int_{w'}^\infty dj \frac{d(a_1-a_2)}{dj} e^{-(a_1-a_2)} \int_{a_2}^\infty e^{-a_3}(a_1 a_3)^{1/\alpha}. \tag{91}$$

In the first integral the integration bounds over a_1 is from 0 to W^α and in the second the relation $w' - w = a_1^{1/\alpha} - a_2^{1/\alpha}$ holds. Hence one obtains

$$d_1 = \Gamma\left(1+\frac{1}{\alpha}\right) \int_0^{W^\alpha} da_1 a_1^{1/\alpha} e^{-a_1}$$
$$+ \int_{W^\alpha}^\infty da_1\left(1 - \frac{da_2}{da_1}\right) a_1^{1/\alpha} e^{-a_1+a_2} \Gamma\left(1+\frac{1}{\alpha}, a_2\right). \tag{92}$$

The second contribution $(j=j')$ is

$$d_2 := \overline{(j-w)(j'-w')}\big|_{j'=j}$$
$$= \int_{w'}^\infty dj \frac{da_2}{dj} e^{-a_1}(a_1 a_2)^{1/\alpha}$$
$$= \int_{W^\alpha}^\infty da_1 \frac{da_2}{da_1} e^{-a_1}(a_1 a_2)^{1/\alpha}. \tag{93}$$

One has for the disorder correlator

$$\widetilde{\Delta}(W) = d_1 + d_2 - \left(\int_0^\infty da_1 e^{-a_1} a_1^{1/\alpha}\right)^2. \tag{94}$$

Using $a_2 = (a_1^{1/\alpha} - W)^\alpha$, $da_2/da_1 = (1-wa_1^{-1/\alpha})^{\alpha-1}$, and the variable $y = a_2^{1/\alpha}$, $a_1^{1/\alpha} = y + W$, one finds

$$\widetilde{\Delta}(W) = -\Gamma\left(1+\frac{1}{\alpha}\right)\Gamma\left(1+\frac{1}{\alpha}, W^\alpha\right)$$
$$+ \alpha \int_0^\infty dy(y+W)e^{-(y+W)^\alpha}$$
$$\times \left[y^\alpha + e^{y^\alpha}\Gamma\left(1+\frac{1}{\alpha}, y^\alpha\right)[(y+W)^{\alpha-1} - y^{\alpha-1}]\right]. \tag{95}$$

Integration by part of the last term finally yields

$$\widetilde{\Delta}(w) = -\Gamma\left(1+\frac{1}{\alpha}\right)\Gamma\left(1+\frac{1}{\alpha}, w^\alpha\right) + w\Gamma\left(1+\frac{1}{\alpha}\right)e^{-w^\alpha}$$
$$+ \int_0^\infty dy e^{-(y+w)^\alpha + y^\alpha}\Gamma\left(1+\frac{1}{\alpha}, y^\alpha\right). \tag{96}$$

We recall that

$$\Gamma(a,x) = \int_x^\infty dz z^{a-1} e^{-z}. \tag{97}$$

Hence we find a fixed-point function continuously dependent on α, and $\zeta = 2 - 2/\alpha$ yielding a unique form for each value of $0 < \zeta < 2$.

The value at $w=0$ has a simple expression,

$$\widetilde{\Delta}(0) = \Gamma\left(1+\frac{2}{\alpha}\right) - \Gamma\left(1+\frac{1}{\alpha}\right)^2. \tag{98}$$

We find that the function $\widetilde{\Delta}(w)$ has a cusp with

$$-\Delta'(0^+) = \frac{\Gamma\left(1+\frac{1}{\alpha}\right)}{\alpha}. \tag{99}$$

Since there are *a priori* w^α terms (we recall $\alpha > 1$), we want to understand at which order the expansion in $|w|$ breaks down.

More explicit expressions can be obtained in special cases. For the box distribution, i.e., $\alpha=2$, we find

$$\widetilde{\Delta}(w) = \frac{e^{-w^2}}{4w}[2w - e^{w^2}\sqrt{\pi}(2w^2+1)\text{erfc}(w) + \sqrt{\pi}]$$
$$+ \frac{1}{2}\sqrt{\pi}\left[we^{-w^2} - \Gamma\left(\frac{3}{2}, w^2\right)\right], \tag{100}$$

which has a power series expansion in $|w|$ around $w=0$,

$$\widetilde{\Delta}(w) = \left(1 - \frac{\pi}{4}\right) - \frac{\sqrt{\pi}w}{4} + \frac{w^2}{3} - \frac{\sqrt{\pi}w^3}{24} - \frac{w^4}{30} + \frac{\sqrt{\pi}w^5}{120} + \frac{w^6}{210}$$
$$- \frac{\sqrt{\pi}w^7}{672} - \frac{w^8}{1512} + \frac{\sqrt{\pi}w^9}{4320} + \frac{w^{10}}{11880} + O(w^{11}). \tag{101}$$

Equation (100) together with Eq. (70) is checked numerically in Sec. V, see Fig. 11.

However for α noninteger the situation is more complicated. Despite the presence of w^α terms (we recall $\alpha > 1$), the one-sided second derivative at $\Delta''(0^+)$ seems to exists. Numerically one finds that for α noninteger, but close to 1, e.g., $\alpha=3/2$, the third derivative at 0 exists, but does not go to zero with a finite slope. Analytically, one obtains an expansion around $\alpha=1$, as

$$\widetilde{\Delta}(w) = \Delta_0(w) + (\alpha-1)\Delta_1(w) + O(\alpha-1)^2 \tag{102}$$

with

$$\Delta_0(w) = e^{-w}, \tag{103}$$

$$\Delta_1(w) = (w-2)\Gamma(0,w) + e^{-w}[-(w+2)\log(w) - 4],$$
(104)

with the incomplete Γ function defined in Eq. (97). Note that

$$\partial_w^2 \Delta_1(w) = -e^{-w}[w\log(w) + 1]$$

and the Taylor expansion of Eq. (104) around 0 is then

$$\Delta_1(w) = (-4 + 2\gamma) + (2-\gamma)w - \frac{w^2}{2} + \left[\frac{11}{36} - \frac{\ln(w)}{6}\right]w^3$$
$$+ \left[\frac{\ln(w)}{12} - \frac{13}{144}\right]w^4 + O(w^5),$$
(105)

whose logarithmic part can be summed up as

$$\Delta_1(w) = [2 - w - e^{-w}(w+2)]\ln(w) + \text{analytic in } |w|.$$
(106)

These expansions confirms that for the Weibull class at non-integer α the second derivative at 0^+, $\Delta''(0^+)$, exists, but not the third one.

Finally let us note that if ρ_m^{III} is scaled as α one should recover class I from the large-α limit of class III, i.e., one can indeed check from Eq. (79) and (109) that $\lim_{\alpha \to \infty} \alpha^2 \tilde{\Delta}^{\mathrm{III},\alpha}(w/\alpha) = \tilde{\Delta}^{\mathrm{I}}(w)$. [The indices refer to the class.] An example of the limit procedure is given below.

3. Calculation of $\Delta(w)$ for class II (Frechet)

We define again $a_1 = a_w(j)$, $a_2 = a_{w'}(j)$, $a_3 = a_{w'}(j')$ with

$$j - w = -a_1^{-1/\alpha},$$
(107)

$$j - w' = -a_2^{-1/\alpha},$$
(108)

$$j' - w' = -a_3^{-1/\alpha}.$$
(109)

One sees that j can only vary in the interval $[-\infty, w]$, and that $j' > j$ is equivalent to $a_3 > a_2$. As for Weibull, there are two pieces,

$$d_1 := \overline{(j-w)(j'-w')}\big|_{j'=j}$$
$$= \int_{-\infty}^{w} dj \frac{d(a_1 - a_2)}{dj} e^{-(a_1 - a_2)} \int_{a_2}^{\infty} da_3 e^{-a_3}(a_1 a_3)^{-1/\alpha},$$
(110)

where the relation $W = w' - w = a_2^{-1/\alpha} - a_1^{-1/\alpha}$ holds. This yields

$$d_1 = \int_0^{\infty} da_1 \left(1 - \frac{da_2}{da_1}\right) a_1^{-1/\alpha} e^{-a_1 + a_2} \Gamma\left(1 - \frac{1}{\alpha}, a_2\right).$$
(111)

The second contribution is

$$d_2 := \overline{(j-w)(j'-w')}\big|_{j'=j}$$
$$= \int_{-\infty}^{w} dj \frac{da_2}{dj} e^{-a_1}(a_1 a_2)^{-1/\alpha}$$
$$= \int_0^{\infty} da_1 \frac{da_2}{da_1} e^{-a_1}(a_1 a_2)^{-1/\alpha}.$$
(112)

One has for the disorder correlator

$$\tilde{\Delta}(W) = d_1 + d_2 - \left(\int_0^{\infty} da_1 e^{-a_1} a_1^{-1/\alpha}\right)^2.$$
(113)

Using the variable $y = a_1^{-1/\alpha}$, $a_2^{-1/\alpha} = y + W$, one finds

$$\tilde{\Delta}(W) = \alpha \int_0^{\infty} dy\, y(y+W)^{-\alpha} e^{-y^{-\alpha}}$$
$$+ \alpha \int_0^{\infty} dy\, y[y^{-1-\alpha} - (y+W)^{-1-\alpha}] e^{-y^{-\alpha} + (y+W)^{-\alpha}}$$
$$\times \Gamma\left(1 - \frac{1}{\alpha}, (y+W)^{-\alpha}\right) - \Gamma\left(1 - \frac{1}{\alpha}\right)^2.$$
(114)

As for the Weibull class, see Eq. (96), we can integrate by part the second term into

$$-\lim_{\Lambda \to \infty} \int_0^{\Lambda} dy\, e^{-y^{-\alpha} + (y+W)^{-\alpha}} \frac{d}{dy}\left[y\Gamma\left(1 - \frac{1}{\alpha}, (y+W)^{-\alpha}\right)\right]$$
$$+ \Lambda\Gamma\left(1 - \frac{1}{\alpha}\right),$$
(115)

where the last term comes from the upper bound in the partial integration, after putting $y \to \Lambda \to \infty$ there. Rewriting it as $\int_0^{\Lambda} dy\, \Gamma(1 - 1/\alpha)$, and using the fact that the first term in Eq. (114) cancels, we arrive at the simple final expression for the Frechet class,

$$\tilde{\Delta}(w) = -\Gamma\left(1 - \frac{1}{\alpha}\right)^2 + \int_0^{\infty} dy\left[\Gamma\left(1 - \frac{1}{\alpha}\right) - e^{-y^{-\alpha} + (y+w)^{-\alpha}}\Gamma\left(1 - \frac{1}{\alpha}, (y+w)^{-\alpha}\right)\right]. \quad (116)$$

We find a fixed-point function, which depends continuously on α, hence on $\zeta = 2 + 2/\alpha$ with a unique form for each value of ζ, in the domain $0 < \zeta < 2$.

We can obtain the small-w behavior easily from Eq. (114). The value at zero,

$$\tilde{\Delta}(0) = \Gamma\left(1 - \frac{2}{\alpha}\right) - \Gamma\left(1 - \frac{1}{\alpha}\right)^2,$$
(117)

is found consistent with the results from the previous section on the distribution of the critical force,

$$\overline{[w - u(w)]^n} = \rho_m^n \Gamma\left(1 - \frac{n}{\alpha}\right).$$
(118)

One sees that $\tilde{\Delta}(0)$ is defined for $\alpha > 2$ and diverges as $\alpha \to 2^+$. As discussed in the previous section this is because in the Frechet class the distribution of the critical force has

algebraic tails and an infinite nth moment for $\alpha \leq n$. We thus consider $\alpha > 2$. The fixed-point function has a cusp, with from Eq. (116),

$$-\widetilde{\Delta}'(0^+) = \frac{\Gamma(1 - 1/\alpha)}{\alpha}, \tag{119}$$

and a well-defined Taylor expansion in $|w|$,

$$\widetilde{\Delta}(w) = \Gamma\left(\frac{\alpha - 2}{\alpha}\right) - \Gamma\left(1 - \frac{1}{\alpha}\right)^2 + \frac{\Gamma\left(-\dfrac{1}{\alpha}\right)w}{\alpha^2} + \frac{\alpha w^2}{4\alpha + 2}$$

$$- \frac{(\alpha + 1)\Gamma\left(\dfrac{1}{\alpha}\right)w^3}{36\alpha + 24} + \frac{\alpha^3 \Gamma\left(3 + \dfrac{2}{\alpha}\right)w^4}{48[2\alpha(4\alpha + 9) + 9]}$$

$$+ \frac{\alpha^2(\alpha + 1)(\alpha^2 - 4)\Gamma\left(2 + \dfrac{3}{\alpha}\right)w^5}{240(15\alpha^2 + 32\alpha + 16)} + O(w^6). \tag{120}$$

The large-w behavior of the fixed-point function is quite different from the other classes. Indeed $\widetilde{\Delta}(w)$ decays to zero rather slowly for large w. This can be seen by writing

$$\widetilde{\Delta}(w) = t_1(w) + t_2(w) - \Gamma\left(1 - \frac{1}{\alpha}\right)^2,$$

$$t_1(w) = \int_0^\infty dy\, e^{-y^{-\alpha} + (y+w)^{-\alpha}} \int_0^{(y+w)^{-\alpha}} dt\, t^{-1/\alpha} e^{-t},$$

$$t_2(w) = \int_0^\infty dy\, \Gamma\left(1 - \frac{1}{\alpha}\right)[1 - e^{-y^{-\alpha} + (y+w)^{-\alpha}}]. \tag{121}$$

The leading term for large w comes from $t_1(w)$, via a series of approximations,

$$t_1(w) \approx \int_0^\infty dy\, e^{-y^{-\alpha} + (y+w)^{-\alpha}} \int_0^{(y+w)^{-\alpha}} dt\, t^{-1/\alpha}$$

$$= \frac{\alpha}{\alpha - 1} \int_0^\infty dy\, e^{-y^{-\alpha} + (y+w)^{-\alpha}} (w+y)^{1-\alpha}$$

$$\approx \frac{\alpha}{\alpha - 1} \int_0^\infty dy\, (w+y)^{1-\alpha} = \frac{w^{2-\alpha}\alpha}{(\alpha - 2)(\alpha - 1)}, \tag{122}$$

whereas $t_2(w)$ is of order $1/w^\alpha$ plus a constant, since one can simply expand the exponential function for large w. For $\alpha = 3$ the function $\widetilde{\Delta}(w)$ and the asymptotics Eq. (122) are plotted on Fig. 6.

IV. AVALANCHE-SIZE AND WAITING-TIME DISTRIBUTIONS

A. Avalanche-size distribution

Successive avalanches, or jumps, occur at a discrete set of $w = w_i$ such that $u(w_i^-) = j_i$ and $u(w_i^+) = j_i + s_i$, where $s = s_i > 0$ is
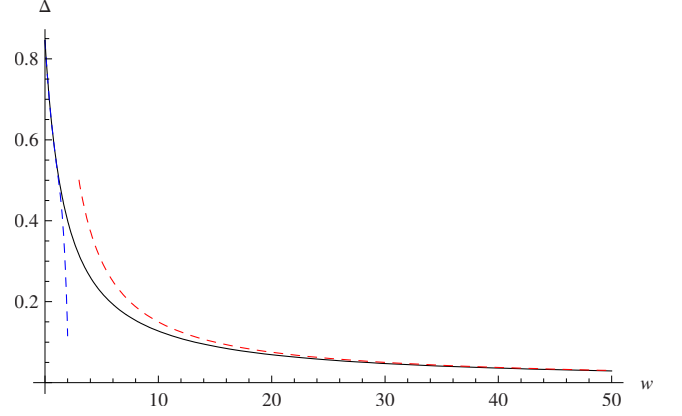

FIG. 6. (Color online) $\widetilde{\Delta}(w)$ from Eq. (116) for $\alpha = 3$ (bold). One clearly sees the long tail for $w \to \infty$. The asymptotic behavior for large w from Eq. (122) is shown (dashed and/or red) as the small-w expansion (blue and/or dashed).

the *size of the avalanche*. The *waiting time* between consecutive avalanches is denoted $W = w_i - w_{i-1}$. It is not properly a time, but we will term it here loosely waiting time since for a driving with a constant velocity it is the waiting time $t_w = W/v$, with here $v = 0^+$ (in that limit the jump time is negligibly shorter). Here we compute the joint distribution of avalanche sizes and waiting times. In Sec. V we discuss an algorithm to generate the sequence of avalanches and the Markov-chain property.

There are two useful probabilities for which the general expressions for the discrete model are easy to write. The first is, for $w' > w$,

$$P_w(j; w') := \text{Prob}\{u(w) = j \text{ and next avalanche is in } [w', \infty]\}. \tag{123}$$

When $u(w) = j$ the next avalanche occurs at $w'' > w$ such that $m^2(j - w'') = F_j$. Thus to realize $w'' > w'$ we need $F_j < m^2(j - w')$. Hence one has

$$P_w(j; w') = \{1 - H(m^2(j - w'))\} \prod_{k=-\infty}^{j-1} H(m^2(k - w)). \tag{124}$$

For $w = w'$, $P_w(j; w) = P_w(j)$ defined in Eq. (17). Of interest is the differential waiting-time distribution

$$P_w(w')dw' = -dw'\, \partial_{w'} \sum_{j=-\infty}^{\infty} P_w(j; w')$$

$$= \text{Prob(given } w, \text{ the next avalanche is in}$$

$$[w', w' + dw']). \tag{125}$$

The joint (integrated) probability is more involved,

$$P_w(j, w', S)dw' := \text{Prob}(u(w) = j \text{ and next avalanche is in}$$

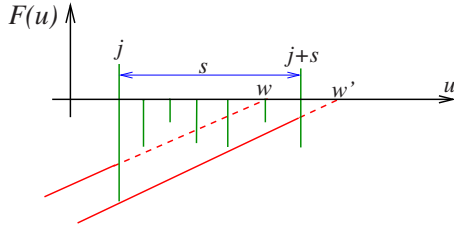$$[w', w' + dw'] \text{ and of size } s > S). \tag{126}$$

One has

FIG. 7. (Color online) Geometrical construction for the size of an avalanche

$$P_w(j, w', S) = \prod_{p=1}^{S} H(m^2(p + j - w'))(-\partial_{w'} P_w(j; w'))$$

(127)

and, of course, $P_w(j, w', S=0) = -\partial_{w'} P_w(j; w')$, i.e., the probability that $u(w)=j$ and that the next avalanche occurs at w' (per unit dw'). Of particular interest is

$$P_w(w', s > S) := \sum_j P_w(j, w', S)$$

$$= \text{Prob(next avalanche is in } [w', w' + dw'] \text{ and of size } s > S)$$

(128)

This is illustrated in Fig. 7.

We now consider the limit $m \to 0$ in which the continuum limit can be used, and extract the distributions of waiting times and avalanche sizes. We find that they depend on the same single scale ρ_m as defined in the previous sections. The waiting-time distribution is denoted below $P(w)$ [and sometimes $P(W)$], and has thus the scaling form

$$P(w) = \rho_m^{-1} \widetilde{P}(w/\rho_m).$$

(129)

However, to simplify notations, unless specified, we drop below the tilde on $\widetilde{P}$ and formally replace $\rho_m \to 1$ (formally, since all statements below are about scaling forms in the limit $m \to 0$). When no confusion is possible we use the symbol w for either the argument of $u(w)$ and the waiting time $w = w_i - w_{i-1}$, and use W for the waiting time when confusion is possible. Similarly the avalanche-size distribution is loosely noted with the same symbol,

$$P(s) = \rho_m^{-1} \widetilde{P}(s/\rho_m)$$

(130)

and we perform the same simplification in notations, and similarly for the joint distribution. The dependence on ρ_m can be restored by replacing in the final formulas

$$j \to \frac{j}{\rho_m},$$

(131)

$$w \to \frac{w}{\rho_m}, \quad s \to \frac{s}{\rho_m},$$

(132)

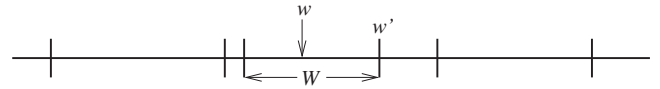similarly for S and W, and correcting the normalizations of probabilities to 1.

FIG. 8. The probability $P_w(w')$ to have a point w in the interval of size W preceding w'.

B. Waiting-time distribution

Using the method introduced in the previous section, see especially Eq. (21)ff, one finds that the continuum limit for the probability $P_w(j; w')$ is

$$P_w(j; w') dj = da_{w'}(j) e^{-a_w(j)},$$

(133)

and we use again the notation $a_1 = a_w(j)$ and $a_2 = a_{w'}(j)$.

1. Class I (Gumbel)

We recall Eq. (75) for class I,

$$j - w = -f_c^0 + \ln a_1,$$

$$j - w' = -f_c^0 + \ln a_2,$$

(134)

where f_c^0 is a nonfluctuating constant, and as in Eq. (79) $a_2 = e^{-W} a_1$. Thus one finds

$$P_w(j; w') dj = e^{-W} da_1 e^{-a_1}.$$

(135)

Integrating over a_1 in $[0, \infty[$ one obtains

$$P_w(w') = \theta(w' - w) e^{w-w'}.$$

(136)

From Eq. (136) we can infer the distribution $P(W)$ of waiting times W. Since the probability that a uniformly chosen w on the real axis falls in an interval of size W is $WP(W)/\int dW WP(W)$ (see Fig. 8), and that then the probability of of $w' - w$ is uniform, i.e., $\theta(0 < w' - w < W)/W$, multiplying the two expressions one finds the general relation

$$\frac{\int_{w'-w}^{\infty} dW P(W)}{\int_0^{\infty} dW W P(W)} = P_w(w').$$

(137)

This is true only in the small-m limit (because of uniform measure assumption). For any member of class I we find the distribution of "waiting time" W (restoring the dependence on ρ_m),

$$P(W) = \rho_m^{-1} e^{-W/\rho_m}.$$

(138)

2. Class III (Weibull)

Let us consider now class III. One has, following the notation in Sec. III D 2,

$$j - w = -f_c^0 + a_1^{1/\alpha},$$

(139)

$$j - w' = -f_c^0 + a_2^{1/\alpha}.$$

(140)

Using the variable $y > 0$ such that $a_2^{1/\alpha} = y$ and $a_1^{1/\alpha} = y + W$ one now finds from Eq. (133)

$$P_w(j; w') dj = \alpha y^{\alpha - 1} e^{-(y + W)^\alpha} dy. \qquad (141)$$

Integrating with respect to y, taking $-\partial_{w'}$ and integrating by part we obtain

$$P_w(w') = \alpha(\alpha - 1) \int_0^\infty dy\, y^{\alpha - 2} e^{-(y + w' - w)^\alpha}. \qquad (142)$$

We recall that $\alpha > 1$, hence the integral is always convergent. From Eq. (137) we obtain

$$\langle W \rangle^{-1} = P_w(w) = \alpha \Gamma\left(2 - \frac{1}{\alpha}\right) \qquad (143)$$

and, taking $-\partial_{w'}$ on both sides of Eq. (137) we obtain for class III

$$P(W) = \frac{\alpha(\alpha - 1)}{\Gamma\left(2 - \frac{1}{\alpha}\right)} \int_0^\infty dy\, y^{\alpha - 2} (y + W)^{\alpha - 1} e^{-(y + W)^\alpha}. \qquad (144)$$

If $\alpha > 2$ it can be integrated by part into

$$P(W) = \frac{(\alpha - 1)(\alpha - 2)}{\Gamma\left(2 - \frac{1}{\alpha}\right)} \int_0^\infty dy\, y^{\alpha - 3} e^{-(y + W)^\alpha}. \qquad (145)$$

For completeness let us give the result for $\alpha = 2$, which corresponds to a box distribution for the forces

$$P_w(w') = \sqrt{\pi}\, \mathrm{erfc}(W), \qquad (146)$$

$$P(W) = \frac{2}{\sqrt{\pi}} e^{-W^2} \theta(W), \qquad (147)$$

which is a simple one-sided Gaussian.

3. Class II (Fréchet)

Let us consider now class II (Frechet). One has

$$j - w = -a_1^{-1/\alpha}, \qquad (148)$$

$$j - w' = -a_2^{-1/\alpha}. \qquad (149)$$

Using the variable $y > 0$ such that $a_1^{-1/\alpha} = y$ and $a_2^{-1/\alpha} = y + W$ one now finds from Eq. (133)

$$P_w(j; w') dj = \alpha(y + W)^{-\alpha - 1} e^{-y^{-\alpha}} dy. \qquad (150)$$

Integrating with respect to y, taking $-\partial_{w'}$ we obtain

$$P_w(w') = \alpha(\alpha + 1) \int_0^\infty \frac{dy}{(y + W)^{2 + \alpha}} e^{-y^{-\alpha}}. \qquad (151)$$

We recall that $\alpha > 0$ hence the integral is always convergent. From Eq. (137) we obtain

$$\langle W \rangle^{-1} = P_w(w) = \alpha \Gamma\left(2 + \frac{1}{\alpha}\right). \qquad (152)$$

Deriving again Eq. (137) with respect to W, we obtain

$$P(W) = \frac{(\alpha + 1)(\alpha + 2)}{\Gamma\left(2 + \frac{1}{\alpha}\right)} \int_0^\infty \frac{dy}{(y + W)^{3 + \alpha}} e^{-y^{-\alpha}}. \qquad (153)$$

One easily checks that Eq. (153) is correctly normalized.

C. Joint avalanche-size and waiting-time distribution

The continuum limit of Eq. (127) can be written as

$$P_w(j, w', S) dj = [-\partial_{w'}(da_2 e^{-a_1})] e^{-a_3 + a_2}, \qquad (154)$$

where we use the same notations $a_w(j) = a_1$, $a_{w'}(j) = a_2$ as above and in addition $a_{w'}(j' = j + S) = a_3$. We remind the reader that in order to include ρ_m, S is rescaled as j and w.

1. Class I (Gumbel)

Consider now class I. In addition to Eq. (134) one has

$$j + S - w' = -f_c^0 + \ln a_3. \qquad (155)$$

Hence we have $a_2 = e^{-W} a_1$ and $a_3 = e^{-W - S} a_1$ where

$$P_w(j, w', S) dj = [-\partial_{w'} e^{-W}(da_1 e^{-a_1})] e^{-a_1 e^{-W}(e^S - 1)}$$
$$= e^{-W} da_1 \exp(-a_1 [1 + e^{-W}(e^S - 1)]). \qquad (156)$$

Integrating over j and a_1, respectively, we obtain the joint distribution

$$P_w(w', s > S) = \theta(w' - w) \frac{1}{e^{w' - w} + e^S - 1}. \qquad (157)$$

Again this is the probability that if one observes the system at w, the next avalanche occurs at w' *and* has size $s > S$. This allows one to find the joint probability $P^+(W, s > S)$ that $w_{n+1} - w_n = W$ and the *next* avalanche is $s_{n+1} > S$ (see Appendix E for further notations and definitions). Indeed one has, by the same reasoning as above,[1]

$$\frac{\int_{w' - w}^\infty dW\, P^+(W, s > S)}{\int_0^\infty dW\, W P^+(W, 0)} = P_w(w', s > S). \qquad (158)$$

This yields for class I

$$P^+(W, s > S) = \frac{e^W}{(e^W + e^S - 1)^2}. \qquad (159)$$

Integrating over W this yields the cumulative joint waiting-time and avalanche-size distribution for class I,

$$P(w > W, s > S) = \frac{1}{\exp(W) + \exp(S) - 1}. \qquad (160)$$

Setting $W = 0$ gives the (rescaled) avalanche-size distribution for class I

---

[1]Note one could also imagine to divide by $\int_0^\infty dW\, W P^+(W, s > S)$, but this is wrong.

$$P(s) = e^{-s}, \quad P(s > S) = e^{-S}. \tag{161}$$

Setting $S=0$, and deriving with respect to W reproduces the waiting-time distribution (138). We thus obtain that the avalanche exponent, such that $P(s) \sim s^{-\tau}$ at small $1 \ll s \ll \rho_m$, is here $\tau=0$. We can give the lowest moments,

$$\langle ws \rangle = \frac{\pi^2}{6} \approx 1.64493, \tag{162}$$

$$\langle w \rangle = \langle s \rangle = 1, \tag{163}$$

$$\langle w^2 \rangle = \langle s^2 \rangle = 2, \tag{164}$$

in units of ρ_m. We also note that the relation

$$\frac{\langle s^2 \rangle}{\langle s \rangle} = -2\Delta'(0^+) \tag{165}$$

is obeyed, using $\tilde{\Delta}'(0^+) = -1$ from Eq. (87). This relation between the cusp and the second moment holds quite generally [61] and is used here as a useful check.

2. Class III (Weibull)

Consider now class III, i.e., Eq. (140) and

$$j + S - w' = -f_c^0 + a_3^{1/\alpha}. \tag{166}$$

This leads to

$$P_w(j, w', S) dj = \left[-\partial_{w'} \frac{da_{w'}(j)}{dj} dj e^{-a_{w(j)}} \right] e^{-a_{w'}(j+S) + a_{w'}(j)}. \tag{167}$$

Now setting as before $y = a_2^{1/\alpha} = j - w'$, the only derivative in the bracket to be taken is of the variable y, i.e., $-\partial_{w'} y = 1$. In short hand this gives

$$P_w(j, w', S) dj = -\partial_{w'} \alpha y^{\alpha-1} dy e^{-(y+W)^\alpha - (y+S)^\alpha + y^\alpha}$$
$$= \alpha(\alpha-1) y^{\alpha-2} dy e^{-(y+W)^\alpha - (y+S)^\alpha + y^\alpha}. \tag{168}$$

Integrating over y (i.e., j) it yields

$$P_w(w', s > S) = \alpha(\alpha-1) \int_0^\infty dy\, y^{\alpha-2} e^{-(y+W)^\alpha - (y+S)^\alpha + y^\alpha}. \tag{169}$$

The final result for the joint probability for class III takes the form

$$P^+(W, s > S) = \frac{\alpha}{\Gamma\left(1 - \frac{1}{\alpha}\right)} (-\partial_W) \int_0^\infty dy [y^{\alpha-2}$$
$$\times e^{-(y+W)^\alpha - (y+S)^\alpha + y^\alpha}]. \tag{170}$$

Integrating over W yields the (rescaled) cumulative distribution for class III,

$$P(w > W, s > S) = \frac{\alpha}{\Gamma\left(1 - \frac{1}{\alpha}\right)} \int_0^\infty dy\, y^{\alpha-2} e^{-(y+W)^\alpha - (y+S)^\alpha + y^\alpha}. \tag{171}$$

Setting $W=0$, we obtain the avalanche-size distribution,

$$P(s > S) = \frac{\alpha}{\Gamma\left(1 - \frac{1}{\alpha}\right)} \int_0^\infty dy\, y^{\alpha-2} e^{-(y+S)^\alpha}. \tag{172}$$

On the other hand, setting $S=0$ in Eq. (171) gives back the waiting-time distribution (144).

Let us comment on these results. Since Eq. (172) can be Taylor expanded in S around $S=0$, it is clear that for class III also the avalanche exponent is again $\tau=0$. For large S, the decay of Eq. (172) is $P(s > S) \sim P(S) \sim \exp(-S^\alpha)$, i.e., a stretched exponent decay with exponent $\delta=\alpha$. Next, one checks that the general relation involving the cusp is obeyed,

$$\frac{\langle s^2 \rangle}{\langle s \rangle} = \frac{\Gamma\left(2 + \frac{1}{\alpha}\right)}{\alpha} \rho_m = -2\Delta'(0^+), \tag{173}$$

using Eq. (99), a useful check on our calculations.

One can also obtain simple expressions for the lowest moments (in units of ρ_m),

$$\langle s \rangle = \langle w \rangle = \frac{1}{\alpha\Gamma\left(2 - \frac{1}{\alpha}\right)}, \tag{174}$$

$$\langle sw \rangle = \frac{\Gamma\left(1 + \frac{1}{\alpha}\right) H_{-1/\alpha}}{\Gamma\left(-\frac{1}{\alpha}\right)} \tag{175}$$

as a function of the harmonic number $H_n = \sum_{k=1}^n 1/k$, i.e., $H_{-1/\alpha} := \gamma_E + \psi(1 - 1/\alpha)$, $\psi(x) := \Gamma'(x)/\Gamma(x)$. From these one can construct a fully universal dimensionless ratio,

$$\frac{\langle sw \rangle}{\langle s \rangle \langle w \rangle} = -\frac{\pi(\alpha-1)^2 H_{-1/\alpha}}{\alpha^2 \sin\left(\frac{\pi}{\alpha}\right)}. \tag{176}$$

Finally one can check that for $\alpha \to \infty$, one recovers class I distribution (160). More precisely

$$\lim_{\alpha \to \infty} P(w > W/\alpha, s > S/\alpha)$$
$$= \lim_{\alpha \to \infty} \frac{1}{\Gamma\left(2 - \frac{1}{\alpha}\right)} \int_0^\infty dx\, x^{-1/\alpha} \exp\left(-x\left[\left(1 + \frac{W}{\alpha x^{1/\alpha}}\right)^\alpha\right.\right.$$
$$\left.\left. + \left(1 + \frac{S}{\alpha x^{1/\alpha}}\right)^\alpha - 1\right]\right) \tag{177}$$

$$= \int_0^\infty dx \exp(-x[e^W + e^S - 1]) = (160), \qquad (178)$$

where we have used $x = y^\alpha$ as variable and $\lim_{\alpha \to \infty}(1 + W/\alpha)^\alpha = \exp(W)$ and that the factors of $x^{1/\alpha}$ could be dropped.

3. Class II (Fréchet)

Consider now class II, i.e., Eq. (140) and

$$j + S - w' = -\rho_m a_3^{-1/\alpha}, \qquad (179)$$

hence $S = a_2^{-1/\alpha} - a_3^{-1/\alpha} = y + W - a_3^{-1/\alpha}$. This leads to

$$P_w(j, w', S)dj = [-\partial_{w'}\alpha(y + W)^{-\alpha-1}dye^{-y^{-\alpha}}]$$
$$\times e^{(y+W)^{-\alpha} - (y+W-S)^{-\alpha}}$$
$$= \alpha(\alpha + 1)(y + W)^{-\alpha-2}dye^{-y^{-\alpha}}$$
$$\times e^{(y+W)^{-\alpha} - (y+W-S)^{-\alpha}}. \qquad (180)$$

The domain of integration depends on whether $W > S$ or $S > W$, and can be expressed as

$$P_w(w', s > S) = \alpha(\alpha + 1)\int_{\max(0, S-W)}^\infty \frac{dy}{(y + W)^{\alpha+2}}$$
$$\times e^{-y^{-\alpha} + (y+W)^{-\alpha} - (y+W-S)^{-\alpha}} \qquad (181)$$

$$= \alpha(\alpha + 1)\int_{\max(W,S)}^\infty \frac{dy}{y^{\alpha+2}}$$
$$\times e^{-(y-W)^{-\alpha} - (y-S)^{-\alpha} + y^{-\alpha}}. \qquad (182)$$

This translates with the same arguments as for Eq. (171) into

$$P(w > W, s > S) = \frac{\int_{\max(W,S)}^\infty \frac{dy}{y^{\alpha+2}}e^{-(y-W)^{-\alpha} - (y-S)^{-\alpha} + y^{-\alpha}}}{\int_0^\infty \frac{dy}{y^{\alpha+2}}e^{-y^{-\alpha}}}. \qquad (183)$$

As for the Weibull and Gumbel universality classes, this expression is symmetric in S and W. We therefore conclude that for all three classes

$$P(w) = P(s). \qquad (184)$$

This property is proved with slightly more general argument in Appendix D. It is of course valid only for the *rescaled distributions* in the limit $m \to 0$ in the sense described above (at the level of the discrete model w is a continuous variable while s is discrete).

The resulting distribution of (rescaled) avalanche size thus reads

$$P(s) = \frac{(\alpha + 1)(\alpha + 2)}{\Gamma\left(2 + \frac{1}{\alpha}\right)}\int_0^\infty \frac{dy}{(y + s)^{3+\alpha}}e^{-y^{-\alpha}} \qquad (185)$$
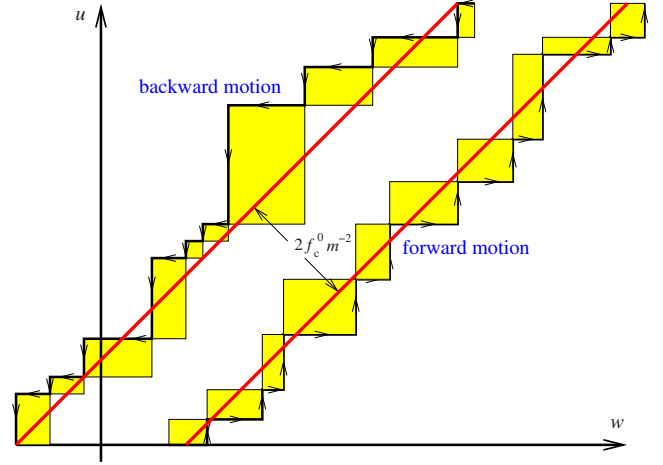
with (in units of ρ_m)

FIG. 9. (Color online) The plot shows $u(w)$ for the forward motion with $m^2\langle w - u\rangle = f_c$, and the backward motion with $m^2\langle u - w\rangle = f_c$. Both trajectories are indicated with arrows. The world line $u(w)$ fluctuates around $w \pm f_c^0 m^{-2}$. These fluctuations have a geometrical interpretation as the yellow and/or shaded region, whose area is related to the expectation $\langle ws\rangle$.

$$\langle s\rangle^{-1} = \alpha\Gamma\left(2 + \frac{1}{\alpha}\right), \qquad (186)$$

$$\langle s^2\rangle/\langle s\rangle = \frac{-2\Gamma(-1/\alpha)}{\alpha^2} = -2\Delta'(0^+), \qquad (187)$$

the last equality being a check, using Eq. (119). Note that $P(s)$ has power-law decay for *large* s, i.e., $P(s) \approx s^{-(2+\alpha)}$. The avalanche exponent however is still $\tau = 0$, since it is related to *small* avalanches (i.e., $s \ll \rho_m$). The Frechet class yields to a cutoff for large avalanches (i.e., $s \gg \rho_m$) which is itself a power law.

4. Local fluctuations of the area of the hysteresis loop

Figure 9 illustrates a typical hysteresis loop for uncorrelated random force landscape, for convenience assumed to have a symmetric distribution $P(-f) = P(f)$. The plot shows $u(w)$ for the forward motion with $m^2\langle w - u\rangle = f_c > 0$ (disorder or translational averages) and the backward motion $m^2\langle u - w\rangle = f_c$. Both curves $u(w)$ fluctuate around $w \pm f_c^0/m^2$, and the enclosed area A of the hysteresis loop exhibits a uniform part $\bar{A} = 2|f_c^0(m)|w$, computed in Sec. III C for each class, plus a fluctuating part $\tilde{A}$,

$$A = \bar{A} + \tilde{A}, \quad \tilde{A} = m^2\sum_i w_i s_i. \qquad (188)$$

It has a geometrical interpretation as the area of the yellow and/or shaded region. Its average value per unit length over a large sample $w \in [0, M]$ is

$$\frac{1}{M}\langle\tilde{A}\rangle = m^2\frac{\langle ws\rangle}{\langle s\rangle}, \qquad (189)$$

since the number of avalanches is $\Sigma_i = N$, $\Sigma_i s_i = M$ hence $\langle s\rangle = M/N$. Note in passing that one has also $\Sigma_i w_i = M$, hence
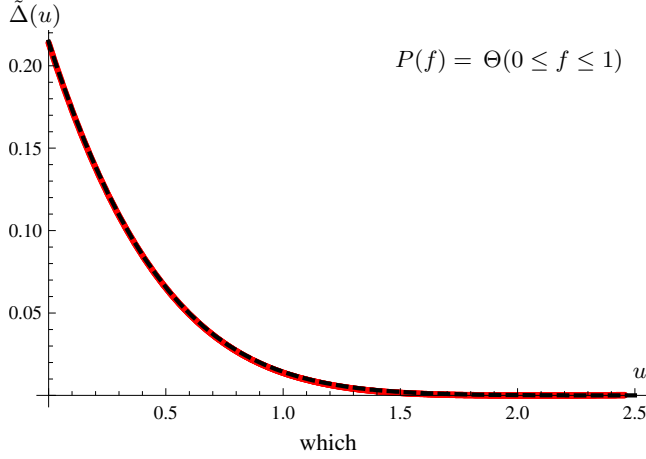
FIG. 10. (Color online) Numerically calculated $\tilde{\Delta}(u)$ as a function of u (red, fat) for the box distribution $P(f)=\Theta(f)\Theta(1-f)$, and comparison with analytical result (black, dashed) from Eq. (100); $\tilde{A}=1$, $\tilde{\alpha}=0$, $A=1/2$, $\rho_m=\sqrt{2}/m$, $m^2=10^{-5}$; there is no adjustable parameter.

$\langle s\rangle=\langle w\rangle$, i.e., the first moments of s and w are always equal. (We neglect boundary contributions which for uncorrelated disorder scale subdominantly.) Similarly one can consider the moments of the local hysteresis area,

$$\frac{1}{M}\sum_i (w_i s_i)^p = \frac{\langle (ws)^p\rangle}{\langle s\rangle}. \tag{190}$$

They can be obtained from the moments of the variable $a=ws$. Hence it is useful to compute the distribution of this variable for the three classes. This is performed in Appendix D.

Let us give the result for the (rescaled) distribution of the Gumbel class,

$$P(a>A) = \int_0^\infty dx \frac{e^x}{(e^x+e^{A/x}-1)^2} = \int_1^\infty dy \frac{1}{(y+e^{A/\ln(y)}-1)^2}, \tag{191}$$

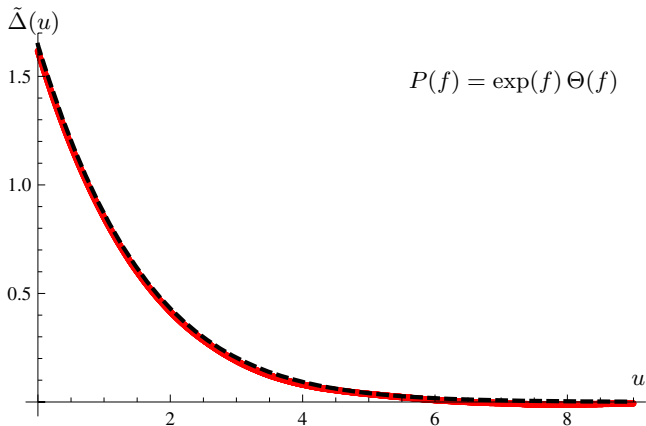from which we give some moments,

FIG. 11. (Color online) $\tilde{\Delta}(u)$ as a function of u for the exponential distribution (red, fat), and comparison with analytical result from Eq. (85) (black, dashed); $\rho_m^{-1}=m^2=0.003$, no adjustable parameter.
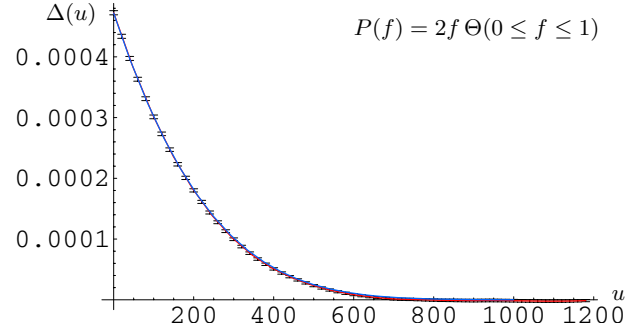

FIG. 12. (Color online) $\Delta(u)$ vs u for $\alpha=3$ (Weibull class); $m^2=0.0001$. No adjustable parameter. Red is data with error bars. Blue is the analytic solution (96) for $\alpha=3$. The other parameters used in Eq. (50)ff are $\tilde{A}=1/\gamma$ and $\tilde{\alpha}=\frac{1}{\gamma}-1$. We have chosen $\gamma=1/2$ as an example, hence $\tilde{\alpha}=1$, $\alpha=3$, $\tilde{A}=2$, $A=\frac{1}{3}$. We use $m^2=0.0001$, with 10^7 disorder points. One finds f_c/m^2: -599.8 (numerics) versus -597.79 (analytic). The parameter free numerical result for $\Delta(u)$ is compared with the analytical one, and found in excellent agreement.

$$\langle a\rangle = 1.64493, \quad \langle a^2\rangle = 18.3995,$$

$$\langle a^3\rangle = 547.343, \quad \langle a^4\rangle = 30\,764.6, \tag{192}$$

measured in units of ρ_m^2.

V. NUMERICS FOR THE TOY MODEL

A. Basic definitions

In this section we study numerically the discrete model of the last section. We consider the following four different disorder distributions:

(i) Box:

$$P_1(f) = 1 \quad \text{if } f \in [0,1], \text{ and } 0 \text{ else.} \tag{193}$$

(ii) Exponential:

$$P_2(f) = \exp(f) \quad \text{if } f>0 \text{ and } 0 \text{ else.} \tag{194}$$

(iii) Random bond (RB): Short-ranged correlated potential. The resulting force at site i is $f_i=e_i-e_{i+1}$ where the energies e_i are uncorrelated random variables distributed with the box distribution $P_1(e)$. We call this distribution $P_3(f)$.

(iv) Class III with $\alpha=3$:

$$P_4(f) = 2f\Theta(0\leq f\leq 1). \tag{195}$$

Note that power-law-distributed forces can be generated by defining $f := x^\gamma$, with $x\in[0,1]$ uniformly distributed. This yields

$$P(f) = \frac{1}{\gamma}f^{1/\gamma-1}\Theta(0\leq f\leq 1), \tag{196}$$

with $\gamma=1/2$ for Eq. (195).

We integrate numerically the equation of movement (8), first at $\eta=0$. This is the discrete model defined in Sec. III A. In practice, for given w, we move the particle as long as the
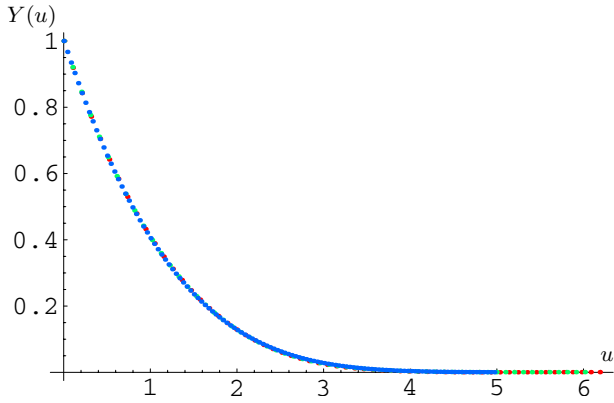
FIG. 13. (Color online) *Rescaled* disorder correlator: The function $Y(u)$ is the rescaled version of $\Delta(u)$ such that $Y(0)=1$ and $\int_u Y(u)=1$. The data is the same as on Figs. 10 and 11 with in addition RB disorder (i.e., random potential): Blue is the box distribution in [0,1], red the exponential, green is RB. This shows that for $m=0.003$ the different microscopic disorders yield very similar rescaled correlators, although the unrescaled ones are different. For the difference between rescaled disorders see Fig. 14.

force, i.e., the right-hand side of Eq. (8) is positive. The point at which we stop defines $u(w)$. We then update $w \to w+1$. This is an approximation to the process defined in Sec. III A, but since jumps as well as waiting times diverge when $m \to 0$, the scaling limit is the same. A second algorithm, described in Appendix C, was used to independently compute $P(w)$ and $P(s)$ (not shown), and check the present results.

B. $\Delta(w)$

We have shown on Figs. 10–12 comparisons between the numerically computed functions $\Delta(u)$ and the analytical predictions. The corresponding analytical results are referenced in the corresponding captions. Hence there is *no adjustable parameter* in Figs. 10–12 and the agreement is excellent.

A general important question at depinning is whether the random bond class (i.e., uncorrelated potentials) flows to the random field one (uncorrelated forces). This appears clearly in Fig. 13, where we plot the rescaled (as explained in the caption) $\Delta(u)$, for the three disorders $P_1(f)$, $P_2(f)$, and $P_3(f)$, defined in Eq. (193) ff. The crossover as the mass decreases from RB disorder to the random-force (RF) disorder can also nicely be seen in our simulations, presented on Fig. 2. One expects that the random short-ranged energy model, i.e., $f_i = e_i - e_{i+1}$ with e_i distributed with $P_{RB}(e)$ should flow to the random-force model with $P(f) = \int_e P_{RB}(f+e)P_{RB}(e)$, i.e., the convolution of $P_{RB}(e)$ and $P_{RB}(-e)$. This is because the rare large forces are isolated and become uncorrelated. This predicts that the box distribution for e should flow to the $\alpha=3$ class III.

We have seen on Fig. 13 that the *shapes* of the correlator functions $\Delta(u)$ (i.e., their rescaled form as explained in the caption) are rather similar for the various universality classes, while their unrescaled forms are very different. These rescaled forms obtained from the analytical calculations are compared in Fig. 14.
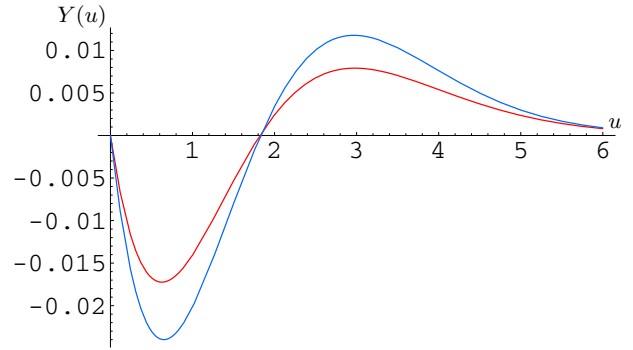

FIG. 14. (Color online) Comparison of the analytical results for the various classes. The function $Y(u)$ is the rescaled version of $\Delta(u)$ such that $Y(0)=1$ and $\int_{u>0} Y(u)=1$. Plotted here are the (small) differences $Y_I(x) - Y_{III,2}(x)$ (red) and $Y_I(x) - Y_{III,3}(x)$ (blue). The index refers to class, and α. This explains why the various classes are very close on Fig. 13.

C. Shocks and avalanches

In Fig. 1 we have shown the avalanches, also called dynamical shocks: As a function of w, we plot $w - u_w$ (minus its average), for different masses. First consider the smallest mass, $m^2 = 0.03$. We see that $w - u_w$ is growing linearly with w, before it jumps. The linear parts are those, at which the particle is localized by a large disorder force, before jumping (in zero time at $\eta v = 0$) to a new position (vertical parts). When decreasing the mass, we see that the linear parts, i.e., the "time" (i.e., distance in w) between jumps, as well as the jumps itself become larger, while sharing parts of their trajectories. This can be interpreted as merging of the (dynamical) shocks.

In Fig. 15 we show the avalanche-size and waiting-time distributions for $P(f)$ being the box distribution. It clearly shows that avalanche-size and waiting-time distributions are
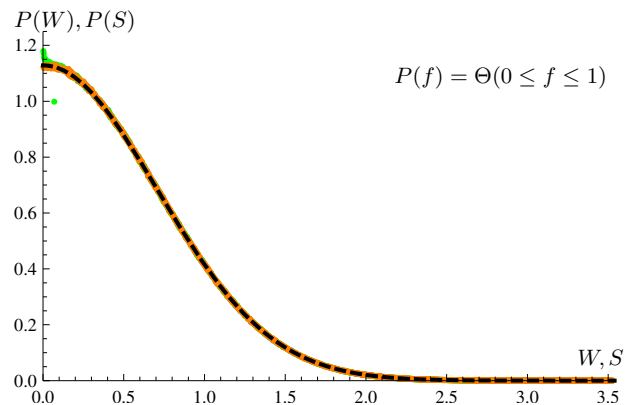

FIG. 15. (Color online) $P(W)$ (orange dots) and $P(S)$ (green dots) as a function of W and S, respectively, for the box distribution $P(f) = \Theta(f)\Theta(1-f)$, and comparison with analytical result (black, dashed) from Eq. (100); $\tilde{A}=1$, $\tilde{\alpha}=0$, $A=1/2$, $\rho_m = \sqrt{2}/m$, $m^2 = 10^{-5}$; there is no adjustable parameter. One sees that the two distributions are identical, with $P(W)$ plotted on top of $P(S)$. However for small avalanche sizes S, the numerics has not yet converged against the analytical result, i.e., finite-size corrections are present and visible on the plot.
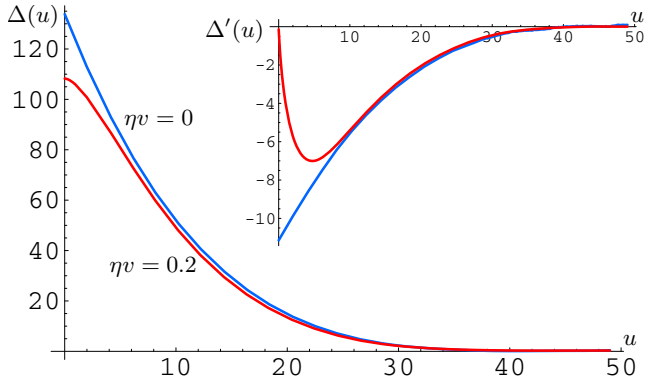
FIG. 16. (Color online) Rounding of $\Delta(u)$ through a finite velocity; $\eta v = 0.2$. Inset: $\Delta'(u)$. The disorder distribution is $P(f) = \Theta(0 \leq f \leq 1)$, $m^2 = 0.003$.

identical, as follows for all disorder classes from Eq. (D3). Moreover, the result is in agreement with the parameter free prediction of Eq. (172), using ρ_m defined in Eq. (59).

D. Finite velocity

In this section, we consider the equation of motion at finite velocity v, or rather at finite ηv, since the latter is the parameter entering all equations.

The algorithm for finite ηv is as follows: We generalize the position $u_t \equiv u(w_t)$ of the point to now take noninteger values. It follows the Langevin equation

$$\eta \frac{d}{dt} u_t = f_{[u_t]} + m^2(u_t - w_t) \tag{197}$$

where

$$[u] := \text{largest integer} \leq u. \tag{198}$$

Condition (198) reflects that the disorder only changes at discrete values of u.

In practice, we discretize (197) with a step size $\delta t = 1/100$, integrating this discretized equation of motion in time following the Itô scheme, and using $w_t = vt$,

$$\eta[u_{t+\delta t} - u_t] = \delta t[f_{[u_t]} + m^2(u_t - w_t)]. \tag{199}$$

To guarantee that our time discretization is fine enough, we report "maxslide," the maximum of Eq. (199) encountered in a simulation. For the simulation shown on Fig. 16, this was 0.05. The figure shows $\Delta(u)$ at $\eta v = 0$, calculated with the discrete algorithm used in the previous sections, and $\Delta(u)$ at $\eta = 1$ and $v = 0.2$. The microscopic disorder is a box distribution for the force, given by Eq. (193). The result clearly shows a *rounding of the cusp* by the nonzero velocity.

VI. LONG-RANGE CORRELATED FORCES

In addition to the three universality classes for short-range (SR) correlated forces, there is also a family of universality classes for long-range (LR) correlated forces. Consider a Gaussian distributed force landscape with no bias $\overline{F(u) - F(u')} = 0$ and second moment,
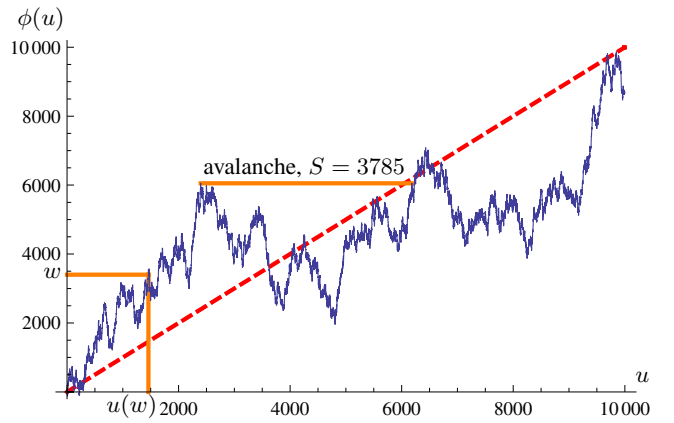

FIG. 17. (Color online) $\phi(u)$ defined in Eq. (201) for f a random walk with $D = 1.67 \times 10^3$ (blue). The dashed (red) line denotes $\phi(u) = u$. We show explicitly the graphical construction of $u(w)$ for $w = 3400$, as well as a larger avalanche of size $S = 3785$. The system is discretized with step size 1 in u direction.

$$\overline{[F(u) - F(u')]^2} = 2\sigma|u - u'|^\gamma. \tag{200}$$

We focus on $\gamma = 1$, i.e., a Brownian-force landscape, but one expects a continuously varying fixed point as a function of γ. Although in most cases random-force landscapes at depinning have short-ranged correlations, these more exotic LR landscapes exhibit some interesting properties. Note that *in the statics* the (very) LR correlated random potential landscape corresponding to the case $\gamma = 1$ was studied by Sinai [71]. It was found that shocks are dense there.

Quite remarkably, exact results can be obtained for this model for any nonzero velocity $v > 0$, as noticed by Alessandro, Beatrice, Bertotti, and Montorsi [66] who introduced this model, hence referred to as the ABBM model, as a realistic description of the Barkhausen effect in metallic ferromagnets, and compared the results to experiments. The mass term originates from the magnetostatic fields: the demagnetizing field (resulting from the effective monopoles sitting at the end of the sample) provides a long-ranged restoring force which acts as a spring, precisely as in the model considered in this paper (see also discussions in Refs. [2,72]).

We first obtain some results on the quasistatic model, then we recall some results of the ABBM analysis at $v > 0$, and obtain from it the renormalized correlator at nonzero velocity. We then discuss how these results match at $v \to 0^+$.

A. Quasistatic motion

The forward process $u = u(w)$ is defined as the *smallest* root of

$$\phi(u) = u - m^{-2}F(u) = w. \tag{201}$$

For $\gamma = 1$ the process $\phi(u)$ is a Brownian motion (BM) of diffusion constant $D = \sigma / m^4$ and upward drift $b = 1$. The time of the Brownian is $t \equiv u$. From Fig. 17 one sees that it becomes a first-passage-time problem, i.e., $u = u(w)$ is the first time the process $\phi(u)$ reaches altitude w. Conversely the process $w(u) = \max_{u' \leq u} \phi(u')$ is the maximum position over all previous times reached by a Brownian motion, see Fig.
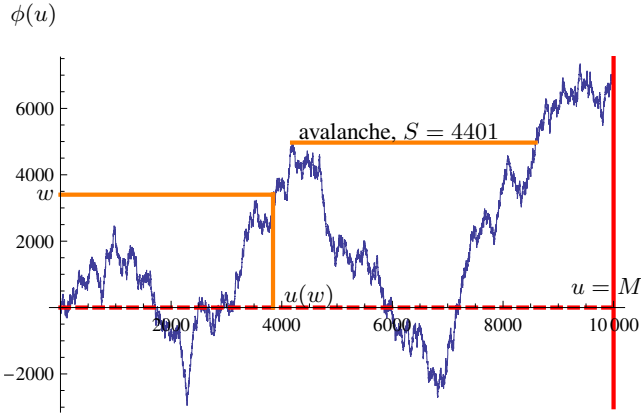
FIG. 18. (Color online) $\phi(u)$ defined in Eq. (201) for f a random walk with $D = 1.67 \times 10^3$ (blue). The dashed (red) line denotes $\phi(u) = 0$ (walk with no drift). We show explicitly the graphical construction of $u(w)$ for $w = 3400$, as well as a larger avalanche of size $S = 4401$. The system is discretized with step size 1 in u direction.

18. To avoid pathologies we assume a cutoff which makes $F(u)$ smooth at very short scales; equivalently we can discretize in u direction, as was done to generate Fig. 17. In AppendixE we have collected some useful properties of first-passage times and maxima of the Brownian motion that we now use extensively. We refer to this appendix for all details.

1. Avalanche distribution

From Fig. 17 one sees that the avalanche distribution $P(s)$ identifies with the return probability to the origin of the BM with a drift $b = 1$ and diffusion constant $D = \sigma/m^4$,

$$P(s) \approx P(s; W_0) = \frac{s_0^{1/2}}{2\sqrt{\pi}} s^{-3/2} \exp\left(-\frac{s}{4s_m} - \frac{s_0}{4s} + \sqrt{\frac{s_0}{4s_m}}\right),$$

(202)

where $u = s$, $P(u; W)$ is defined in Eq. (E7), $b = 1$, and $D = \sigma/m^4$. W_0 is a nonuniversal short-distance scale. We have defined $s_0 := W_0^2/D$ and $s_m := D$ the short-scale and large-scale cutoffs for the avalanche size. In the limit of small m one has $s_0 \ll s_m$, allowing one to drop the last term in Eq. (202). There are many small avalanches of the order of s_0, i.e. the distribution is concentrated at s_0. However the moments $\langle s^p \rangle$ for $p > 1/2$ are dominated by large avalanches. For $s \gg s_0$ one has

$$P(s) = \frac{\langle s \rangle}{2\sqrt{\pi s_m}} \frac{1}{s^{3/2}} e^{-s/(4s_m)},$$

(203)

$$s_m = D = \sigma m^{-4},$$

(204)

and $\langle s \rangle = \sqrt{s_m s_0}$. This is exactly the distribution found in the mean-field theory of sandpiles [73] and of the random-field Ising model, and was recently shown to hold, using FRG [61,74], for elastic manifolds in $d = 4$. The random-walk picture goes back to the so-called *Galton process* [75] for survival of family names (see [76] for a recent discussion in the context of depinning) which exhibits the same mean-field power-law behavior at the threshold.

2. Two-point conditional distribution

It turns out that the one-point-probability and critical-force distribution is a subtle issue for this model, due to the long-range nature of the landscape and the choice of boundary conditions. We do not discuss it in details here, but some considerations are given in AppendixF. A full solution requires a separate study.

We can still offer some simple remarks. If we know, e.g., by observation in a numerical simulation or an experiment, that the process is such that $u(w_1) = w_1$, then one can easily compute, from the Markov property of Brownian motion, the probabilities of all *future* events, i.e., the *conditional probability* for $u(w_2), \ldots, u(w_n)$ with $w_1 < w_2 < \ldots < w_n$,

$$P_{w_2 \ldots w_n}(u_2, \ldots, u_n | u(w_1) = u_1)$$
$$= P(u_2 - u_1; w_2 - w_1) \times \cdots \times P(u_n - u_{n-1}; w_n - w_{n-1}),$$

(205)

where $P(u; w)$ is the first-passage-time probability defined in Eq. (E7). Computing the moments one finds

$$\overline{u(w_n) - w_n} = u(w_1) - w_1,$$

(206)

$$\overline{[u(w_n) - w_n - u(w_p) - w_p]^2}^c = 2D|w_n - w_p| = \frac{2\sigma}{m^4}|w_n - w_p|,$$

(207)

for any $n, p \geq 1$. This defines the renormalized correlator

$$\Delta(0) - \Delta(w) = \sigma w,$$

(208)

i.e., it is exactly the bare disorder correlator. Note that although this result was derived from a conditional probability, it is independent of the choice of u_1 and w_1 *provided* all points w_i to which it applies are *larger* than w_1. Note also that although the two-point correlator is the bare one, the higher cumulants are different: they are nontrivial and can be easily computed from Eq. (206). Hence the system flows to a nontrivial fixed point. Remarkably, one can check that Eq. (208) is an exact fixed point of the two-loop FRG equation for $\Delta'(u)$, i.e., the derivative of Eq. (7),[2] using the value $\zeta = \epsilon = 4 - d$ (here $\zeta = 4$ which is the correct value for the present model).

We can also check that Eq. (208) satisfies the general relation

$$-\frac{2\Delta'(0^+)}{m^4} = 2\frac{\sigma}{m^4} = 2s_m = \frac{\langle s^2 \rangle}{\langle s \rangle}.$$

(209)

In fact, we can also check some of the general relations discussed in [61,74] for the so-called higher Kolmogorov cumulants, defined there,

---

[2]To obey Eq. (7) one should take $\Delta(0) = +\infty$ from the long-range character, or consider a box size in u space, which modifies the FRG analysis.

$$G(\lambda) := \overline{\exp(\lambda(\ u(w) - w - u(w') - w')) - 1}$$
$$= \exp\left(\left[w - w'\right]\left(\frac{1 - \sqrt{1 - 4\lambda s_m}}{2s_m} - \lambda\right)\right) - 1$$
$$= \left(\frac{1 - \sqrt{1 - 4\lambda s_m}}{2s_m} - \lambda\right)(w - w') + O[(w - w')^2]$$

(210)

for $w > w' \geq w_1$, using formula (E6) for the Laplace transform of the first passage time probability with $b = 1$ and $D = s_m$. This is related to the fact that the full distribution of avalanche sizes at the tree level (i.e., in mean field) in the field theory coincides with the distribution of return times of the one-dimensional Brownian motion.

B. Motion at finite velocity $v > 0$

Let us now consider the case $w(t) = vt$, i.e., a particle pulled by a spring at constant velocity,

$$\partial_t u(t) = F(u(t)) + m^2[vt - u(t)].$$

(211)

For simplicity, we set $\eta = 1$ (it can be restored by setting $t \to t/\eta$ and $v \to \eta v$). For $v > 0$ and since it is an overdamped equation of motion (no overshoot), the instantaneous velocity $v_t := \partial_t u$ is positive (possibly after a short transient), hence one can write $v_t = \mathbf{v}(u(t))$, which satisfies

$$\partial_t v_t = F'(u(t))v_t + m^2(v - v_t),$$

(212)

$$\partial_u \mathbf{v}(u) = m^2\left[\frac{v}{\mathbf{v}(u)} - 1\right] + F'(u).$$

(213)

Since for the Brownian-force landscape $F'(u)$ is a white noise, the second equation is a standard Langevin equation, hence the probability to observe $\mathbf{v}$ at u, given that the velocity is $\mathbf{v}_0$ at u_0 satisfies the Fokker-Planck equation,

$$\partial_u P = \partial_{\mathbf{v}}[\sigma \partial_{\mathbf{v}} P + (\partial_{\mathbf{v}} E(\mathbf{v}))P],$$

(214)

$$E(\mathbf{v}) = -m^2 v \ln \mathbf{v} + m^2 \mathbf{v},$$

(215)

with δ function initial condition. For $u \to \infty$ it converges to the equilibrium measure

$$P_{eq}(\mathbf{v}) = Z^{-1} e^{-E(\mathbf{v})/\sigma} = \frac{(m^2/\sigma)^{m^2 v/\sigma}}{v \Gamma(m^2 v/\sigma)} \mathbf{v}^{m^2 v/\sigma} e^{-m^2 \mathbf{v}/\sigma}.$$

(216)

One can also directly work with Eq. (212), rewriting it as a stochastic equation [77],

$$dv_t = dF(t) + m^2(v - v_t)dt.$$

(217)

$\overline{dF(t)^2} = 2\sigma v_t dt$ is a Brownian motion up to a time reparametrization, and the factor v_t can be seen by writing $\int du(\frac{dF(u)}{du})^2 = \int dt v_t^{-1}(\frac{dF(t)}{dt})^2$. In Itô prescription this yields the Fokker-Planck equation for the probability $Q(v_t = \mathbf{v}, t | v_0, t_0)$ of velocity $\mathbf{v}$,

$$\partial_t Q = \partial_{\mathbf{v}}[\sigma \partial_{\mathbf{v}}(\mathbf{v}Q) + m^2(\mathbf{v} - v)Q]$$

(218)

$$= \partial_{\mathbf{v}}[\sigma \partial_{\mathbf{v}}(\mathbf{v}Q) + \mathbf{v}(\partial_{\mathbf{v}} E(\mathbf{v}))Q].$$

(219)

Hence the steady-state solution for $t \to \infty$ is $Q_{eq} \sim \mathbf{v}^{-1} P_{eq}$, the velocity factor originating from the change of variable from u to t. One has [66]

$$Q_{eq}(\mathbf{v}) = \frac{(m^2/\sigma)^{m^2 v/\sigma}}{\Gamma(m^2 v/\sigma)} \mathbf{v}^{-1 + m^2 v/\sigma} e^{-m^2 \mathbf{v}/\sigma},$$

(220)

which yields the average velocity $\bar{\mathbf{v}}^Q = v$, as expected, and the connected expectation of the square of the velocity $\overline{\mathbf{v}^{2Q,c}} = v\frac{\sigma}{m^2}$. Note that the average velocity using P is $\bar{\mathbf{v}}^P = v + \frac{\sigma}{m^2}$, hence it does not even vanish as $v \to 0^+$: this is because most (in fact, as $m \to 0$, all) of the u segments belong to avalanches, yielding a finite average velocity if weighted by du, but that the fraction of time spent on them goes to zero, consistent with $v \to 0^+$.

ABBM also noted that the correlation function

$$C(t - t_0) := \int dv_t dv_0 (v_t - v)(v_0 - v) Q(v_t, t | v_0, t_0) Q_{eq}(v_0)$$

(221)

satisfies the very simple equation (see also [77])

$$\partial_t C = -m^2 C,$$

(222)

obtained by multiplying Eq. (218) by $(v_t - v)(v_0 - v)Q_{eq}(v_0)$, integrating over $v_t = \mathbf{v}$ and v_0 and using the fact that the current $J = \sigma \partial_{\mathbf{v}} \mathbf{v} Q + m^2(\mathbf{v} - v)Q$ vanishes at $\mathbf{v} = 0$ and $\mathbf{v} \to \infty$. After integration by parts one obtains Eq. (222).

From this we can now obtain the renormalized disorder Δ at $v > 0$ and discuss the crossover. One first notes that from the definition (5), inserting $w = vt$ and $w' = vt'$ and taking two derivatives, one has

$$C(t - t') = \overline{(v_t - v)(v_{t'} - v)} = -v^2 m^{-4} \Delta''(v(t - t')).$$

(223)

Since from Eq. (222) and above,

$$C(t) = v\sigma m^{-2} e^{-m^2 t},$$

(224)

we obtain

$$\Delta''(w) = -\frac{\sigma}{v} m^2 e^{-m^2 w/v}.$$

(225)

Integrating twice we finally obtain

$$\Delta(0) - \Delta(w) = \sigma w - \frac{\sigma v}{m^2}(1 - e^{-m^2 w/v}),$$

(226)

a formula valid for any $v > 0$. The integration constant has been fixed by either of the two equivalent conditions: (i) no cusp at $w = 0$; (ii) the large-w behavior is the same as in the bare model, and as in the statics, i.e., in the limit $v \to 0$, given by Eq. (208). A nonzero velocity $v > 0$ thus smoothens the cusp in a boundary layer of size $w \sim v/m^2$, but the function remains nonanalytic: there is a *subcusp*, i.e., a nonzero $\Delta'''(0^+)$; indeed one has at small w

$$\Delta(0) - \Delta(w) = \frac{m^2\sigma}{2v}w^2 - \frac{m^4\sigma}{6v^2}w^3 + O(w^4). \qquad (227)$$

This indicates continuity of $u(w(t))$ but jumps in its derivative, the velocity. It remains to be understood whether this feature is more general or if it is tied to the long-range nature of the random force landscape.

The distribution of avalanches times (in t) and sizes (in u) at $v > 0$ can be extracted by studying the returns "near" the origin of the process, i.e., the return to the origin inside the potential well $E(\mathbf{v})$. This is given by Eq. (212) or equivalently by

$$d\mathbf{v} = m^2\left(\frac{v}{\mathbf{v}} - 1\right)du + \sqrt{2\sigma}dB, \qquad (228)$$

where $dB(u)$ is a standard unit Brownian motion. Near $\mathbf{v} = 0$ we can first ignore the drift term $-m^2 du$. Define the change of variables $y = 2\sigma u$, then $\mathbf{v}(u) = r(y = 2\sigma u)$ $= \sqrt{\Sigma_{i=1}^{\tilde{d}} x_i^2(y)}$ is the norm of a $\tilde{d}$-dimensional BM in the variable y [78], which satisfies

$$dr = \frac{\tilde{d} - 1}{2r}dy + dB(y), \qquad (229)$$

$$\tilde{d} = 1 + \frac{m^2 v}{\sigma}. \qquad (230)$$

This yields the avalanche-size exponent $\tau = 2 - \tilde{d}/2$, for $\tilde{d} \le 2$, from the power-law decay of first return probabilites of a Brownian near the origin, see Appendix G,

$$\tau = \frac{3}{2} - \frac{m^2 v}{2\sigma} \qquad (231)$$

below a critical velocity $v \le \sigma/m^2$. This result was anticipated in Refs. [79,80]. Note that the definition of avalanches at $v > 0$ is not clear cut and requires a small velocity cutoff noted $\mathbf{v}_0$. In Appendix E 3 it is shown that

$$P(s) = \frac{1}{\Gamma(\tau - 1)}\frac{1}{s}\left(\frac{s_0}{s}\right)^{\tau-1}e^{-s_0/s}, \qquad (232)$$

$$s_0 = \mathbf{v}_0^2/(4\sigma) \qquad (233)$$

for $\mathbf{v}_0 \ll v$. Since the drift is neglected Eq. (233) holds only for $s \le s_m = \sigma/m^4$, the large scale cutoff. The drift provides a large velocity cutoff $\mathbf{v}_> = \sigma/m^2$ in Eqs. (216) and (220), and a large relaxation time cutoff $t_> = m^{-2}$, with $s_m = \mathbf{v}_> t_>$. For larger velocity $v > \sigma/m^2$ the behavior changes qualitatively. It corresponds to $\tilde{d} > 2$, see Appendix G, and the most probable velocity in $Q_{eq}(\mathbf{v})$ is no longer near $\mathbf{v} = 0$.

More details and the solution including the drift term are given in Appendix E 3 for the various regimes. In particular it is shown that one recovers the quasistatic size distribution obtained above in the limit $v = 0^+$.[3] For $v \le \sigma/m^2$ the random walk $\mathbf{v}(u)$, in the continuum limit, comes back infinitely of-

ten near the origin (i.e., near $\mathbf{v}_0$), hence the role of the drift term is mainly to cut off the rare large avalanches, very much similar to the statics (see, e.g., the discussion in [61,74]). For $v > \sigma/m^2$ the random walk in velocity space is still certain to come back near the origin but only because of the drift. There are then two types of avalanches. In a fraction of them (computed in Appendix E 3) the instantaneous velocity $\mathbf{v}$ does not reach v: these avalanches are still described by the model without the drift (first-return "time," conditioned to return) and lead to power-law distributions. In the rest, the velocity reaches v and equilibrates in the well $E(\mathbf{v})$; the "time" between two returns at small $\mathbf{v}_0 \ll v$ can then be estimated as $\sim(\mathbf{v}_0)^{-m^2 v/\sigma}$ proportional to the inverse equilibrium probability (either P_{eq} or Q_{eq} depending on whether one is interested in avalanche size or duration). Typically there will be a bunch of small avalanches of the first kind separated by one of the second kind. Eventually at larger velocities returns to the origin $\mathbf{v}_0 \ll v$ become very rare events and there is no real sense in which one can talk about avalanches.

VII. DEPINNING AND EXTREME STATISTICS OF RECORDS

A. Model without a mass: Records without drifts

For a particle pulled through a random-force landscape it is also possible to consider the problem without a parabola. The problem is easier to solve, but the correspondence with the FRG calculations is much less clear. Let us give here some elementary results.

We now have to solve for the smallest root $u(f)$ of

$$f = -F(u) \qquad (234)$$

where f is the applied force. We study the case where the force is continually increased. The process $u(f)$ then has jumps from u_i to u_{i+1} as the force crosses the values f_i, which form an increasing sequence. These values are called the *record values* for the process $F(u)$, and the u_i the *record times*. Statistics of records thus naturally occurs in the physics of depinning. The problem is to find the running maximum (i.e., the record) of an *unbiased* process, while in the case of a mass it had a drift. In the absence of a drift the only scale in the problem is the system size M.

1. Uncorrelated forces

Let us start with the discrete model of uncorrelated forces studied in Sec. III A, characterized by a force distribution $P_f(F)$ for each site. A similar problem was studied in [81] (Sec. IV B). There the probability distribution of the full record value sequence $(f_1 < f_2, \ldots < f_n, \ldots)$ was obtained for a semi-infinite line. It can be mapped onto a sum of indepen-

---

[3]Note however that these results are for a pure Brownian landscape. If the force landscape is smooth at short scale u_0, Eq. (233)

holds only for $s_0 \gg u_0$. For $s_0 \le u_0$ the short-scale cutoff function for $P(s)$ is more complicated, but this has no consequence for the behavior for $s_0 \ll s \ll s_m$ still given by Eq. (233). In the small v limit, there is a further crossover velocity $v_c = \sqrt{4\sigma u_0}$ below which the short-scale cutoff function progressively becomes the one of the quasistatic limit.
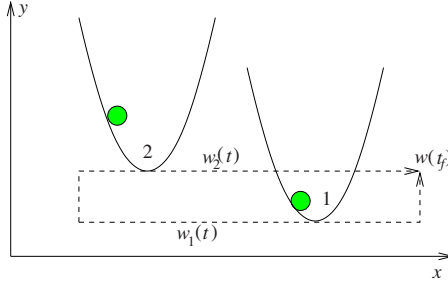
FIG. 19. (Color online) Two particles dragged through a random-energy landscape by parabolic potentials (springs) whose centers have identical starting and final positions but follow different paths $\{w_1(t)\}$ and $\{w_2(t)\}$.

dent variables as follows: The sequence distribution can be obtained from

$$\Phi(f_n) = \sum_{i=0}^{n} a_i \qquad (235)$$

for any $n > 1$, where the a_i are independent positive random variables, each with an exponential distribution $P(a)da = e^{-a}da$. The function

$$\Phi(f) = -\ln \int_{-\infty}^{f} dF P_f(F) \qquad (236)$$

describes the tail of the distribution, here the smallest f. For stretched exponential tails, as in class I, the growth is $f_n \sim n^{1/\gamma}$, while for power-law tails, as in class II, the growth is exponential in n.

Another set of results, remarkably universal, is known [62,63] for the probability $P(N|M)$ of the number of records N, here equal to the number of jumps, for a system of size M (notations are inverted as compared to [62]). Then for an uncorrelated sequence of F_i it was shown [82] that at large M

$$N = \ln M + \xi\sqrt{\ln M}, \qquad (237)$$

where ξ is a univariate Gaussian random variable [65,66]. Hence the translationally averaged avalanche size in absence of a mass should be

$$\frac{1}{N}\sum_{i=1}^{N} s_i = \frac{M}{N} \to \frac{M}{\ln M}, \qquad (238)$$

i.e., it is the typical avalanche size $\frac{M}{N}$. In the language of records the avalanche sizes $s_i = u_{i+1} - u_i$ are the time intervals between successive records, also called *record ages*. The translational average grows unboundedly with system size. Hence there are very few avalanches and they are almost as large as the system. Note that, at variance with the results on the sequence f_i, this result is *independent* of the distribution $P_f(F)$ for continuous distributions.

2. Forces correlated as a random walk

In the case of a landscape obtained as a discrete-time random walk, $F_i = F_{i-1} - \eta_i$ where η_i are uncorrelated random variables drawn from the same *symmetric* continuous distri-
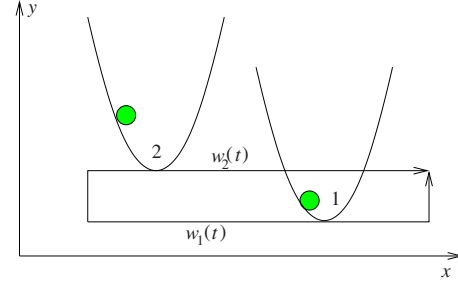
bution $P(-\eta) = P(\eta)$, it was recently obtained in Ref. [62] that

$$\sum_{M=N-1}^{\infty} P(N|M)z^M = \frac{(1 - \sqrt{1-z})^{N-1}}{\sqrt{1-z}}. \qquad (239)$$

Equivalently

$$P(N|M) = 2^{-2M+N-1}\binom{2M-N+1}{M} \underset{M\to\infty}{\sim} \frac{1}{\sqrt{\pi M}} e^{-N^2/(4M)}.$$

Hence for large sizes M, the average number of jumps behaves as [62]

$$\bar{N} \approx \frac{2}{\sqrt{\pi}}\sqrt{M}. \qquad (240)$$

There are also results for the jump sizes s_i, named *record ages* l_i in Ref. [62]. The typical jump size is $s_{\text{typ}} = M/\bar{N} = \sqrt{\pi M}/2$, while the average maximal jump size is $\overline{s_{\text{max}}} = 0.626\,508M$ and the average minimal jump size is $\overline{s_{\text{min}}} = \sqrt{M/\pi}$ [62].

B. Model with a mass: Records with a drift

The usual problem of records with drifts [63] consists in studying the sequence

$$Y_i = X_i + ci \qquad (241)$$

with $c > 0$ where the X_i are symmetric random variables. One way to present the correspondence to the depinning model with a mass[4] is that

$$X_i = -F_i, \quad c = m^2. \qquad (242)$$

The set of (upper) records Y_{i_p}, $p = 1, \ldots, N$, $i = 1, \ldots, M$, i.e., successive highest values, are the values $m^2 w_p$ at which a jump from $u_p = i_p$ to $u_{p+1} = i_{p+1}$ occurs in the process $u(w)$.

1. Short-range correlations

In the case of IID random variables with a drift it was shown that the total number of records N up to time M grows linearly as $N \sim r(c)M$ with (normal) fluctuations which were

---

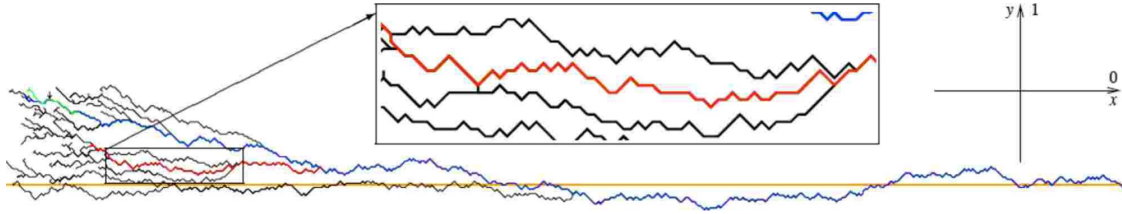[4]One can also set $X_i = -F_i/m^2$ and $c = 1$ as in Sec. VI.

FIG. 21. (Color online) Trajectories of particles dragged from left to right by a parabolic well. Trajectories starting at different random initial positions all converge towards the same trajectory, with the same position at a given time (which is not visible on the plot). The minimum position of the parabola in y direction is indicated by a straight (orange and/or grey) line. At the right, we show our coordinate system. The inset at the top is a blowup of part of the curve. It shows a deviation from the no crossing property which holds for $N=1$ (Middleton theorem [87]): Trajectories which are together can split up, even if later on they join again (see text).

characterized [63,64]. However obtaining analytic results, even for $r(c)$, for a general distribution was found difficult and some results were obtained only for special distributions $P(F)$ [63,64]. The function $r(c)$ is related to the avalanche density $1/\langle s \rangle = r(c)$, which is finite in presence of a mass, and is computed here for small $m^2 = c$. We solved the problem for arbitrary distributions $P(F)$ and found universality in the small c limit, with three classes. In addition we obtained the joint distribution $P(w,s)$ of (i) the time s between one record and the next; (ii) the difference in value w with the previous record.[5] These results were given in Sec. IV.

2. Long-range correlations

Let us now extend the discussion of Ref. [62] to records with drift, i.e., depinning with a mass. Again we consider the random walk $X_i = X_{i-1} + \eta_i$ with IID random variables $\eta = -F$ of distribution $P_f(\eta)$. The alert reader will note that $P_f(\eta)$, $P_{\text{ava}}(s)$, and $P(s)$ below denote three different probabilities and functions. $P_f(\eta)$ produces a correlated sequence $X_n - X_0 = \sum_{i=1}^n \eta_i$. For $n \geq 1$ we set

$$P(n) = \text{Prob}(X_n < X_0 - cn) = \text{Prob}(Y_n < Y_0),$$

$$Q(n) = \text{Prob}(X_i < X_0 - ci, i = 1, \ldots, n) \qquad (243)$$

$$= \text{Prob}(Y_i < Y_0, i = 1, \ldots, n). \qquad (244)$$

The Sparre-Andersen theorem [83–85] states that

$$Q(z) := \sum_{n=0}^{\infty} Q(n) z^n = \exp\left(\sum_{n=1}^{\infty} \frac{P(n)}{n} z^n \right), \qquad (245)$$

setting $Q(0) = 1$ by convention. We denote $F(n) := Q(n-1) - Q(n)$ the first passage probability that Y_n crosses Y_0 between steps $n-1$ and n. As in [62] the joint distribution of record ages (jump sizes) s_i and number N of records is

$$P(\{s\}, N|M) = F(s_1)F(s_2) \cdots F(s_{N-1})Q(s_N)\delta_{\sum_i^N s_i = N}. \qquad (246)$$

While for $c = 0$, $P(n) = 1/2$ independent of n, leading to Eq. (239) and the very universal results of [62] quoted above, for

$c > 0$ the sequence $P(n)$, hence $Q(n)$, usually depends on the details of the distribution $P(\eta)$. Hence apart from the asymptotic behavior at large n (hence M), one expects less universality.

The following formulas are still valid: The generating function for the probability to have N records given M, $P(N|M) = \sum_{\{s\}} P(\{s\}, N|M)$ can be written as

$$\sum_{M=N-1}^{\infty} z^M P(N|M) = F(z)^{N-1} Q(z), \qquad (247)$$

where $F(z) := \sum_{n=1}^{\infty} F(n) z^n = 1 - (1-z)Q(z)$. For instance the generating function for the average number of jumps is obtained by multiplying Eq. (247) by N, and summing over N,

$$\sum_{M \geq 0} z^M \bar{N}(M) = \frac{1}{(1-z)^2 Q(z)}. \qquad (248)$$

Similar results hold for higher moments.

If one considers $P_f(\eta)$ with a finite second moment, the X_i are in the universality class of the Brownian motion and one should recover the results of Sec. VI using that [85]

$$P(n) \sim n^{-1/2} e^{-nS(c)}, \quad Q(n) \sim n^{-3/2} e^{-nS(c)} \qquad (249)$$

with a common function $S(c) = O(c^2)$ at small c. For instance, if $P_f(\eta)$ is a univariate Gaussian, $P(n) = \frac{1}{2}[1 - \text{erf}(c\sqrt{n/2})] \approx (2\pi c^2 n)^{-1/2} e^{-c^2 n/2}$ for large n. We will not study the Brownian case in detail, since it was already discussed in Sec. VI, and we refer to Ref. [85] for a detailed asymptotic analysis [as well as a nice proof of Eq. (245)].

Of course we expect that stable distributions play a special role. Here we detail one example of a Levy-type random-force landscape, for which the results for the records with drift are particularly simple, and present a nice generalization of Ref. [62], although they may not be as universal. Consider the Cauchy distribution,

$$P_f(\eta) = \frac{a}{\pi(\eta^2 + a^2)}, \qquad (250)$$

such that the distribution of $X_n - X_0$ is also Cauchy with parameter $a \to na$. Quite extraordinarily,

---

[5]With the same method one can obtain the difference in value w with the next record.
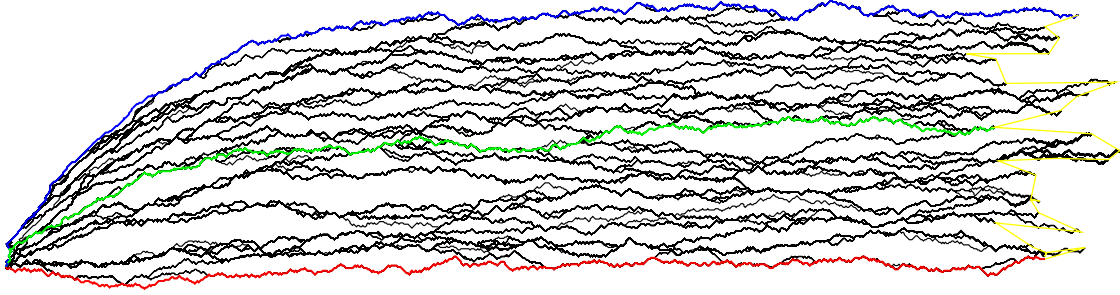
FIG. 22. (Color online) Trajectories of 200 particles dragged from left to right. All particles start at (0,0). However, they sit in different potential wells (as described in the main text). As can be seen, they mostly move together on preferred trajectories, before separating again. The end points are joined by yellow lines. $m^2 = 0.003$. The particles in the two outer wells, as the center one, are marked in colors (red and/or blue, green). The well was moved for a total of 1000 steps.

$$P(n) = \int_{cn}^{\infty} \frac{nadx}{\pi[x^2 + (na)^2]} = \int_{c}^{\infty} \frac{adx}{\pi[x^2 + (a)^2]} =: p$$

is independent of n, with $0 < p = \arctan(a/c)/\pi < 1/2$ for $c > 0$. Hence $Q(z) = (1-z)^{-p}$ and $F(z) = 1 - (1-z)^{1-p}$, and

$$Q(n) = \frac{\Gamma(n+p)}{\Gamma(1+n)\Gamma(p)}, \qquad (251)$$

$$F(n) = (1-p)\frac{\Gamma(n+p-1)}{\Gamma(1+n)\Gamma(p)}. \qquad (252)$$

Using Eq. (248) one finds the average number of records (i.e., of jumps),

$$\bar{N} = \frac{\Gamma(2+M-p)}{\Gamma(1+M)\Gamma(2-p)} \underset{M \to \infty}{\sim} \frac{M^{1-p}}{\Gamma(2-p)}, \qquad (253)$$

which grows as a power law of the size. Higher moments grow with the same scale,

$$\overline{N^2} = -\bar{N} + \frac{2\Gamma(3+M-2p)}{\Gamma(1+M)\Gamma(3-2p)}. \qquad (254)$$

Hence at large M the connected fluctuations are

$$\overline{N^2} - \bar{N}^2 = \left[\frac{2}{\Gamma(3-2p)} - \frac{1}{\Gamma(2-p)^2}\right]M^{2(1-p)}, \qquad (255)$$

and in all cases the results of Ref. [62] are recovered for $p = 1/2$, the case without drift. The full distribution takes a scaling form at large M,

$$P(N|M) \approx M^{p-1} g_p(NM^{p-1}). \qquad (256)$$

Summing Eq. (247) with this scaling ansatz at large M, i.e., $x := -\ln z \approx 1 - z$ small yields

$$\int_0^{\infty} dM M^{p-1} e^{-Mx} g_p(NM^{p-1}) \approx x^{-p} e^{-Nx^{1-p}}$$

with $g_{1/2}(y) = e^{-y^2/4}/\sqrt{\pi}$.

From Eq. (246) one sees that the distribution of avalanche sizes (i.e., record ages) is $P_{\rm ava}(s) = F(s)$ for $s = 1, 2, \ldots$. For fixed p and large s it decays from Eq. (252) as a power law with $\tau = 2 - p$,

$$P_{\rm ava}(s) = F(s) \approx \frac{s^{-(2-p)}}{-\Gamma(p-1)}. \qquad (257)$$

This leads to a simple interpretation in terms of a directed random walk with traps of independent random release times s_i, distributed as $P(s) \sim s^{-(1+\mu)}$ and $1/2 \leq \mu = 1 - p < 1$. M is the total time t and N the distance x traveled. As is well known, for $\mu < 1$, $x \sim t^{\mu}$ and the distribution of $z = t/x^{1/\mu} = M/N^{1/(1-p)}$ is a Levy stable distribution $L_{\mu}(z)$ with positive support, which is indeed the solution of Eq. (256), $g_p(y) = \mu^{-1} y^{1-1/\mu} L_{\mu}(y^{-1/\mu})$.

Although the strong universality of the symmetric case does not hold, we expect that all processes in the class of the Cauchy process remain critical even with a drift which has a power-law distribution of avalanches given above, and a continuously varying exponent. For stable processes intermediate between Cauchy and Gaussian, avalanches should be cut at a finite scale, which diverges with different exponents as $c \to 0$. The situation of stable processes broader than the Cauchy distribution remains open.

VIII. GENERAL CONSIDERATIONS ABOUT AN N-COMPONENT DISPLACEMENT FIELD

Up to now, we have considered particles, and more generally elastic objects and manifolds, whose position is a one-component function. We now consider particles or elastic objects embedded in higher dimensions $N > 1$. For simplicity, we focus on a particle, but the considerations in this short section can be extended to d-dimensional elastic manifolds. In the next section we consider an application to a particle driven in a two-dimensional random-energy landscape.

Consider two particles, which see the same random-energy landscape, but which sit in different parabolas, labeled 1 and 2. These parabola are chosen with the same curvature m^2 but their centers differ, and can have very different trajectories, which we call $\{w_1(t)\}$ and $\{w_2(t)\}$. An interesting case is when the trajectories differ but the end points coincide $w_1(t_{i,f}) = w_2(t_{i,f})$ as in the example of Fig. 19. In that example it is clear that

$$|\overline{u_{w_1}(t_f) - u_{w_2}(t_f)}| \approx \sqrt{2}\frac{f_c}{m^2}. \qquad (258)$$

This is because there should be a nonzero critical force, f_c, and that each particle lags behind each parabola center $w_i(t)$,
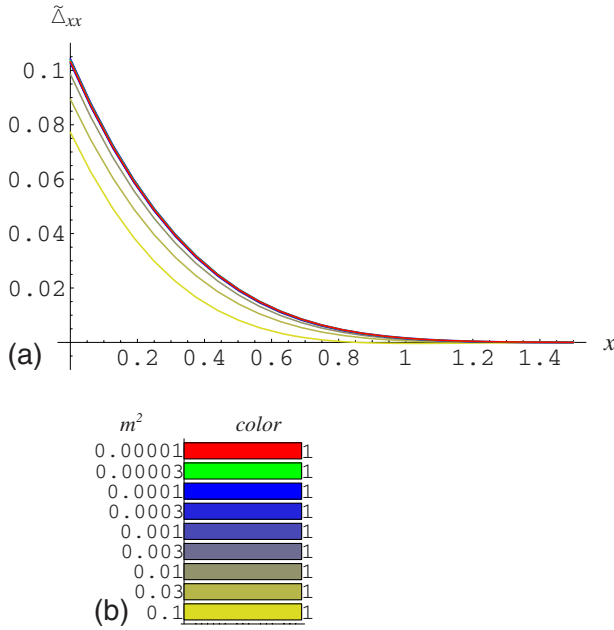
FIG. 23. (Color online) Scaling collapse for $\widetilde{\Delta}_{xx}(x,0)$ $:= m^{-4+2\zeta_x}\Delta_{xx}(xm^{\zeta_x},0)$, with $\zeta_x=1.595$. The scaling collapse is perfect except for the two largest masses.

up to fluctuations, roughly in minus the direction of drift. Thus the process u_w depends on the trajectory $w(t)$, and to define a single valued function u_w, we have to restrict to a single well-defined trajectory $w(t)$ in a quasistatic limit. Consider now Fig. 20. Both parabolas move with the same velocity v in x direction. They are completely characterized by their position $\vec{w}=\{x=x_0+vt,\vec{y}\}$, with $\vec{w}\in\mathbb{R}^N$, $\vec{y}\in\mathbb{R}^{N-1}$. Especially note that without loss of generality, x_0 can be put to 0. Again we integrate the Langevin equation (1), to define $\vec{u}(\vec{w})$.

A more difficult question is whether $\vec{u}(\vec{w})$ depends on the initial condition $\vec{u}(t_0)$, and since we have set x_0 to 0, implicitly on the starting time t_0. One expects (see next section for how it occurs) that the dependence of $\vec{u}(\vec{w})$ on t_0 disappears in the limit of $t_0\rightarrow-\infty$, and this is the limit we are interested in. This could be checked, similar to the *exact sampling* method, see, e.g., [86], by starting at time t_0, and checking that at the time of interest t, all trajectories from all possible initial conditions have converged towards a single one. If not, one starts at an earlier time t_{-1}, and checks again, repeating this procedure until all trajectories have converged. This defines a function $\vec{u}(\vec{w})$, which is now independent of the initial time and conditions. In the next section it will be checked numerically that for a particle driven through a two-dimensional bounded random-energy landscape, all trajectories indeed converge, see Figs. 21 and 22. It is also found there that the so-called no crossing property (Middleton theorem [87]) does not hold for $N=2$: although violations appear to be rare there are some instances of two trajectories splitting up. This results from a second particle (more properly, a second trajectory of the same particle with a different initial condition) arriving at a later time on the same site: it then feels a stronger drive from the parabola and may jump forward and pass the first particle. An example is shown in Fig. 21.

Having given an unambiguous definition of $\vec{u}(\vec{w})$, we can calculate connected correlation functions of its moments, which again define Δ (now a tensor), and higher cumulants. For this tensor the driving direction x will play a special role (for $N>2$ we expect isotropy in the other $N-1$ direction. The calculation is done for a particle in the next section. Other definitions of $\vec{u}(\vec{w})$ could of course be given. The simplest one is to pick a fixed but different driving direction. From statistical isotropy of the disorder the results should be the same up to the rotation. We defer the study of more complicated driving processes to future work.

IX. A PARTICLE DRAGGED IN TWO DIMENSIONS: $D=0$, $N=2$

We now study particles dragged through a two-dimensional random-energy landscape.

The algorithm works as follows: We generate a random-energy landscape on a square lattice. A particle in addition sees a parabolic well. The total energy is the sum of both. We will mostly use a box distribution for the energy of a site, uniform in $[0, 1]$. Energies on different sites are uncorrelated. We then update all particle positions: If a particle can move in a direction such that and lower its potential energy, it will do so. If there are several such directions, it will choose the one with the lowest final energy. We allow moves to the eight nearest neighbors numbered from 1 to 8 (starting at the center 0),

8	1	2
7	0	3
6	5	4

If a move is possible, we perform it and then try other moves again, until the particle finally becomes stuck. If several moves are possible, we take the one which results in the largest descent in energy, i.e., we go into the direction of the maximum force. Only then, we update the position of the parabola, by moving it from w to $w+dw=w+vdt$. We record the particle position as a function of time t.

We first show numerically that there is a unique attractor trajectory (see Fig. 21). We start particles at random positions, but in the same parabolic well. Then move the parabola in a given direction (here always to the right, also denoted the x direction). One sees that trajectories converge, and particles will have the same position at a given time (not visible on Fig. 21, which only shows the world lines.) This convergence can be understood from the fact that if two "particles" (in fact these are the same particle but with different initial conditions) meet at a site at the same time, their future evolution is identical. Hence the deep sites with low energies where the particle becomes temporarily stuck act as sinks where the trajectories merge. Clearly, the particle needs to be trapped long enough for the process to be efficient.

Our proper simulation is done with many particles (here 200), each sitting in a parabola which are displaced by one
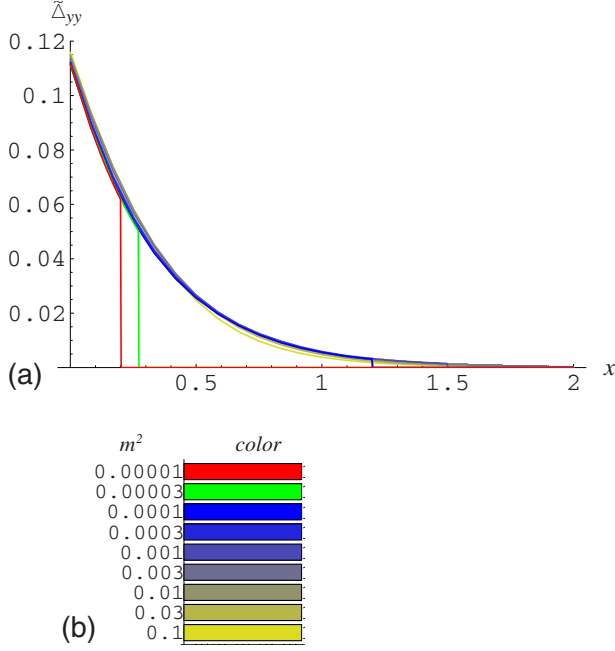
FIG. 24. (Color online) Scaling collapse for $\tilde{\Delta}_{yy}(x,0)$ $:= m^{-4+2\zeta_y}\Delta_{yy}(xm^{\zeta_x},0)$, with $\zeta_x=2$ and $\zeta_y=1$. The descending lines indicate that no data have been collected for larger values, due to an insufficient choice of parameters. Good scaling collapse.

unit (or in general by dy) to the top. This gives us data points in the y direction. In the x direction (in which we move the parabolas), we use that after some time t the parabola has been displaced by a distance vt. We denote the minimum of the parabola $w_{t,y}$ and its ith component $w_{t,y}^i$ as

$$w_{t,y} := (vt,y), \quad w_{t,y}^0 := vt, \quad w_{t,y}^1 := y. \quad (259)$$

The particle sitting in this parabola will have position $u_{w_{t,y}}$, with components $u_{w_{t,y}}^i$. We then define $\Delta^{ij}(tv,y)$ as

$$\Delta^{ij}((t'-t)v,y) := m^4 \overline{(u_{w_{t,0}}^i - w_{t,0}^i)(u_{w_{t',y}}^j - w_{t',y}^j)}^c. \quad (260)$$

The connected symbol c indicates that we have subtracted the critical force. $\Delta^{ij}(x,y)$ has the following symmetry properties:

$$\Delta^{ii}(x,y) = \Delta^{ii}(x,-y), \quad (261)$$

$$\Delta^{01}(x,0) = 0, \quad (262)$$

$$\Delta^{01}(0,y) = -\Delta^{10}(0,y). \quad (263)$$

This is a consequence of the relabeling symmetry in Eq. (260) $\Delta^{ij}(x,y) = \Delta^{ji}(-x,-y)$ and obvious covariance under the parity symmetry $y \to -y$. For smaller and smaller masses, there will be more and more data points. Steps in the x direction are necessarily discretized, of size $dw = vdt$. This poses an additional problem not present for $N=1$: there choosing a dw too large results in a loss in precision (since some smaller jumps may be overrun) but does not have dramatic consequences for large jumps, especially does not
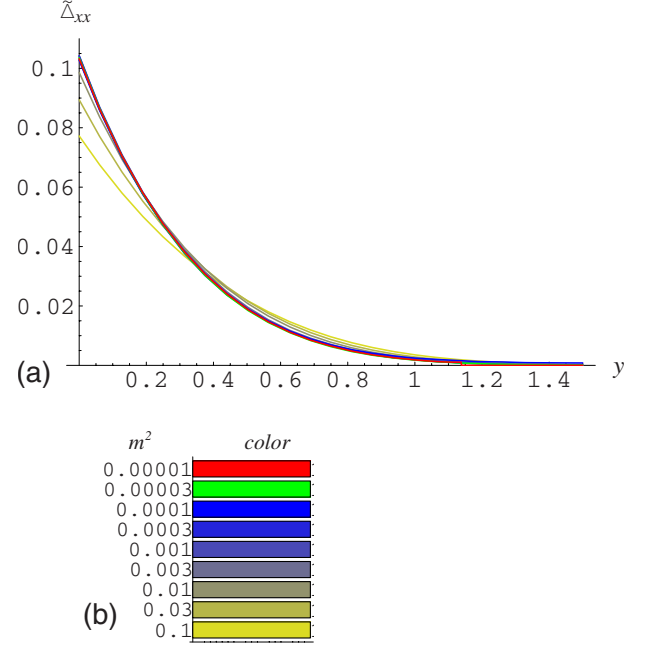

FIG. 25. (Color online) Scaling collapse for $\tilde{\Delta}_{xx}(0,y)$ $:= m^{-4+2\zeta_x}\Delta_{xx}(0,ym^{\zeta_y})$, with $\zeta_x=1.595$ and $\zeta_y=1$. The scaling collapse is excellent for all but the three largest masses.

change the end point $u(w)$, due to Middleton's theorem [87]. In contrast, for $N=2$, if the parabola is not moved adiabatically, the particles will see a strong force forward, and therefore be more likely to move forward, instead of sideward, thus embarking on a different trajectory. This may alter the whole trajectory over a much larger region. In practice, we decided to never move the parabola by more than one unit, before checking whether a move could be made. It may be a possible source for finite-size corrections. These will disappear *if, and only if* the critical force scales to zero for $m \to 0$, since the energy gain for an elementary move is

$$\frac{m^2}{2}[(u+1-w)^2 - (u-w)^2] = m^2\left(u-w+\frac{1}{2}\right) \approx f_c. \quad (264)$$

However, f_c goes slowly towards 1, by which it is bounded. Unfortunately we find, e.g., $f_c(m^2=0.01)=0.464\,602$, $f_c(m^2=0.0001)=0.785\,073$. This might indicate that the step size we have used is still too large. We have not attempted to use a smaller step size due to the enormous computing powers needed. We nevertheless believe that the results are valid for the following reason: f_c measures the time average of u_w-w, but we have to know the forward force exerted by the spring, when the particle *arrives* at the trap. Clearly, this must be much smaller, otherwise in a few steps the force would have increased by 1, which is sufficient to overcome *any* barrier for the box-distributed random energies, and the particle would not remain pinned for a long time. However we see diverging trapping times in the simulations, thus the argument using Eq. (264) is not valid.

We now present data for the force-force correlators in Figs. 23–27, for masses ranging from $m^2=0.1$ to $m^2=10^{-5}$,
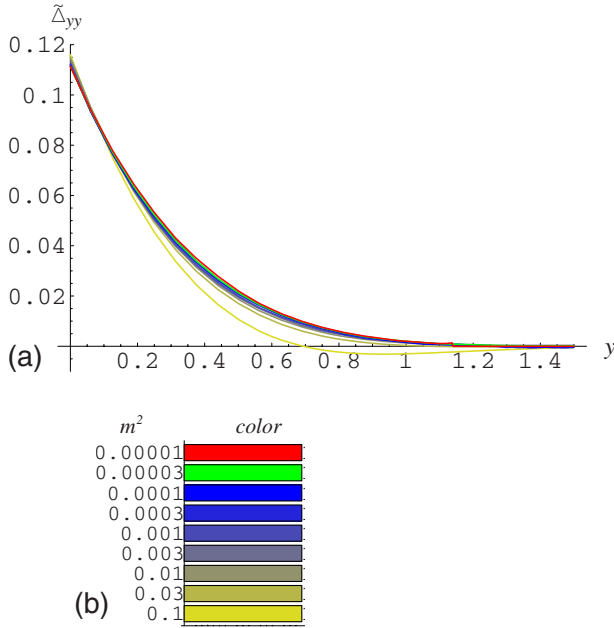
FIG. 26. (Color online) Scaling collapse for $\widetilde{\Delta}_{yy}(0,y)$ $:= m^{-4+2\zeta_y}\Delta_{xx}(0,ym^{\zeta_y})$, with $\zeta_y=1$. The collapse is good, except for the three largest masses.

descending in half decades. A first and important qualitative conclusion to be drawn is that all correlators not only depend on x, but also on y. This is in contradiction to the fixed-point structure used by Ertaş and Kardar [67], whose Δ_{ij} depends only on x and not on y.

Our aim is to determine the scaling exponents ζ_x and ζ_y from the finite-mass scaling ansatz, suggested by the FRG equations for this problem [68],

$$\widetilde{\Delta}_m^{ij}(x,y) := m^{-4+\zeta_i+\zeta_j}\Delta^{ij}(xm^{-\zeta_x},ym^{-\zeta_y}), \qquad (265)$$

and supposing that $\widetilde{\Delta}_m \to \widetilde{\Delta}$ for $m \to 0$. We find that for $\Delta_{xx}(x,0)$, $\Delta_{yy}(x,0)$, $\Delta_{xx}(0,y)$, $\Delta_{yy}(0,y)$, and $\Delta_{xy}(0,y)$ *separately* such a scaling collapse is possible. There is no doubt that $\zeta_y=1$, with consistently rather small errors: the scatter from the different estimations is $\zeta_y=1.009\pm0.015$.

However, the results for ζ_x are less consistent. We find different values, depending on which quantity we consider. There is a clean data collapse on Fig. 24 for $\widetilde{\Delta}_{yy}$ with $\zeta_x=2$; however on Figs. 23 and 25 for $\widetilde{\Delta}_{xx}$ the best collapse is with $\zeta_{xx}=1.6$; finally on Fig. 27 for $\widetilde{\Delta}_{xy}$, the best scaling collapse is for $\zeta_x=1.25$, where however some of the data are noisy (but note that at least the data for the second-smallest mass, which are already very difficult to obtain, and for some of the larger masses, show only little noise, such that noise does not seem to be an issue here). Let us recall for comparison that for $N=1$ a particle driven in a random-energy landscape with a box distribution belongs to universality class III with $\alpha=3$, i.e., $\zeta_x=4/3$, see Secs. III C 3 and III D 2. (For a box random *force* it is $\alpha=1$ and $\zeta=1$.)

To conclude, we have shown that the unique attractor trajectory can be defined for the particle with $N=2$, and that the disorder correlator $\Delta_{ij}(x,y)$ can be measured.
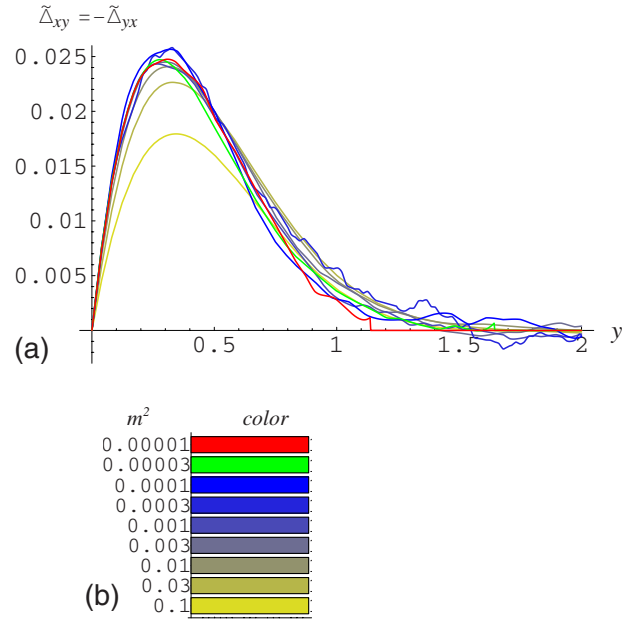

FIG. 27. (Color online) Scaling collapse for $\widetilde{\Delta}_{xy}(0,y)$ $:= m^{-4+\zeta_x+\zeta_y}\Delta_{xy}(0,ym^{\zeta_y})$, with $\zeta_x=1.25$ and $\zeta_y=1$. The signal-to-noise ratio is rather big. In order to improve the statistics, we have used (after numerical verification) that $\widetilde{\Delta}_{xy}(0,y)=-\widetilde{\Delta}_{yx}(0,y)$, to plot $\frac{1}{2}[\widetilde{\Delta}_{xy}(0,y)-\widetilde{\Delta}_{yx}(0,y)]$. Fair scaling collapse, except for the two largest masses.

X. CONCLUSION

To conclude we have shown how the renormalized disorder correlator $\Delta(w)$, central to the functional RG theory of depinning, can be measured for a manifold of internal dimension d driven by a spring in an $N=1$ random landscape. This correlator contains information about the stick slip motion of the interface.

We have solved analytically the case $d=0$ of a particle in a short-range correlated pinning-force landscape, finding three universality classes. In each case we have obtained the universal fixed-point forms for $\Delta(w)$ for quasistatic driving, i.e., the depinning fixed point. In all cases it exhibits the famous cusp at $w=0^+$. We have also obtained the distribution of critical forces, avalanche sizes and waiting times, and checked the general relations conjectured to hold between their moments and the cusp $\Delta'(0^+)$. While the exponent ζ can take various values depending on the class, the avalanche-size exponent was found to be $\tau=0$ in all cases, which invalidates, at least at a naive level, the conjecture $\tau=2-2/(d+\zeta)$. We also found that the distribution of avalanche sizes and waiting times are *identical* in the scaling limit.

We have extended our results to a particle driven in force landscapes with the correlations of a random walk. In the Brownian case, known as the ABBM model for interface motion and Barkhausen noise, it is possible to solve for any driving velocity and check the quasistatic limit. Remarkably this model has much in common with the mean field theory of avalanches and recent FRG results for avalanche distributions in $d=4$. Since $\zeta=4$, the avalanche exponent for $v=0^+$

obeys, in that case, the conjecture $\tau = 2 - 2/(d+\zeta)$.

In each case we have emphasized the connections between the depinning problem for a particle and the extremal statistics of records, with and without drifts.

These exact results in $d=0$ provide interesting checks and interpretations of the functional RG theory, and help us understand what we should expect for manifolds.

Finally, we started addressing the problem of depinning for $N>1$, mostly numerically; even for a particle it is quite nontrivial. We have checked numerically the consistency of the method, based on the ergodicity in presence of driving via a quadratic well. Numerous open problems remain.

ACKNOWLEDGMENTS

APPENDIX A: DYNAMICAL ACTION AND OBSERVABLES

In this section we establish the relation between the effective action and observables; this is an extension to the dynamics of the proof given in [57,88] for the statics. This relation allows one to measure the correlator of the dynamical FRG as explained in the text. Since the dynamical field theory is significantly more complicated than the static replica field theory, the arguments presented here may be slightly less general and rely on further assumptions about the nature of the quasistatic limit and its ergodic properties, some remaining to be demonstrated, as, e.g., extensions to $N>1$ components is less straightforward than in the statics [57,88]. At a formal level, however, the arguments are rather similar.

We use notations of the text and consider the following equation of motion:

$$\eta \partial_t u(x,t) = F_x[u(t);w(t)] + \xi(x,t),$$

$$F_x[u;w] = m^2[w(x) - u(x)] + \nabla_x^2 u(x) + F(x,u(x)), \quad \text{(A1)}$$

where $w(t)$ is given, and $\xi(x,t)$ is the thermal noise. We denote in general implicitly $u_{xt}^s = u(x,t;u_0(x,t_0),F,\xi)$ the solution for given initial condition, disorder, and thermal noise.

1. Definition of functionals

Let us first recall the definition of the useful functional of the dynamical field theory. We write the dynamical [Martin-Siggia-Rose (MSR)] action $\mathcal{S}$ in compact notation as

$$\mathcal{S}[u,\hat{u}] = \hat{u} \cdot g^{-1} \cdot u + \hat{u} \cdot A^{(0)}[u] - \frac{1}{2} \hat{u} \cdot B^{(0)}[u] \cdot \hat{u} + O(\hat{u}^3) \quad \text{(A2)}$$

For any "vectors" u,v we denote $u \cdot v := \int_{xt} u_{xt} v_{xt}$ (and additional index contraction for $N>1$), A and B are, respectively,

vector and matrix functionals. g_{xy} can be an arbitrary (time independent) symmetric matrix but the usual choice is (in Fourier) $g_q^{-1} = q^2 + m^2$. The functionals defining the bare action are

$$A^{(0)}[u]_{xt} = \eta \partial_t u_{xt}, \quad \text{(A3)}$$

$$B^{(0)}[u]_{xt,x't'} = 2\eta T \delta_{xx'} \delta_{tt'} + \Delta_0(u_{xt} - u_{x't'}) \delta_{xx'}, \quad \text{(A4)}$$

which is the standard MSR action averaged over disorder. The statistical tilt symmetry (STS) of the bare action states that $A^{(0)}[u]$ and $B^{(0)}[u]$ are invariant under the change $u_{xt} \to u_{xt} + \phi_x$. It implies the same symmetry for $A[u]$ and $B[u]$. The generating function of connected correlations is

$$\exp(W[w,\hat{w}]) := \int \mathcal{D}[u]\mathcal{D}[\hat{u}]\exp(-\mathcal{S}[u,\hat{u}] + \hat{u} \cdot g^{-1} \cdot w$$
$$+ \hat{w} \cdot g^{-1} \cdot u), \quad \text{(A5)}$$

where the sources have been redefined, following [57,88], in a convenient way for the following. It also admits an expansion similar to the action

$$W[w,\hat{w}] = \hat{w} \cdot g^{-1} \cdot w - \hat{w} \cdot \hat{A}[w] + \frac{1}{2}\hat{w} \cdot \hat{B}[w] \cdot \hat{w} + O(\hat{w}^3), \quad \text{(A6)}$$

where the STS implies that $\hat{A}[w]$ and $\hat{B}[w]$ are invariant under the change $w_{xt} \to w_{xt} + \phi_x$. Finally the effective action functional Γ is defined as usual as the Legendre transform of W,

$$W[w,\hat{w}] + \Gamma[u,\hat{u}] = \hat{u} \cdot g^{-1} \cdot w + \hat{w} \cdot g^{-1} \cdot u. \quad \text{(A7)}$$

It admits the expansion

$$\Gamma[u,\hat{u}] = \hat{u} \cdot g^{-1} \cdot u + \hat{u} \cdot A[u] - \frac{1}{2}\hat{u} \cdot B[u] \cdot \hat{u} + O(\hat{u}^3). \quad \text{(A8)}$$

STS implies the same symmetry for $A[u]$ and $B[u]$ as for $A^{(0)}[u]$ and $B^{(0)}[u]$.

2. Relations to observables

The functional W is directly related to observables, i.e., correlation functions, in the following way: Consider the average over solutions of the equation of motion,

$$\overline{\langle e^{\int_{xt} \hat{w} \cdot g^{-1} \cdot u^s} \rangle_{\xi,u_0}} = \int \mathcal{D}[u]\mathcal{D}[\hat{u}]e^{-\mathcal{S}_w[u,\hat{u}] + \hat{w} \cdot g^{-1} \cdot u_{xt}}$$

$$= \int \mathcal{D}[u]\mathcal{D}[\hat{u}]u e^{-\mathcal{S}[u,\hat{u}] + \hat{u} \cdot g^{-1} \cdot w + \hat{w} \cdot g^{-1} \cdot u} = e^{W[w,\hat{w}]}. \quad \text{(A9)}$$

Here $\mathcal{S}_w$ is the MSR action in presence of w, while $\mathcal{S} \equiv \mathcal{S}_{w=0}$ is the action defined above, in the absence of w. As usual, to take into account the initial conditions (if necessary) all time integrals start at t_0 and an additional integral $\mathcal{D}[u_0]P[u_0]$ fixes its probability at $t=t_0$. Expanding the above average, one finds

$$W[w,\hat{w}] = \hat{w} \cdot g^{-1} \cdot \overline{\langle u \rangle}_w + \frac{1}{2}\hat{w} \cdot g^{-1} \cdot (\overline{\langle uu \rangle}_w$$
$$- \overline{\langle u \rangle}_w \overline{\langle u \rangle}_w) \cdot g^{-1} \cdot \hat{w} + O(\hat{w}^3). \quad (A10)$$

Note that the (matrix) average $\overline{\langle uu \rangle} - \overline{\langle u \rangle \langle u \rangle}$ is not the connected thermal average but the connected double (disorder+thermal) average. Note the index w which indicates that the above averages, e.g., $\langle u_{xt} \rangle_w$, are averages with respect to $\mathcal{S}_w$, i.e., in presence of the (given) driving w_{xt}. Comparing with Eq. (A6) we obtain

$$\overline{\langle u_{xt} \rangle}_w = w_{xt} - g_{xy}\hat{A}_{yt}[w], \quad (A11)$$

$$\overline{\langle u_{xt}u_{x't'} \rangle}_w - \overline{\langle u_{xt} \rangle}_w \overline{\langle u_{x't'} \rangle}_w = g_{xy}g_{x'y'}\hat{B}_{yt,y't'}[w], \quad (A12)$$

where summation (integration) over repeated indices is implicit. Until now w_{xt} is arbitrary. For a uniform driving w_t one has

$$\overline{\langle (w_t - \bar{u}_t) \rangle} = m^{-2}\frac{1}{L^d}\int_y \hat{A}_{yt}[w], \quad (A13)$$

$$\overline{\langle (w_t - \bar{u}_t)(w_{t'} - \bar{u}_{t'}) \rangle} - \overline{\langle (w_t - \bar{u}_t) \rangle}\,\overline{\langle (w_{t'} - \bar{u}_{t'}) \rangle}$$
$$= m^{-4}\frac{1}{L^{2d}}\int_{yy'} \hat{B}_{yt,y't'}[w]. \quad (A14)$$

These are the (spatially) local parts of the $\hat{A}$ and $\hat{B}$ functionals, and we expect

$$\lim_{L \to \infty} \lim_{\partial_t w(t) \to 0^+} \lim_{T \to 0} \frac{1}{L^d}\int_y \hat{A}_{yt}[w] = f_c, \quad (A15)$$

$$\lim_{L \to \infty} \lim_{\partial_t w(t) \to 0^+} \lim_{T \to 0} \frac{1}{L^{2d}}\int_{yy'} \hat{B}_{yt,y't'}[w] = L^{-d}\hat{\Delta}(w_t - w_{t'}). \quad (A16)$$

More relations can be derived, e.g., by considering the formal expansion (symbolically)

$$W[w + \delta w, \hat{w}]$$
$$= \sum_{n_1 n_2} \frac{1}{n_1! n_2!}\overline{\langle \hat{u} \cdots \hat{u}u \cdots u \rangle}_w^c (g^{-1}\delta w)^{n_1}(g^{-1}\hat{w})^{n_2}. \quad (A17)$$

Hence one has

$$\overline{\langle \hat{u}_{x't'}u_{xt} \rangle}_w = g_{xx'}^{-1}\delta_{tt'} - (\boldsymbol{\nabla}_w\hat{A}[w])_{x't',xt}. \quad (A18)$$

Let us also recall that the quadratic parts of W and Γ are (always)

$$W_{\text{quad}}[w,\hat{w}] = \hat{w} \cdot g^{-1} \cdot R \cdot g^{-1} \cdot w + \frac{1}{2}\hat{w} \cdot g^{-1} \cdot C \cdot g^{-1} \cdot \hat{w}, \quad (A19)$$

$$\Gamma_{\text{quad}}[u,\hat{u}] = \hat{u} \cdot R^{-1} \cdot u - \frac{1}{2}\hat{u} \cdot D \cdot \hat{u}, \quad (A20)$$

where R and C are the exact response and correlation functions (in the absence of w) and $C = R^t DR$.

Finally, it is useful to mention the terms without disorder,

$$A[u] = a \cdot u, \quad (A21)$$

$$\boldsymbol{\nabla}_u A[u] = a^t, \quad (A22)$$

$$g^{-1} + a = R^{-1}, \quad (A23)$$

$$\hat{A}[w] = \hat{a} \cdot w, \quad (A24)$$

$$\boldsymbol{\nabla}_w\hat{A}[w] = \hat{a}^t, \quad (A25)$$

$$g^{-1} - \hat{a} = g^{-1} \cdot R \cdot g^{-1}, \quad (A26)$$

with

$$\hat{a} \cdot (1 + g \cdot a) = a, \quad (A27)$$

$$\hat{a} = a \cdot (1 + g \cdot a)^{-1} \quad (A28)$$

3. Legendre transform

Our aim is to relate the functionals $\hat{A}$ and $\hat{B}$, which are observables as established above, to the functionals A and B associated to the effective action.

Let us thus perform the Legendre transform. In this transformation one defines the functionals $w[u,\hat{u}]$ and $\hat{w}[u,\hat{u}]$ which allow to compute Γ from W using Eq. (A7). One has

$$w = g \cdot \frac{\delta\Gamma}{\delta\hat{u}} = u + g \cdot A[u] - g \cdot B[u] \cdot \hat{u} + O(\hat{u}^2), \quad (A29)$$

$$\hat{w} = g \cdot \frac{\delta\Gamma}{\delta u} = \hat{u} + g \cdot \boldsymbol{\nabla}_u A[u] \cdot \hat{u} - \frac{1}{2}g \cdot \boldsymbol{\nabla}_u\hat{u} \cdot B[u] \cdot \hat{u} + O(\hat{u}^3). \quad (A30)$$

The inverse relations are useful as well,

$$u = g \cdot \frac{\delta W}{\delta\hat{w}} = w - g \cdot \hat{A}(w) + g \cdot \hat{B}(w) \cdot \hat{w} + O[\hat{w}^2], \quad (A31)$$

$$\hat{u} = g \cdot \frac{\delta W}{\delta w}$$
$$= \hat{w} - g \cdot \boldsymbol{\nabla}_w\hat{A}[w] \cdot \hat{w} + \frac{1}{2}g \cdot \boldsymbol{\nabla}_w\hat{w} \cdot \hat{B}[w] \cdot \hat{w} + O(\hat{w}^3). \quad (A32)$$

From Eqs. (A29) and (A31) one deduces that

$$w - u = g \cdot A[u] + O(\hat{u}) = g \cdot \hat{A}[w] + O(\hat{w}). \quad (A33)$$

This implies that

$$A[u] = \hat{A}[w]|_{\hat{u}=0} = \hat{A}[u + g \cdot A[u]], \qquad (A34)$$

which allows in principle to compute one functional from the other. One has the equivalent relation

$$\hat{A}[w] = A[w - g \cdot \hat{A}[w]], \qquad (A35)$$

Moreover

$$B[u] = -g^{-1} \cdot dw/d\hat{u}, \qquad (A36)$$

where $\hat{u}$ should be set to zero at the end. We have used a notation which makes the position of the indices clear. From Eq. (A30),

$$d\hat{w}/d\hat{u} = 1 + g \cdot \nabla_u A[u] - g \cdot \nabla_u \hat{u} \cdot B[u] + O(\hat{u}^2). \qquad (A37)$$

Note the subtle difference with

$$dw/du = 1 + g \cdot A[u]\overleftarrow{\nabla}_u - g \cdot B[u] \cdot \hat{u}\overleftarrow{\nabla}_u + O(\hat{u}^2). \qquad (A38)$$

This means that [at least at order $O(\hat{u}) = O(\hat{w})$, but eventually even exact]

$$g^{-1} \cdot dw/du = [g^{-1} \cdot d\hat{w}/d\hat{u}]^t. \qquad (A39)$$

From Eq. (A31) follows

$$\begin{aligned} B[u] &= -g^{-1} \cdot dw/d\hat{u} \\ &= -g^{-1} d\{u + g \cdot \hat{A}[w] - g \cdot \hat{B}[w] \cdot \hat{w} + O(\hat{w}^2)\}/d\hat{u} \\ &= d\{-\hat{A}[w] + \hat{B}[w] \cdot \hat{w} + O(\hat{w}^2)\}/d\hat{u} \\ &= \hat{A}[w]\overleftarrow{\nabla}_w \cdot g \cdot B[u] + \hat{B}[w] \cdot d\hat{w}/d\hat{u}, \qquad (A40) \end{aligned}$$

where it is implicit that $\hat{u}$ is set to zero at the end. It implies

$$\{1 - (\nabla_w \hat{A}[w])^t \cdot g\} \cdot B[u] = \hat{B}[w](1 + g \cdot \nabla_u A[u]) + O(\hat{u}). \qquad (A41)$$

This can also be written as

$$(d\hat{u}/d\hat{w})^t \cdot B[u] = \hat{B}[w] \cdot d\hat{w}/d\hat{u}. \qquad (A42)$$

Equivalently,

$$B[u] = (d\hat{w}/d\hat{u})^t \cdot \hat{B}[w] \cdot d\hat{w}/d\hat{u}. \qquad (A43)$$

Finally, the relation between the $\hat{B}$ and B functionals can be written as

$$B[u] = (1 + g \cdot \nabla_u A[u])^t \cdot \hat{B}[w] \cdot (1 + g \cdot \nabla_u A[u]), \qquad (A44)$$

where in this relation u and w are related via

$$w - u = g \cdot A[u] = g \cdot \hat{A}[w]. \qquad (A45)$$

It can also be written equivalently as

$$\hat{B}[w] = (1 - g \cdot \nabla_w \hat{A}[w])^t \cdot B[u] \cdot (1 - g \cdot \nabla_u \hat{A}[w]). \qquad (A46)$$

4. Evaluation of the functionals

Let us now evaluate the functionals $\hat{A}_{xt}[\{w_{yt}\}]$ and $\hat{B}_{xt,x't'}[\{w_{yt}\}]$ in various situations.

Let us consider first $T > 0$ *equilibrium dynamics*, i.e., a driving function w_{yt} which evolves infinitely slowly between $w_{yt_1} = w_1(y)$ and $w_{yt_2} = w_2(y)$ such that the system always remains in equilibrium (i.e., we consider the limit $t_2 - t_1 \to \infty$ at fixed $w_1 - w_2$). From Eq. (A11) and STS it is clear that $\hat{A}[w] = \hat{A}[0] = 0$ in that limit. This implies $u = w$ in Eq. (A45) and also $A[u] = 0$. It then implies that $\hat{B}[w] = B[w]$ and one recovers the results of Refs. [57,88] for the statics using replicas. More precisely one expects in that limit that $\hat{B}_{yt,y't'}[w] = B_{yt,y't'}[w] = \partial_{w_1(y)}\partial_{w_2(y')}R[w_1, w_2]$, where $\hat{R} = R$ is the two-replica functional of the statics. Hence it is a statement *only* about the infinitely separated time part of the $B[w]$ functional and not about the smaller time separation part (which contains the renormalization of η and highly complicated activated dynamics as described in [33]).

Consider now $T = 0$ and $w_{yt} = w(t) = vt$. From translational invariance $\hat{A}_{xt}[w]$ [see, e.g., Eq. (A11)] can only be a time and space independent v-dependent constant (assuming boundary conditions do not break translational invariance) which we choose to call $f(m, v)$. Because of Eq. (A45) one must have the equality

$$\hat{A}_{xt}[w] = A_{xt}[u] = f(m, v) \qquad (A47)$$

and $u = w - m^{-2}f(m, v) = vt - m^{-2}f(m, v)$ in Eq. (A45). The difference with the equilibrium statics is that this constant is nonzero. This is allowed despite the STS symmetry because we are considering the $T = 0$ limit first and the fact that $w(t)$ depends on t cannot be ignored even for $v = 0^+$. In that limit one has $f_c(m, v = 0^+) = f^\uparrow_c = -f_c(m, v = 0^-)$. Of course the fact that the constant depends uniquely on v assumes some ergodicity property, similarly if $w(t)$ is a more complicated adiabatic function there could be in general some history dependence. These issues have been discussed in Sec. VIII. For $N = 1$ we will rely on Middleton's theorem [87] which proves unicity of the solution. Note that at $T > 0$ Eq. (A47) remains true with a $f(m, v, T)$ such that $f(m, 0, T) = 0$ in agreement with the discussion of the previous paragraph.

Since the derivative of a constant is zero, using Eqs. (A47) and (A44) we find that at $T = 0$ with the choice $w = vt$ one has

$$B_{yt,y't'}[u = u(t) = vt - m^{-2}f(m,v)] = \hat{B}_{yt,yt'}[w] = \hat{\Delta}(v(t - t')). \qquad (A48)$$

Denoting $B_{yt,yt'}[u] = \Delta(u(t) - u(t'))$ gives

$$\Delta(w) = \hat{\Delta}(w), \qquad (A49)$$

a result on which is based our measurement of $\Delta(w)$ here and in [60].

APPENDIX B: CALCULATION OF SOME INTEGRALS

Here we compute the integrals in Eq. (84) of the main text. We need

$$\int_a^\infty ds e^{-s} \ln s = e^{-a} \ln a - \mathrm{Ei}(-a) \qquad (B1)$$

$$\mathrm{Ei}(-a) = -\int_a^\infty dt e^{-t}/t. \qquad (B2)$$

This gives

$$\tilde{\Delta}(W) = (1 - e^{-W}) \int_0^\infty da e^{-a(1-e^{-W})} \ln(a) e^{-ae^{-W}} \ln(ae^{-W})$$

$$- (1 - e^{-W}) \int_0^\infty da e^{-a(1-e^{-W})} \ln(a) \mathrm{Ei}(-ae^{-W})$$

$$+ e^{-W} \left(\gamma_E^2 + \frac{\pi^2}{6} + X\gamma_E \right) - \gamma_E^2. \qquad (B3)$$

Consider the integral

$$- \int_0^\infty da e^{-a(1-e^{-W})} \ln(a) \mathrm{Ei}(-ae^{-W})$$

$$= \int_0^\infty da e^{-a(1-e^{-W})} \ln a \int_{ae^{-W}}^\infty dt e^{-t}/t$$

$$= \int_1^\infty db \int_0^\infty da e^{-a(1-e^{-W})} \ln a \int_{ae^{-W}}^\infty dt e^{-tb}$$

$$= \int_1^\infty \frac{db}{b} \int_0^\infty da \ln a e^{-a(1-e^{-W})-ae^{-W}b}$$

$$= \int_1^\infty \frac{db}{b} \frac{1}{(1-e^{-W}) + be^{-W}}$$

$$\times \int_0^\infty da e^{-a}\{\ln a - \ln((1-e^{-W}) + be^{-W})\}$$

$$= -\gamma_E \frac{W}{1-e^{-W}} - \frac{1}{6(1-e^{-W})}$$

$$\times \left[\pi^2 - 3W^2 + 3\ln^2(e^W - 1) + 6\,\mathrm{Li}_2\left(\frac{1}{1-e^X}\right) \right]. \qquad (B4)$$

This yields

$$\tilde{\Delta}(x) = \frac{x^2}{2} - \frac{1}{2}\log^2(e^x - 1) - \mathrm{Li}_2\left(\frac{1}{1-e^x}\right), \qquad (B5)$$

which can be rewritten as Eq. (85) in the main text.

APPENDIX C: AVALANCHE PROCESS AND MARKOV CHAIN

It is useful to recast the avalanche process for the discrete model of uncorrelated forces as a Markov chain, and define an algorithm for easy use in the numerics.

Let us index jumps by n, they occur at positions $u_n^- := u_n$ (integer), where the force is F_n (real). Note that the w position of the jump is $w_n = u_n - m^{-2}F_n$. Given (u_n, F_n) one finds the next jump (u_{n+1}, F_{n+1}) by the following algorithm:

$$u_{n+1} = u_n + s_n, \quad F_{n+1} = f_{s_n}, \qquad (C1)$$

$$s_n = \min(p = 1, 2, \ldots \text{ such that } f_p < F_n + m^2 p), \qquad (C2)$$

where $f_1, f_2, \ldots$ are a sequence of IID random variables of distribution $P_0(f)$. The s_n (integers greater or equal to one) are the size of the avalanche and are determined at the same time. The variables (s_n, F_{n+1}) form a Markov chain with conditional probability $P(s_n, F_{n+1}|F_n)$.

$$P(s, F'|F) = P_0(F')\theta(F + m^2 s > F') \prod_{k=1}^{s-1} H(F + m^2 k), \qquad (C3)$$

$$P(s|F) = [1 - H(F + m^2 s)] \prod_{k=1}^{s-1} H(F + m^2 k), \qquad (C4)$$

$$H(F) = \int_F^\infty df P_0(f), \qquad (C5)$$

which is normalized $\Sigma_{s \geq 1} P(s|F) = 1$ using that $1 - H_1 + (1-H_2)H_1 + (1-H_3)H_1 H_2 + \cdots = 1 - H_1 H_2 H_3 \ldots$ and the fact that the H_k tend to zero as k increases.

Starting from, for instance, $P_0(F_0)$, the distribution for F_n is given by

$$P_n(F_n) = P(F_n|F_{n-1})P(F_{n-1}|F_{n-2}) \cdots P(F_1|F_0)P_0(F_0), \qquad (C6)$$

$$P(F'|F) = \sum_{s \geq 1} P(s, F'|F). \qquad (C7)$$

It converges to a stationary probability, noted $\tilde{P}(F)$, which satisfies

$$\sum_{s \geq 1} P(s, F'|F)\tilde{P}(F) = \tilde{P}(F'). \qquad (C8)$$

Once we find $\tilde{P}(F)$ the joint distribution of (s_n, F_{n+1}, F_n) is known,

$$P(s_n, F_{n+1}, F_n) = P(s_n F_{n+1}|F_n)\tilde{P}(F_n). \qquad (C9)$$

Hence the avalanche-size distribution is

$$P(s) = \int dF P(s|F)\tilde{P}(F). \qquad (C10)$$

The sequence of waiting times is such that

$$w_{n+1} - w_n = W_n = s_n - m^{-2}(F_{n+1} - F_n). \qquad (C11)$$

Hence the joint size and waiting-time distribution is

$$P(W, s) = \int dF dF' \delta(W - s + m^{-2}(F' - F))P(s, F'|F)\tilde{P}(F). \qquad (C12)$$

The problem is thus to determine the solution of Eq. (C8). One can formally write it as an infinite product,

$$\tilde{P}(F_0) = \int dF_1 dF_2 \ldots \prod_{k=1}^{\infty} P(F_{k-1}|F_k), \qquad \text{(C13)}$$

$$P(F'|F) = P_0(F') \sum_{s \geq 1} \theta(F + m^2 s > F') \prod_{k=1}^{s-1} H(F + m^2 k), \tag{C14}$$

which however also contains an infinite number of integrations. This method does not seem very practical (see, however, [64]) and in the text we obtain the result by another method.

APPENDIX D: GENERAL RESULTS FOR UNCORRELATED DISORDER

Proof that $P(w) = P(s)$. Suppose that the following variable transformation holds between $j - w$, and the corresponding

$$f(j - w) = a_w(j) \tag{D1}$$

up to a constant shift and a rescaling. We recall that $f(y) = \exp(y)$ (Gumbel), $f(y) = y^{\alpha}$, $y > 0$ (Weibull), and $f(y) = (-y)^{-\alpha}$, $y < 0$ (Fréchet).

Then

$$P_w(w', s > S) = \int dy f''(y) e^{-f(y+W) - f(y+s) + f(y)}, \tag{D2}$$

where integration bounds depend on the class (real axis for Gumbel, positive axis for Weibul, and negative axis for Fréchet). Using the relations in the text one finds that the joint waiting-time and avalanche-size distribution is

$$P(w > W, s > S) = \frac{\int_0^{\infty} dy f''(y) e^{-f(y+W) - f(y+S) + f(y)}}{\int_0^{\infty} dy f''(y) e^{-f(y)}}, \tag{D3}$$

where the denominator is such that the distribution is properly normalized. Also note that for some choice of variables, one has to be careful with the bounds of integration, see the Fréchet class, Eq. (183).

This formula shows that avalanche-size and waiting-time distribution are equal for all microscopic (uncorrelated) disorder: $P(S) = P(W)$.

The distribution of the local area $a = ws$ defined in the text can be obtained as follows:

$$P(a > A) = \int_0^{\infty} dW \int_0^{\infty} dS [\partial_w \partial_s P(w > W, s > S)] \theta(WS - A)$$

$$= \int_0^{\infty} dW \int_0^{\infty} dS P(w > W, s > S) \partial_W \partial_S \theta(WS - A)$$

$$= \int_0^{\infty} dW \int_0^{\infty} dS P(w > W, s > S)$$

$$\times [\delta(A - WS) - WS \delta'(A - WS)]$$

$$= -A \frac{\partial}{\partial A} \int_0^{\infty} dW \int_0^{\infty} dS P(w > W, s > S) \delta(A - WS). \tag{D4}$$

We note a subtle point that when writing the last term as the derivative with respect to A of $-A \int P(w > W, s > S) \delta(A - WS)$, the explicit derivative of A cancels the first term.

Inserting the integral representation (D3) for $P(w > W, s > S)$ yields

$$P(a > A) = \frac{-\frac{A\partial}{\partial A} \int_0^{\infty} \frac{dW}{W} \int_0^{\infty} dy f''(y) e^{-f(y+W) - f(y+A/W) + f(y)}}{\int_0^{\infty} dy f''(y) e^{-f(y)}}. \tag{D5}$$

Note that boundary terms from the partial integration in Eq. (D4) vanish except for $w = 0$ or $s = 0$, in which case $A = 0$. Thus we could possibly have a term $\sim \delta(A)$. However we know that for $w = 0$ we do not have a diverging probability for an avalanche, and vice versa for w and s exchanged. The above result can also be written as

$$P(a > A) = \frac{-\frac{A\partial}{\partial A} \int_0^{\infty} dw \int_0^{\infty} dy f''(y) e^{-f(y+e^w) - f(y+Ae^{-w}) + f(y)}}{\int_0^{\infty} dy f''(y) e^{-f(y)}}. \tag{D6}$$

For the Gumbel class, $f(y) = e^y$, and this yields the formula given in the text.

APPENDIX E: FIRST-PASSAGE TIMES AND AVALANCHE DISTRIBUTIONS

In this appendix we recall the basic method of the backward diffusion equation to compute distributions of first passage times on a half line and an interval, and then extend it to compute the first-passage-time distribution in the velocity-diffusion equation of the ABBM model.

1. First-passage-time distribution on a half line

Let us call $T(w'; w)$ the first-passage time at w' of a BM starting at position $w < w'$ at time 0. Let us recall that the generating function

$$G(w', p; w) = \langle e^{-pT(w'; w)} \rangle \tag{E1}$$

satisfies the diffusion equation and boundary conditions

$$D \partial_w^2 G + b \partial_w G = pG,$$

$$G(w', p; w') = 1, \quad G(w', p = 0; w = -\infty) = 0 \tag{E2}$$

for $b > 0$. To see that, one introduces the diffusion kernel on $x \in [-\infty, w']$ in presence of an absorbing boundary at $x = w'$, which satisfies

$$\partial_t P = D\partial_x^2 P - b\partial_x P = D\partial_w^2 P + b\partial_w P,$$

$$P(x,t=0|w,0) = \delta(x-w), \quad P(w',t|w,0) = 0. \quad \text{(E3)}$$

By definition of the exit time one has for $p>0$,

$$G(w',p;w) = -\int_0^\infty dt e^{-pt}\partial_t \int_{x<w'} P(x,t|w,0)$$

$$= 1 - p\int_{x<w'} \hat{P}(x,p|w,0), \quad \text{(E4)}$$

with $\hat{P}$ the Laplace transform of P. The latter satisfies

$$p\hat{P}(x,p|w,0) - \delta(x-w) = (D\partial_w^2 + b\partial_w)\hat{P}(x,p|w,0). \quad \text{(E5)}$$

Multiplying with $-p$ and integrating over x from $-\infty$ to w' yields Eq. (E2).

The solution of Eq. (E2) including the boundary conditions is

$$G(w',p;w) = \exp\left(\frac{b-\sqrt{4pD+b^2}}{2D}(w'-w)\right). \quad \text{(E6)}$$

For $b\geq 0$ it satisfies $\lim_{p\to 0} G(w,p;w')=1$. It is then inverted into the probability $P(u;w'-w)du$ that $T(w';w)\in[u,u+du[$,

$$P(u;W) = \frac{W}{\sqrt{4\pi D}}u^{-3/2}\exp\left(-\frac{(bu-W)^2}{4Du}\right)\theta(u), \quad \text{(E7)}$$

where $W=w'-w$. Note that for negative drift $b<0$ one has

$$\lim_{p\to 0} G(w,p;w') = 1-q,$$

$$q := \text{Prob}(T(w';w)=\infty) = 1 - \exp\left(-\frac{|b|(w'-w)}{D}\right) \quad \text{(E8)}$$

since in that case there is a finite probability q that the walk starting at w never hits $x=w'$.

The Laplace transform (LT) of the probability to be at w at time t can be written as the probability to arrive there for the first time, and then repeatedly going with and against the drift, coming always back to w,

$$\text{LT}_{t\to p}\frac{w_0}{\sqrt{4\pi Dt}}e^{-(w-bt)^2/(4Dt)} = \frac{w_0}{\sqrt{4pD+b^2}}e^{\frac{b-\sqrt{4pD+b^2}}{2D}w}$$

$$\approx \frac{w_0^2}{2D}G(0,p;-w)\frac{1+\Pi_0^-(p)}{1-\Pi_0^+(p)\Pi_0^-(p)}, \quad \text{(E9)}$$

where $\Pi_0^+(p)=G_{b=|b|}(w_0,p;0)$ is the return probability going along the drift, and $\Pi_0^-(p)=G_{b=-|b|}(w_0,p;0)$ going against the drift (with $w_0>0$ a small cutoff which allows one to cross 0 in the microscopic model). Equation (E9) expresses that the probability to be near $x=0$ is a sum of nth passage time events; the factor $w_0^2/2D=dt=dw^2/(2D)$ is the change of measure from time to space.

Similarly consider the problem of the last passage time t_0 of a Brownian at $w=0$, with initial condition $w=0$ at $t=0$. Its Laplace transform can again be expressed as a geometric series

$$\Pi_{\text{last}}(p) = [1-\Pi_0^-(0)]\frac{\Pi_0^+(p)}{1-\Pi_0^+(p)\Pi_0^-(p)} \approx \frac{1}{\sqrt{1+\dfrac{4Dp}{b^2}}}. \quad \text{(E10)}$$

Hence

$$\Pi_{\text{last}}(t_0) = \frac{|b|}{\sqrt{4\pi Dt_0}}e^{-b^2 t_0/(4D)}, \quad \text{(E11)}$$

$$\langle t_0\rangle = \frac{2D}{b^2}, \quad \langle t_0^2\rangle = \frac{12D^2}{b^4}. \quad \text{(E12)}$$

2. First-passage-time distribution on an interval

Consider now a Brownian starting at w in an interval $[w_a,w_b]$. Consider the functions $G_a(w,p)$, $G_b(w,p)$, and $G(w,p)=G_a(w,p)+G_b(w,p)$ which satisfy the same differential equation (E2) but with boundary conditions

$$G_a(w_a,p) = 1, \quad G_a(w_b,p) = 0,$$

$$G_b(w_b,p) = 1, \quad G_b(w_a,p) = 0. \quad \text{(E13)}$$

Then $G(w,p)=\langle e^{-pT_{ab}(w)}\rangle$ is the generating function for the first exit time $T_{ab}(w)$ of the interval $[w_a,w_b]$ by a walker starting at $w\in[w_a,w_b]$ at time zero. It satisfies Eq. (E2) with boundary conditions $G(w_a,p)=1$ and $G(w_b,p)=1$. One finds

$$G_a(w,p) = e^{b/2D(w_a-w)}\frac{\sinh(\mu(w_b-w))}{\sinh(\mu(w_b-w_a))}, \quad \text{(E14)}$$

$$G_b(w,p) = e^{b/2D(w_b-w)}\frac{\sinh(\mu(w-w_a))}{\sinh(\mu(w_b-w_a))}, \quad \text{(E15)}$$

$$\mu = \frac{1}{2D}\sqrt{4Dp+b^2}. \quad \text{(E16)}$$

One checks that $G(w,p=0)$ irrespective of the sign of b as the walk is certain to exit the interval. The function $G_a(w,p)$ [respectively, $G_b(w,p)$] is the same generating function restricted to walks exiting in w_a (respectively, w_b), with normalizations

$$p_a = G_a(w, p = 0) = \frac{\exp\left(\dfrac{b}{D}(w_b - w)\right) - 1}{\exp\left(\dfrac{b}{D}(w_b - w_a)\right) - 1}, \quad \text{(E17)}$$

$$p_b = G_b(w, p = 0) = 1 - p_a, \quad \text{(E18)}$$

for $b > 0$.

One way to derive these results is to introduce the diffusion kernel $P(x, t | w, 0)$ with absorbing boundary conditions at $x = w_a$ and $x = w_b$. Its expression reads in Laplace

$$P(x, p | w, 0) = \begin{cases} e^{b/2D(x-w)} \dfrac{\sinh(\mu(x - w_a)) \sinh(\mu(w_b - w_0))}{D\mu \sinh(\mu(w_b - w_a))} & \text{for } w_a < x < w, \\[3mm] e^{b/2D(x-w)} \dfrac{\sinh(\mu(w_b - x)) \sinh(\mu(w - w_a))}{D\mu \sinh(\mu(w_b - w_a))} & \text{for } w < x < w_b. \end{cases} \quad \text{(E19)}$$

It satisfies the diffusion equation with the proper boundary conditions. This is obtained as follows:

$$G(p, w) = -\int_0^\infty dt\, e^{-pt} \partial_t \int_{w_a}^{w_b} dx\, P(x, t | w, 0)$$
$$= D[\partial_x P(x, p | w, 0)|_{x=w_a} - \partial_x P(x, p | w, 0)|_{x=w_b}], \quad \text{(E20)}$$

where the first term is $G_a(p, w)$ and the second $G_b(p, w)$. They represent the flux from each boundary.

3. Avalanche distribution for the ABBM model

Let $s = T(\mathbf{v}', \mathbf{v})$ be the first passage "time" from $\mathbf{v}$ at time $u = 0$ to $\mathbf{v}' < \mathbf{v}$ at time s, the avalanche size (here defined with some velocity cutoff $\mathbf{v}'$). The generating function $G(\mathbf{v}', p; \mathbf{v}) = \exp(-sp)$ satisfies the backward diffusion equation

$$\sigma \partial_{\mathbf{v}}^2 G + \left(\frac{m^2 v}{\mathbf{v}} - m^2\right) \partial_{\mathbf{v}} G = pG, \quad \text{(E21)}$$

$$G(\mathbf{v}', p; \mathbf{v}') = 1, \quad G(\mathbf{v}', p; +\infty) = 0 \quad \text{(E22)}$$

a. Solution without the drift term

From now on we denote

$$x = \frac{m^2 v}{\sigma}. \quad \text{(E23)}$$

The solution, if one first drops the drift term, is

$$G(\mathbf{v}', p; \mathbf{v}) = \left(\frac{\mathbf{v}}{\mathbf{v}'}\right)^{(1-x)/2} \frac{K_{|1-x|/2}(\mathbf{v}\sqrt{p/\sigma})}{K_{|1-x|/2}(\mathbf{v}'\sqrt{p/\sigma})}. \quad \text{(E24)}$$

One expects that it describes correctly small avalanches.

There are two cases. For $x \leq 1$ one has $G(p=0) = 1$, i.e., the velocity is certain to reach any fixed $\mathbf{v}' > 0$. The leading behavior at small $\mathbf{v}, \mathbf{v}'$ is then for $x < 1$,

$$G - 1 = -C(p/4\sigma)^{(1-x)/2}, \quad \text{(E25)}$$

$$C = -\frac{\Gamma\left(\dfrac{x-1}{2}\right)}{\Gamma\left(\dfrac{1-x}{2}\right)} [\mathbf{v}^{1-x} - (\mathbf{v}')^{1-x}]. \quad \text{(E26)}$$

Inverse Laplace transform from p to s yields a distribution $1/s^\tau$ with the value of $\tau = (3-x)/2$ given in the text. The small avalanche cutoff s_0, necessary since $1/s^\tau$ is not normalizable at small s for $\tau > 1$, is provided by $\mathbf{v}, \mathbf{v}'$ and its full form can in principle be obtained by inverse Laplace transform from p to s of Eq. (A24). Its order of magnitude is easy to read from Eq. (E24) as $s_0 \sim \mathbf{v}^2/\sigma$ (see below for a more precise estimate).

One notes that the limit $\mathbf{v}' \to 0$ can be taken for $x < 1$ for any $\mathbf{v}$. It is then easy to inverse Laplace transform (E24) in that limit and to obtain the probability that if the velocity at $u = 0$ is $\mathbf{v}$, then the next stopping point u' is in the interval $u' \in [s, s+ds]$ as

$$G(0, s; \mathbf{v}) ds = \frac{1}{\Gamma(\mu)} \frac{ds}{s} \left(\frac{s_0}{s}\right)^\mu e^{-s_0/s}, \quad \text{(E27)}$$

$$s_0 = \mathbf{v}^2/(4\sigma), \quad \mu = (1-x)/2. \quad \text{(E28)}$$

Next one can use the stationary distribution to find the probability that choosing a $u = 0$ the next stopping point is at s,

$$\int_0^\infty d\mathbf{v}\, G(0, s; \mathbf{v}) P_{\text{eq}}(\mathbf{v}) = \frac{2\sigma}{\Gamma(\mu)\Gamma(x) v s^\mu} \left(\frac{m^2}{\sigma}\right)^x (4\sigma)^{-\mu}$$

where to be consistent we have assumed $s \ll s_m = \sigma/m^4$.

For $x > 1$, the probability of ever reaching $\mathbf{v}' > 0$ is $G(p=0) = (\frac{\mathbf{v}'}{\mathbf{v}})^{x-1} < 1$, from Eq. (E24). At small $\mathbf{v}, \mathbf{v}'$ (and of the same order) the following expansion holds for $1 < x < 3$:

$$G = \left(\frac{\mathbf{v}'}{\mathbf{v}}\right)^{x-1}\left(1 + \frac{\Gamma\left(\dfrac{1-x}{2}\right)}{\Gamma\left(\dfrac{x-1}{2}\right)}\left(\frac{p}{4\sigma}\right)^{(x-1)/2}[\mathbf{v}^{x-1} - (\mathbf{v}')^{x-1}]\right).$$

$$(E29)$$

$$G = (\mathbf{v}', p; \mathbf{v}) = \left(\frac{\mathbf{v}}{\mathbf{v}'}\right)^{1-x} e^{\frac{m^2 - \sqrt{m^4 + 4p\sigma}}{2\sigma}(\mathbf{v} - \mathbf{v}')} \frac{U\left(1 - \mathbf{v}\dfrac{m^2}{2\sigma}\left[1 + \dfrac{m^2}{\sqrt{m^4 + 4p\sigma}}\right], 2 - x, \dfrac{\sqrt{m^4 + 4p\sigma}}{\sigma}\mathbf{v}\right)}{U\left(1 - \mathbf{V}'\dfrac{m^2}{2\sigma}\left[1 + \dfrac{m^2}{\sqrt{m^4 + 4p\sigma}}\right], 2 - x, \dfrac{\sqrt{m^4 + 4p\sigma}}{\sigma}\mathbf{V}'\right)} \qquad (E30)$$

which reduces for $v = 0^+$ to the expression obtained for quasistatic avalanches,

$$G(\mathbf{v}', p; \mathbf{v})(\mathbf{v}', p; \mathbf{v}) = e^{\frac{m^2 - \sqrt{m^4 + 4p\sigma}}{2\sigma}(\mathbf{v} - \mathbf{v}')}, \qquad (E31)$$

from which, after inverse Laplace, Eq. (202) was obtained.

One can now check that $G(p=0) = 1$ for all x and $\mathbf{v}, \mathbf{v}' > 0$; hence thanks to the drift the walk comes back infinitely often, as announced in the text.

Let us consider the leading behavior at small $\mathbf{v}, \mathbf{v}'$. The expansion has the form

$$G = \frac{A[1 + O(\mathbf{v}^2)] + B\mathbf{v}^{1-m^2 v/\sigma}[1 + O(\mathbf{v})]}{A[1 + O((\mathbf{v}')^2)] + B(\mathbf{v}')^{1-m^2 v/\sigma}[1 + O(\mathbf{v}')]}$$

where A and B are complicated functions of p. Here we focus on the case $v < \sigma/m^2$, then

$$G - 1 = \frac{B}{A}(\mathbf{v}^{1-m^2 v/\sigma} - (\mathbf{v}')^{1-m^2 v/\sigma}). \qquad (E32)$$

This yields

$$G - 1 = \left(\frac{\sqrt{m^4 + 4p\sigma}}{\sigma}\right)^{1-m^2 v/\sigma} \frac{\Gamma\left(-1 + \dfrac{m^2 v}{\sigma}\right)}{\Gamma\left(1 - \dfrac{m^2 v}{\sigma}\right)}$$

$$\times \frac{\Gamma\left(1 - \dfrac{m^2 v}{2\sigma}\left(1 + \dfrac{m^2}{\sqrt{m^4 + 4p\sigma}}\right)\right)}{\Gamma\left(\dfrac{m^2 v}{2\sigma}\left(1 - \dfrac{m^2}{\sqrt{m^4 + 4p\sigma}}\right)\right)}$$

$$\times (\mathbf{v}^{1-m^2 v/\sigma} - (\mathbf{v}')^{1-m^2 v/\sigma}). \qquad (E33)$$

For $p \gg s_m^{-1} = m^4/\sigma$ one can check that this expression reproduces Eq. (E25) above; hence in that case the distribution of small avalanches can be found neglecting the drift. From this

This shows that, *conditioned to returning near zero velocity* the avalanches size distribution has again a tail $1/s^\tau$ for $s \gg s_0$, with $\tau = (1+x)/2 > 1$.

b. Solution with the drift term

Taking into account the drift term in Eq. (E21) reintroduces the large-size cutoff for avalanches at $s_m = \sigma/m^4$.

It is also possible to solve the full problem, with the drift. One finds for the Laplace transform of the first-passage time:

expression Laplace inversion allows, in principle, to obtain the full avalanche distribution. We will not attempt to perform it but note that there is an additional pole structures for $p = p_n$,

$$p_n = -\frac{m^4}{4\sigma} \frac{n(n-x)}{\left(n - \dfrac{x}{2}\right)^2}, \quad n = 1, 2, \dots, \qquad (E34)$$

which implies a decay

$$P(s) \sim e^{-\frac{(1-x)}{(2-x)^2}s/s_m} \qquad (E35)$$

at large $s \gg s_m$.

APPENDIX F: SOME ONE-POINT OBSERVABLES FOR THE BROWNIAN FORCE LANDSCAPE

We present here a few partial results for one-point observables for the Brownian force landscape, deferring a more complete study to the future.

Note that since $F(u)$ is an unbounded Brownian landscape, it has an infinite threshold force $2f_d = \max F(u) - \min F(u)$. However the model studied here of a particle dragged by a parabolic well is well defined, and from it one defines an average critical force,

$$f_c(m) := m^2 \overline{[w - u(w)]} \sim m^{2-\zeta}, \qquad (F1)$$

which diverges[6] as $m \to 0$ for $\zeta > 2$. As discussed in the main text, for $\gamma = 1$ one has $\zeta = 4$.

Let us now examine the one-point probability of the process $u(w)$. Since it is a long-range correlated landscape, there is a subtlety linked to the choice of boundary conditions.

---

[6]Note that in fact this was already the case for some members of class I.

1. Special boundary conditions

If we first fix $u(w=0)=0$, the probability $P_w(u)$ that $u(w)=u$ for $u>0$ is equal to the probability that the first passage time of $\phi(u')$ at w is u, starting at zero. Hence we find

$$P_w(u) = P(u;w), \tag{F2}$$

where $P(u;w)$ is defined in Eq. (E7). In fact, it follows from the Markov property that if we impose $u(w=0)=0$ and leave the future unconstrained, the n-point probability is

$$P_{w_1,\ldots,w_n}(u_1,\ldots,u_n) = P(u_1;w_1)P(u_2-u_1;w_2-w_1) \times \cdots$$
$$\times P(u_n-u_{n-1};w_n-w_{n-1}) \tag{F3}$$

for $0 \le w_1 \le w_2 \ldots \le w_n$. Computing the moments of Eq. (F2) one finds

$$\overline{u(w)-w} = 0, \tag{F4}$$

$$\overline{[u(w)-w]^2} = 2Dw = \frac{2\sigma}{m^4}w, \tag{F5}$$

hence one finds that the critical force $f_c(m)$, which is proportional to the average extension of the spring pulling the particle, is *zero*. On the other hand, the total area of the hysteresis loops per unit length cannot vanish—in fact from Eq. (F5) we can guess that it should grow as $\sqrt{w}$. Hence by contrast with the case of the uncorrelated force landscape, these two quantities cannot be equal.

To understand this apparent paradox let us note that to insure $u(w=0)=0$ one needs to impose rather strong conditions, e.g., $F(u)=0$ for all $u \le 0$. Otherwise, there is a nonzero probability that the BM has taken values $\phi(u)>w=0$ in the past, i.e., for $u<0$, which is in contradiction with $u(w=0)=0$. If we now want to use the hysteresis loop argument in a symmetric way, it would require a similar choice at some prescribed $u(w=W)=0$. But then Eqs. (F2) and (206) do not hold anymore (it holds for a Brownian unconstrained in the future). Since that procedure produces a nonstationary result, we do not discuss it further.

2. A more generic situation

First note that shifting $F(u)$ by a constant leaves (200) unchanged, but also shifts $w-u(w)$ while it does not change the area of the hysteresis loop. Hence comparing $f_c(m)=m^2\overline{[w-u(w)]}$ with the area of the hysteresis loop makes sense only for a statistically symmetric landscape. To eliminate this unimportant shift we can consider a distribution of forces symmetric around zero by setting $F(u=0)=0$. This is one way to fix the problematic zero mode of the Brownian landscape. This does not mean that $u_1 := u(w=0)$ is necessarily at zero. u_1 is the position of the first crossing of $\phi(u)=w=0$ by the BM. The probability distribution of $u_1 \le 0$ is given by (see Appendix E)

$$\Pi_{\text{last}}(u_1) = \frac{m^2}{\sqrt{4\pi\sigma|u_1|}}e^{-m^4|u_1|/(4\sigma)}\theta(-u_1). \tag{F6}$$

This yields a critical force

$$f_c(m) = -m^2\overline{u_1} = \frac{2\sigma}{m^2}, \tag{F7}$$

which makes more sense, i.e., it is positive and obeys the expected scaling.

However, to be a bit more general, what we have just computed is the conditional probability $P_{w_1}[u_1|F(u_a)=f_a]$ with the choice $u_a=0$ and $f_a=0$ (which can be realized using shifts of the axis) *and* the additional choice $w_1=u_a-f_a/m^2$ (hence $w_1=0$). One wonders whether the critical force depends on that choice.

To answer this question, we need to compute $P_{w_1}(u_1|F(0)=0)$ as a function of w_1. There are two cases: If $w_1<0$, then $u_1 \ge 0$ and one has

$$P_{w_1 \le 0}(u_1|F(0)=0)$$
$$= \theta(-u_1)LT^{-1}_{p \to -u_1}G_{b=|b|}(|w_1|,p;0)\Pi_{\text{last}}(p). \tag{F8}$$

This gives

$$P_{w_1 \le 0}(u_1|F(0)=0) = \theta(-u_1)\frac{|b|}{\sqrt{4\pi D|u_1|}}e^{-(|b||u_1|-|w_1|)^2/(4D|u_1|)}.$$

One finds

$$\int du_1 u_1 P_{w_1 \le 0}(u_1|F(0)=0) = -\frac{2D}{b^2} - \frac{|w_1|}{|b|}. \tag{F9}$$

If $w_1>0$ there are two subcases, and the total reads

$$P_{w_1 \ge 0}(u_1|F(0)=0)$$
$$= \theta(-u_1)LT^{-1}_{p \to -u_1}G_{b=-|b|}(w_1,p;0)\Pi_{\text{last}}(p)$$
$$+ \theta(u_1)LT^{-1}_{p \to u_1}G_{b=|b|}(w_1,p;0)$$
$$\times[1-G_{b=-|b|}(w_1,p=0;0)]. \tag{F10}$$

This gives

$$P_{w_1 \ge 0}(u_1|F(0)=0)$$
$$= \theta(-u_1)\frac{|b|}{\sqrt{4\pi D|u_1|}}e^{-(|b||u_1|+w_1)^2/(4D|u_1|)}$$
$$+ \theta(u_1)\frac{w_1}{\sqrt{4\pi D}}u_1^{-3/2}e^{-(|b|u_1-w_1)^2/(4Du_1)}(1-e^{-\frac{|b|}{D}w_1}),$$
$$\tag{F11}$$

which can be checked to be correctly normalized. One obtains

$$\int_{-\infty}^0 du_1 u_1 P_{w_1 \ge 0}(u_1|F(0)=0) = -\left(\frac{2D}{b^2}+\frac{w_1}{|b|}\right)e^{-\frac{|b|}{D}w_1},$$

$$\int_0^{+\infty} du_1 u_1 P_{w_1 \geqslant 0}(u_1 | F(0) = 0) = \frac{w_1}{|b|}\left(1 - e^{-\frac{|b|}{D}w_1}\right).$$

Hence we find, setting $|b| = 1$ and $D = \sigma/m^4$, conditioned to $F(0) = 0$,

$$m^2\overline{(w_1 - u(w_1))} = 2\sigma/m^2, \quad w_1 \leqslant 0,$$

$$m^2\overline{(w_1 - u(w_1))} = 2(m^2 w_1 + \sigma/m^2)e^{-m^4 w_1/\sigma}, \quad w_1 \geqslant 0 \tag{F12}$$

For the past ($w_1 \leqslant 0$) one recovers the previous result, while for the future it decreases to zero at large w_1.

We could try to generalize further by picking a u_a and averaging over f_a with some distribution. Using the condition $w = u - F(u)/m^2$ one can check that

$$P_{w_1}(u_1 | F(u_a) = f_a) = P_{w_1 - u_a + f_a/m^2}(u_1 - u_a | F(0) = 0).$$

Hence we can use the previous calculation. For fixed w_1, u_a, and f_a one has

$$m^2\int du_1(w_1 - u_1)P_{w_1}(u_1 | F(u_a) = f_a) = m^2\int du_1(w_1 - u_1)P_{w_1 - u_a + f_a/m^2}(u_1 - u_a | F(0) = 0)$$

$$= m^2\int du_1'(w_1' - f_a/m^2 - u_1')P_{w_1'}(u_1' | F(0) = 0)$$

$$= \begin{cases} 2\sigma/m^2 - f_a, & \text{for } w_1 - u_a + f_a/m^2 \leqslant 0 \\ 2(m^2 w_1' + \sigma/m^2)e^{-m^4 w_1'/\sigma} - f_a & \text{for } w_1' = w_1 - u_a + f_a/m^2 \geqslant 0, \end{cases} \tag{F13}$$

which can, in principle, be averaged on f_a. It is not clear however at this stage which distribution to choose and how to relate these quantities to the area of the hysteresis loop. Further work is needed to clarify these issues.

APPENDIX G: FIRST RETURN PROBABILITIES IN D DIMENSIONS

In this appendix, we recall standard methods to derive the first return probability in d dimensions, using a regular hypercubic lattice.

Consider a random walk on the integers $\mathbb{Z}$. The probability to return to the origin after t steps ($t = 2m$ even) is [89]

$$u_t = \binom{t}{t/2} 2^{-t}. \tag{G1}$$

This is seen by noting that giving weight a for a step to the right, and $b = 1 - a$ for a step to the left, the probability to be at x after t steps is the same as taking i steps to the right and $t - i$ to the left, with $x = 2i - t$ and equal to $p_x = a^i b^{t-i}\binom{t}{i}$, from which the above result is obtained for $a = b = 1/2$, $i = t/2$. We note $u_0 = 1$.

The probability to return to the origin for the first time after t steps is noted f_t, and we note $f_0 = 0$. In order to be at the origin at time t, we must return for the first time no later than t, and can then make a new excursion. Therefore we have (for $t > 0$ even)

$$u_t = f_2 u_{t-2} + f_4 u_{t-4} + \cdots + f_t u_0. \tag{G2}$$

Introducing the generating functions

$$u(x) := \sum_{m=0}^{\infty} u_{2m}x^m, \quad f(x) := \sum_{m=0}^{\infty} f_{2m}x^m, \tag{G3}$$

Eq. (G2) can be written as

$$u(x) = 1 + f(x)u(x). \tag{G4}$$

This gives for the probabilities (G1)

$$u(x) = \frac{1}{\sqrt{1-x}}, \quad f(x) = 1 - \sqrt{1-x}; \tag{G5}$$

thus the first return probability in $d = 1$ at time t is

$$f_t = \frac{u_t}{t-1}. \tag{G6}$$

At large times,

$$u_{2m} \approx \frac{1}{\sqrt{\pi m}}, \quad f_{2m} \approx \frac{1}{2\sqrt{\pi}m^{3/2}}. \tag{G7}$$

We now want to calculate the same quantities in d dimensions, noted u_t^d and f_t^d. u_t^d is simply

$$u_t^d = (u_t)^d. \tag{G8}$$

As an example, in $d = 2$,

$$u^{d=2}(x) = \frac{2K(x)}{\pi}, \quad f^{d=2}(x) = 1 - \frac{\pi}{2K(x)}, \tag{G9}$$

with K the elliptic K function, and in $d = 3$,

$$u(x) = \left(\frac{2K\left(\frac{1}{2}(1 - \sqrt{1 - x})\right)}{\pi} \right)^2. \qquad (G10)$$

In general, an analytic solution for the coefficients is not possible. We therefore give the asymptotic behavior for large t, i.e., small $1 - x$ such that the series picks up contributions at large times. Noting $s := -\ln x$, we obtain for $d < 2$

$$u^d(x) = \sum_{m=0}^{\infty} u_{2m}^d x^m \approx \int_0^{\infty} dm \frac{1}{(\pi m)^{d/2}} \exp(-sm)$$

$$= \pi^{-d/2} s^{(d/2)-1} \Gamma\left(1 - \frac{d}{2}\right). \qquad (G11)$$

Note that for $d \geq 2$, a uv cutoff is needed, which we discuss below. Using Eq. (G4) yields

$$f^d(x) = 1 - \frac{1}{u^d(x)} \approx 1 - \frac{\pi^{d/2} s^{1-d/2}}{\Gamma\left(1 - \frac{d}{2}\right)}. \qquad (G12)$$

Transforming inverse Laplace gives

$$f_{2m}^d \approx \frac{2 - d}{2} m^{d/2 - 2} \pi^{d/2 - 1} \sin\left(\frac{d\pi}{2}\right) \quad \text{for } d < 2.$$

$$(G13)$$

Let us now consider $d > 2$. Then

$$u^d(x) \approx u^d(1) + \pi^{-d/2} s^{d/2 - 1} \Gamma\left(1 - \frac{d}{2}\right), \qquad (G14)$$

$$u^d(1) \approx 1 + \pi^{-d/2} \zeta\left(\frac{d}{2}\right), \quad d < 2, \qquad (G15)$$

$$u^{d=3}(1) = \frac{\pi}{\Gamma(3/4)^4} = 1.3932\ldots, \qquad (G16)$$

where the approximation for $u^d(1)$ valid for d near 2 was obtained summing using $u_{2m}^d \approx (\pi m)^{-d/2}$ (it gives 1.469 for $d = 3$). Then

$$f^d(x) = 1 - \frac{1}{u^d(x)} \approx 1 - \frac{1}{u^d(1)} + \frac{1}{u^d(1)^2} \pi^{-d/2} s^{d/2 - 1} \Gamma\left(1 - \frac{d}{2}\right)$$

$$+ O(s^{d-2}). \qquad (G17)$$

Note that $1 - 1/u^d(1)$ is the probability that the walk never returns (which equals 0.2822… in $d = 3$). Conditioned to returning, the probability that the first return occurs at $t = 2m$ steps decays at large t as

$$u^d(1) f_{t=2m}^d \approx \frac{1}{u^d(1)} \pi^{-d/2} m^{-d/2} \quad \text{for } d > 2. \qquad (G18)$$

We see that at $d = 2$ the exponent for the first return probability changes direction, and that the amplitudes of both Eqs. (G13) and (G18) go to 0 [90–93].

---

[1] S. Lemerle, J. Ferré, C. Chappert, V. Mathet, T. Giamarchi, and P. Le Doussal, Phys. Rev. Lett. **80**, 849 (1998).

[2] J. S. Urbach, R. C. Madison, and J. T. Markert, Phys. Rev. Lett. **75**, 276 (1995).

[3] G. Blatter, M. V. Feigel'man, V. B. Geshkenbein, A. I. Larkin, and V. M. Vinokur, Rev. Mod. Phys. **66**, 1125 (1994).

[4] T. Nattermann and S. Scheidl, Adv. Phys. **49**, 607 (2000).

[5] G. Gruner, Rev. Mod. Phys. **60**, 1129 (1988).

[6] S. Brazovskii and T. Nattermann, Adv. Phys. **53**, 177 (2004).

[7] S. Moulinet, C. Guthmann, and E. Rolley, Eur. Phys. J. A **8**, 437 (2002).

[8] S. Moulinet, A. Rosso, W. Krauth, and E. Rolley, Phys. Rev. E **69**, 035103(R) (2004).

[9] D. Cule and T. Hwa, Phys. Rev. B **57**, 8235 (1998).

[10] P. Moretti, M. C. Miguel, M. Zaiser, and S. Zapperi, Phys. Rev. B **69**, 214103 (2004).

[11] L. Ponson, D. Bonamy, and E. Bouchaud, Phys. Rev. Lett. **96**, 035506 (2006).

[12] D. S. Fisher, Phys. Rep. **301**, 113 (1998).

[13] D. S. Fisher, Phys. Rev. B **31**, 1396 (1985).

[14] P. Chauve, P. Le Doussal, and K. J. Wiese, Phys. Rev. Lett. **86**, 1785 (2001).

[15] T. Giamarchi and P. Le Doussal, Phys. Rev. B **52**, 1242 (1995).

[16] D. S. Fisher, Phys. Rev. Lett. **56**, 1964 (1986).

[17] M. Kardar, Phys. Rep. **301**, 85 (1998).

[18] D. S. Fisher, Phys. Rev. B **31**, 7233 (1985).

[19] L. Balents and D. S. Fisher, Phys. Rev. B **48**, 5949 (1993).

[20] S. Scheidl and Y. Dincer, e-print arXiv:cond-mat/0006048.

[21] Yusuf Dincer, Master's thesis, Universität Köln, 1999.

[22] P. Le Doussal and K. J. Wiese, Phys. Rev. Lett. **89**, 125702 (2002).

[23] P. Chauve and P. Le Doussal, Phys. Rev. E **64**, 051102 (2001).

[24] P. Le Doussal, K. J. Wiese, and P. Chauve, Phys. Rev. E **69**, 026112 (2004).

[25] P. Le Doussal and K. J. Wiese, Phys. Rev. B **68**, 174202 (2003).

[26] P. Le Doussal and K. J. Wiese, Nucl. Phys. B **701**, 409 (2004).

[27] P. Le Doussal and K. J. Wiese, Phys. Rev. E **72**, 035101(R) (2005).

[28] D. E. Feldman, Phys. Rev. B **61**, 382 (2000).

[29] D. E. Feldman, Int. J. Mod. Phys. B **15**, 2945 (2001).

[30] D. E. Feldman, Phys. Rev. Lett. **88**, 177202 (2002).

[31] G. Tarjus and M. Tissier, Phys. Rev. Lett. **93**, 267008 (2004).

[32] L. Balents and P. Le Doussal, Europhys. Lett. **65**, 685 (2004).

[33] L. Balents and P. Le Doussal, Phys. Rev. E **69**, 061107 (2004).

[34] L. Balents and P. Le Doussal, Ann. Phys. (N.Y.) **315**, 213 (2005).

[35] P. Le Doussal and K. J. Wiese, Phys. Rev. Lett. **96**, 197202 (2006).

[36] P. Le Doussal and K. J. Wiese, Phys. Rev. Lett. **98**, 269704 (2007).

[37] M. Tissier and G. Tarjus, Phys. Rev. Lett. **96**, 087202 (2006).

[38] M. Tissier and G. Tarjus, Phys. Rev. B **74**, 214419 (2006).

[39] A. Fedorenko, P. Le Doussal, and K. J. Wiese, Phys. Rev. E **74**, 041110 (2006).

[40] A. Fedorenko, P. Le Doussal, and K. J. Wiese, Phys. Rev. E **74**, 061109 (2006).

[41] P. Le Doussal, K. J. Wiese, and P. Chauve, Phys. Rev. B **66**, 174201 (2002).

[42] P. Chauve, T. Giamarchi, and P. Le Doussal, Phys. Rev. B **62**, 6241 (2000).

[43] T. Nattermann, S. Stepanow, L. H. Tang, and H. Leschhorn, J. Phys. II **2**, 1483 (1992).

[44] O. Narayan and D. S. Fisher, Phys. Rev. B **48**, 7030 (1993).

[45] P. Chauve, T. Giamarchi, and P. Le Doussal, Europhys. Lett. **44**, 110 (1998).

[46] P. Le Doussal and K. J. Wiese, Phys. Rev. E **67**, 016121 (2003).

[47] P. Le Doussal and K. J. Wiese, Phys. Rev. E **68**, 046118 (2003).

[48] P. Le Doussal, K. J. Wiese, E. Raphael, and Ramin Golestanian, Phys. Rev. Lett. **96**, 015702 (2006).

[49] A. Rosso and W. Krauth, Phys. Rev. B **65**, 012202 (2001).

[50] A. Rosso and W. Krauth, Phys. Rev. Lett. **87**, 187002 (2001).

[51] A. Rosso and W. Krauth, Phys. Rev. E **65**, 025101(R) (2002).

[52] A. Rosso, A. K. Hartmann, and W. Krauth, Phys. Rev. E **67**, 021602 (2003).

[53] D. T. Fuchs, R. A. Doyle, E. Zeldov, S. F. W. R. Rycroft, T. Tamegai, S. Ooi, M. L. Rappaport, and Y. Myasoedov, Phys. Rev. Lett. **81**, 3944 (1998).

[54] P. Paruch, T. Giamarchi, and J.-M. Triscone, Phys. Rev. Lett. **94**, 197601 (2005).

[55] C. J. Bolech and A. Rosso, Phys. Rev. Lett. **93**, 125701 (2004).

[56] A. B. Kolton, A. Rosso, T. Giamarchi, and W. Krauth, Phys. Rev. Lett. **97**, 057001 (2006).

[57] P. Le Doussal, Europhys. Lett. **76**, 457 (2006).

[58] A. A. Middleton, P. Le Doussal, and K. J. Wiese, Phys. Rev. Lett. **98**, 155701 (2007).

[59] P. Le Doussal and K. J. Wiese, Europhys. Lett. **77**, 66001 (2007).

[60] A. Rosso, P. Le Doussal, and K. J. Wiese, Phys. Rev. B **75**, 220201 (2007).

[61] P. Le Doussal, A. A. Middleton, and K. J. Wiese, Phys. Rev. E **79**, 050101(R) (2009).

[62] S. N. Majumdar and R. M. Ziff, Phys. Rev. Lett. **101**, 050601 (2008), and references therein.

[63] J. Krug, J. Stat. Mech.: Theory Exp. 2007, P07001.

[64] R. Ballerini and S. Resnick, J. Appl. Probab. **22**, 487 (1985); Adv. Appl. Probab. **19**, 801 (1987); K. Borovkov, J. Appl. Probab. **36**, 669 (1999).

[65] S. Redner and M. R. Petersen, Phys. Rev. E **74**, 061114 (2006).

[66] B. Alessandro, C. Beatrice, G. Bertotti, and A. Montorsi, J. Appl. Phys. **68**, 2901 (1990).

[67] D. Ertaş and M. Kardar, Phys. Rev. B **53**, 3520 (1996).

[68] A. Fedorenko, P. Le Doussal, and K. Wiese (unpublished).

[69] Pierre Le Doussal and Thierry Giamarchi, Phys. Rev. B **57**, 11356 (1998).

[70] F. Lacombe, S. Zapperi and H. J. Herrmann, Phys. Rev. B **63**, 104104 (2001).

[71] Ya. Sinai, Commun. Math. Phys. **148**, 601 (1992).

[72] S. Zapperi, P. Cizeau, G. Durin, and H. E. Stanley, Phys. Rev. B **58**, 6353 (1998).

[73] M. Stapleton and K. Christensen, e-print arXiv:cond-mat/0510626; D. Dhar and S. N. Majumdar, J. Phys. A **23**, 4333 (1990).

[74] P. Le Doussal and K. Wiese (unpublished).

[75] H. W. Watson and Francis Galton, J. R. Anthropol. Inst. **4**, 138 (1875).

[76] D. S. Fisher, Phys. Rep. **301**, 113 (1998).

[77] B. Alessandro, C. Beatrice, G. Bertotti, and A. Montorsi, J. Appl. Phys. **64**, 5355 (1988).

[78] We thank J. P. Bouchaud for emphasizing this point, and very useful discussions on the ABBM model.

[79] J. P. Bouchaud (private communication), quoted in [72].

[80] G. Durin, G. Bertotti, and A. Magni, J. Appl. Phys. **75**, 5490 (1994).

[81] L. Laloux and P. Le Doussal, Phys. Rev. E **57**, 6296 (1998).

[82] V. B. Nevzorov, Theor. Probab. Appl. **32**, 201 (1987).

[83] W. Feller, *An Introduction to Probability Theory and its Applications* (Wiley, New York, 1968).

[84] E. Sparre Andersen, Math. Scand. **1**, 263 (1953); **2**, 195 (1954).

[85] M. Bauer, C. Godreche, and J. M. Luck, J. Stat. Phys. **96**, 963 (1999).

[86] W. Krauth, *Statistical Mechanics: Algorithms and Computations* (Oxford University Press, Oxford, 2006).

[87] A. A. Middleton, Phys. Rev. Lett. **68**, 670 (1992).

[88] P. Le Doussal (unpublished).

[89] Charles M. Grinstead and J. Laurie Snell, *Introduction to Probability* (American Mathematical Society, Providence, RI, 1997).

[90] STS symmetry implies $\overline{\hat{V}(w)}=0$.

[91] STS implies that $\hat{A}[w]$ and $\hat{B}[w]$ are invariant under the change $w_{xt}\to w_{xt}+\phi_x$, and the same for A,B,A^0,B^0 functionals.

[92] Distributions with unbounded tails $p(f)\sim A\alpha(\alpha+1)f^{2+\alpha}$ at large negative f correspond to $\alpha\to-\alpha$, i.e., $\zeta=2+2/\alpha$, $f_c^0=0$, $m^2\rho_m=(A/m^2)^{1/\alpha}$, [and $c=\Gamma(1-\frac{1}{\alpha})$]. However, they are dominated by rare events with no finite continuum limit for cumulants of order larger than α.

[93] K. Dahmen and J. P. Sethna, Phys. Rev. B **53**, 14872 (1996).